Identification and Characterisation of Protein Phosphatase 1, Catalytic Subunit Alpha (PP1α) as a Regulator of NF-κB in T Lymphocytes

Dissertation

submitted to the
Combined Faculties for the Natural Sciences and for Mathematics
of the Ruperto-Carola University of Heidelberg, Germany
for the degree of Doctor of Natural Sciences
presented by

Diplom-Biologe Thomas Mock
born in Arnsberg (Germany)

January 2012

Identification and Characterisation of Protein Phosphatase 1, Catalytic Subunit Alpha (PP1α) as a Regulator of NF-κB in T Lymphocytes

Oral examination: 19.01.2012

Referees:

Prof. Dr. Philipp Beckhove
German Cancer Research Center, Heidelberg

Prof. Dr. Peter H. Krammer
German Cancer Research Center, Heidelberg

This thesis is based on research conducted in the Division of Immunogenetics at the German Cancer Research Center (DKFZ), under supervision of Prof. Dr. Peter H. Krammer and direct supervision of PD Dr. Rüdiger Arnold in the period from June 2008 to January 2012.

“Es gibt mehr Fragen als Antworten. Es ist ein ungerechter Handel.”

(Haruki Murakami)

Danksagung

An dieser Stelle möchte ich allen, die mich während meiner Doktorarbeit unterstützt und begleitet haben, meinen Dank aussprechen.

Zunächst möchte ich Prof. Peter H. Krammer danken, dass er mir die Möglichkeit gegeben hat meine Doktorarbeit in seiner Arbeitsgruppe anzufertigen. Peter schafft ein professionelles, aber trotzdem familiäres Arbeitsumfeld, in dem eine kritische Auseinandersetzung mit Daten gefordert und gefördert wird und wissenschaftliche Genauigkeit sowie Ehrlichkeit höchste Priorität haben. Ich möchte mich vor allem für sein Vertrauen in die Arbeit und seinen Optimismus bedanken.

Mein besonderer Dank gilt meinem direkten Betreuer PD Dr. Rüdiger Arnold. Dein Verdienst für das Gelingen dieser Arbeit besteht nicht nur aus deiner Aufgabe als direkter wissenschaftlicher Mentor. Wann auch immer nötig, hast du mir den Rücken freigehalten und so den manchmal ohnehin stressigen Laboralltag erleichtert. Durch unsere freundschaftliche Zusammenarbeit und deinen bewundernswerten Optimismus hast du mir über so manches negative Ergebnis am Ende eines langen Tages hinweggeholfen und das Projekt vorangetrieben. Ich konnte in den letzten Jahren viel von dir lernen. Vielen, vielen Dank für alles!!!

Darüber hinaus, möchte ich mich besonders bei Dr. Markus Brechmann bedanken, mit dem ich einen Großteil der letzten Jahre ein Team gebildet habe und durch dessen Ideen und Arbeit diese Dissertation erst möglich geworden ist.

Herrn Prof. Dr. Beckhove danke ich für die Betreuung dieser Arbeit als Erstgutachter. Ferner möchte ich Prof. Dr. Watzl, Prof. Dr. Lanzer und Prof. Dr. Müller für die Betreuung und Begutachtung meiner Promotion danken.

Zudem bedanke ich mich bei dem Rest der „Phosphatase-Gruppe“ mit Rebecca Breuer, Wolfgang Müller und insbesondere Christina Scheiner, die mir als Biologielaborantin zur Seite stand und mir die ein oder andere „undankbare“ Aufgabe im Labor abgenommen hat.

Ein großer Dank auch an alle jetzigen Mitglieder der Abteilung Immungenetik und Ehemaligen, wie Dr. Julia Hoffmann und Dr. Dirk Brenner, für eure Diskussionsbereitschaft, Hilfe, Zuspruch und alle tollen Momente und Ereignisse jenseits des Labors.

Von ganzem Herzen danke ich Nina, ohne die ich diese prägende und intensive Zeit nicht so unbeschadet überstanden hätte.

Zu guter Letzt danke ich meinen Freunden und meiner Familie, insbesondere meinen Eltern, die mich immer bedingungslos auf meinem Weg unterstützt haben und ohne die ich nicht wäre, wo ich bin.

Zusammenfassung

Der Transkriptionsfaktor *nuclear factor-kappa B* (NF-κB) ist für die Aktivierung und das Überleben von T-Lymphozyten essentiell. NF-κB reguliert die Expression von Zytokinen, Wachstumsfaktoren und anti-apoptotischen Genen. Entsprechend ist die physiologische NF-κB-Aktivierung von zentraler Bedeutung für eine effiziente Immunantwort. Verschiedenste Neoplasien weisen Genmutationen auf, die zu einer aberranten, meist konstitutiven NF-κB-Aktivität führen. Diese erlaubt es Tumorzellen, den Zell-intrinsischen Kontrollmechanismen zu entgehen und unkontrolliert zu proliferieren.

Die T-Zell Rezeptor (TZR)-induzierte Signalleitung, die zur Aktivierung von NF-κB führt, basiert größtenteils auf Phosphorylierungsreaktionen, die zu Veränderungen in der Funktion und Aktivität der phosphorylierten Proteine führen. Diese Phosphorylierung von Proteinen ist aber meist transient. Während viele Kinasen und ihre Substrate charakterisiert wurden, ist die Rolle von Phosphatasen in der Modulierung der NF-κB Signalkaskade bisher wenig untersucht.

Um Phosphatasen zu identifizieren, die eine Rolle bei der TZR-induzierten NF-κB-Aktivierung spielen, wurde ein RNA Interferenz (RNAi) Screen in Jurkat T Zellen durchgeführt. Mit Hilfe dieser Methode konnten verschiedene Phosphatasen und Phosphatase-assoziierte Proteine identifiziert werden, welche die NF-κB-Aktivität positiv oder negativ regulieren. Entsprechend wurde die protein phosphatase 1, calalytic subunit alpha (PP1α) als Positivregulator identifiziert. RNAi-vermittelte Verminderung der PP1α-Expression führte zu einer verringerten NF-κB-Aktivität. Umgekehrt führte die Überexpression von PP1α zu einer erhöhten NF-κB-Aktivität. Es konnte jedoch kein deutlicher Einfluss von PP1α im Hinblick auf zytoplasmatische Phosphorylierungsreaktionen im NF-κB-Signalweg detektiert werden. Allerdings wurde festgestellt, dass PP1α, vermutlich Promotor-spezifisch, die Expression einzelner *bona fide* NF-κB-regulierter Gene beeinflusst. Entsprechend führte eine verringerte PP1α-Expression zu einer verminderten DNA-Bindeaktivität von NF-κB. Zudem wurde gezeigt, dass PP1α für die Proliferation von primären humanen $CD4^+$ T-Lymphozyten benötigt wird. Darüber hinaus, induzierte eine verringerte PP1α Expression oder Inhibition der enzymatischen Aktivität der Phosphatase Apoptose in NF-κB-abhängigen kutanen T Zell Lymphom (engl.: *cutaneous T cell lymphoma*, CTCL) Zellen.

In dieser Arbeit konnte ein neuer Regulator der TZR-induzierten NF-κB-Aktivität identifiziert werden. Diese Ergebnisse tragen zu einem genaueren Verständnis der NF-κB-Regulation in T Lymphozyten bei und sind möglicherweise für die zukünftige therapeutische Behandlung von NF-κB-assoziierten Erkrankungen von Bedeutung.

Abstract

The transcription factor nuclear factor-kappa B (NF-κB) is an essential regulator of lymphocyte activation and survival mediating expression of cytokines, growth factors and pro- and anti-apoptotic genes. Hence, NF-κB activation is essential to mount an efficient immune response and to eradicate potential threats. Conversely, several malignancies acquire mutations, resulting in constitutive NF-κB activity, allowing them to escape cell-intrinsic check-point mechanisms.

Signal transduction to NF-κB, emanating from the T cell receptor (TCR), largely relies on phosphorylation of proteins, altering their localisation and activity. However, most phosphorylation events are transient. While multiple kinases and their substrates have been characterised, the role of phosphatases in modulating NF-κB activity is less well understood.

To systematically identify phosphatases that take part in NF-κB signalling upon TCR engagement, a RNA interference (RNAi) genetic screen in Jurkat T cells was performed. Using this approach, several phosphatases and phosphatase-associated proteins were identified that positively or negatively regulate NF-κB activity. Accordingly, protein phosphatase 1, catalytic subunit alpha (PP1α) was identified as a positive regulator of NF-κB activity. While PP1α silencing caused decreased NF-κB activity, PP1α overexpression augmented NF-κB activity upon TCR engagement. Cytoplasmic signalling events, with respect to known phospho-sites in the NF-κB pathway, were not dramatically influenced by the phosphatase. However, PP1α was found to selectively regulate expression of a subset of *bona fide* NF-κB target genes, most likely in a promoter-specific manner. Accordingly, PP1α-silencing caused a significant reduction of NF-κB DNA binding activity. Furthermore, knock down of PP1α or inhibition of its phospholytic activity suppressed proliferation of primary human $CD4^+$ T lymphocytes. In addition, PP1α-silencing or inhibition sensitised a malignant NF-κB-addicted cutaneous T cell lymphoma (CTCL) cell line towards apoptosis.

In summary, the present study identified PP1α as a novel regulator of NF-κB activity in T lymphocytes and implicates the phosphatase as a factor for lymphoma survival. These findings contribute to a more datailed understanding of NF-κB regulation and may have implications for the treatment of NF-κB-associated malignancies in the future.

Table of contents

1. Introduction

1.1 The immune system

The immune system is a complex system, comprising cells, tissues and soluble products that ensure the health of an organism by the ability to recognize, attack and eradicate non-self entities or by the removal of damaged, infected, auto-reactive or transformed cells derived from self. The term immunity (latin: "*immunitas",* exempt from*)* describes the normal functioning of the immune system in a healthy organism. The concept arose in the 16th century, when little was known about the origin of diseases. Individuals that survived the first encounter of an otherwise fatal disease and that remained healthy after a second exposure were said to be "exempt from" or "immune".

The immune system of higher vertebrates (jawed fish and higher) has evolved into two general branches that can be distinguished by their nature to recognize invading pathogens and mount an immune response. The innate (or natural) immune system recognises foreign entities in a totally non-specific or broadly specific and non-selective manner, whereas the adaptive (or acquired) immune system mounts an immune response in an uniquely specific and selective fashion. Although these features sharply separate the innate and adaptive immune systems, the host defence relies on the concerted action of both and their interconnection with each other to maintain an individuals health and persistent immunity.

1.1.1 The innate immune system

The innate immune system is considered to be the first line of defence against a potential pathogenic threat and can be further subdivided into a non-induced and an induced arm (Janeway and Medzhitov, 2002). Non-induced mechanisms include anatomical and physiological barriers that substantially reduce the likelihood of an infection. The former encompassing the skin and mucosae that physically prevent access to the body, the latter consisting of actions (e.g. sneezing) and substances produced by tissues (e.g. mucus) (Janeway and Medzhitov, 2002).

The induced mechanisms of the innate immune response are largely dependent on specialized cells that arise during haematopoiesis from common myeloid progenitors (CMPs). Among the most frequent descendants from CMPs are cells devoted to

phagocytosis and identification of microbial particles. These immune cells possess an arsenal of broad-spectrum sensors (pattern recognition receptors, PRRs) that recognize so called pathogen-associated molecular patterns (PAMPs). PAMPs are common invariant and repetitive molecular structures (e.g. lipopolysaccharide, LPS) shared among a variety of microbes that are normally not present in the host (Iwasaki and Medzhitov, 2010). Among the best-known PRRs is the family of the extra- and intracellular Toll like receptors (TLRs), which were first discovered in *Drosophila* (Hoffmann, 1999; Kawai and Akira, 2010). Upon binding to their ligands, PRRs initiate an intracellular signalling cascade, which induces a transcriptional program leading to a clearance response that takes the form of phagocytosis, target cell lysis and/or induction of inflammation (Akira and Takeda, 2004). In addition to the cellular component of the innate immune system, the humoral constituents of the complement system are an essential part of an innate immune response. The complement system is activated by a series of proteolytic cleavages leading to three principle outcomes: (i) lysis of pathogens, (ii) opsonisation of pathogens, (iii) clearance of immune complexes (Ricklin et al., 2010).

The combination of the humoral and cellular parts of innate immunity will either eliminate a foreign entity or will keep it in check until the slower, but potentially more effective, adaptive immune response can develop.

1.1.2 The adaptive immune system

The class of cells that mediate the adaptive immune response is called lymphocytes. Lymphocytes are further subdivided into B lymphocytes (B cells, B referring to the a*via*n bursa of Fabricius) and T lymphocytes (T cells, T referring to thymus). They originate from so called common lymphoid progenitors (CLPs), which are generated in the bone marrow from multipotent hematopoietic stem cells (HSCs) earlier during haematopoiesis. While B cell precursors mature in the bone marrow, T cell precursors migrate to the thymus, where they eventually differentiate into mature T cells and enter the periphery. Whereas the innate immune system mounts a response in a broad and unspecific fashion, the adaptive immune system employs highly specific, selective and unique recognition receptors, called B or T cell antigen receptors (BCRs or TCRs, respectively). Each lymphocyte expresses thousands of identical copies of a unique given antigen receptor. In contrast to the genetically fixed recognition receptors of the innate immune system, antigen receptors are generated from a large collection of gene fragments, giving rise to an almost limitless repertoire of unique specificity by means of somatic recombination (Tonegawa, 1993). During this process,

potential auto-reactive antigen receptors are generated. To circumvent lymphocyte attacks to an auto-antigen, self-reactive lymphocytes are negatively selected, leading to central tolerance (Starr et al., 2003). Binding of an antigen to a specific antigen receptor on a mature lymphocyte can trigger its clonal expansion and differentiation into daughter effector cells.

B lymphocytes are able to recognize antigen in its intact form. Engagement of the BCR will lead to the activation of the B cell, causing it to proliferate and differentiate into an antibody secreting plasma cell. An antibody is the modified soluble form of the BCR that can enter the circulation to neutralize or mark antigens for clearance from the body. It therefore constitutes the humoral part of the adaptive immune system. T cells can be further subdivided into two subsets: $CD8^+$ cytotoxic T cells (CTLs), which can lyse target cells directly, and $CD4^+$ helper T cells (T_H), which can further differentiate into T_H1, T_H2, T_H17 and T_{reg} cells to assist CTL or B cell mediated responses, depending on the context and type of antigen they encounter (Zhou et al., 2009). Unlike B cells, T cells are not able to recognize a native antigen. The TCR recognizes a bipartite structure on the surface of a host cell, made up of the major histocompatibility complex (MHC) and a short peptide derived from a protein antigen, which is referred to as peptide-MHC complex (p:MHC) (Trombetta and Mellman, 2005).

Clonal expansion of lymphocytes results in short lived daughter effector cells and long-lived memory cells. The antigen-experienced memory cells persist in a resting state after a pathogen is eliminated. During a second encounter with the same pathogen, memory cells undergo more rapid proliferation and differentiation into effector cells. The result is a stronger and faster secondary immune response. The phenomenon of immunological memory is the fourth hallmark of the adaptive immune system besides the concepts of specificity, diversity and tolerance that distinguishes it from the innate immune system.

1.1.3 The interconnection between innate and adaptive immunity

The course of an immune response can be divided into three phases. The first phase includes the non-induced innate immune system. Anatomical and physiological barriers protect against invading pathogens. When a pathogen manages to breach this first passive line of defence, the second phase will start to develop. Tissue-resident phagocytes, like macrophages or dendritic cells (DCs) sense common microbial structures by their PRRs, leading to the production of pro-inflammatory cytokines and chemokines. Cytokines are low molecular weight peptides or glycoproteins that mediate intercellular communication within

the immune system. In the context of the second phase of an immune response cytokines either intensify (e.g. TNFα) or dampen (e.g. IL-10) an immune response. Chemokines are chemoattractant cytokines (e.g. IL-8) that are secreted to recruit more innate immune cells, like neutrophils and monocytes, to the site of infection and thereby amplify the initial cell-mediated response. In addition, activation of complement contributes to pathogen clearance during this phase. In many cases pathogen invasion can be controlled by the innate immune system within the first 4 to 96 hours. However, the innate immune system is limited in cell numbers and its potential to mount a sufficient immune response. If a pathogen surpasses innate immunity, the third phase with the induction of adaptive immunity will be provoked. At the interface of innate and adaptive immunity are so called professional antigen presenting cells (APCs), like macrophages, B cells and most importantly DCs. They are endowed with high rates of antigen processing and their presentation in p:MHC complexes. DCs are activated at sites of inflammation from where they migrate to the lymphoid organs to present p:MHC to T cells and activate them. Recognition of p:MHC by the TCR only is not sufficient to induce T cell activation. To ensure that activation is restricted to an immune response, activated DCs express co-stimulatory ligands. Only recognition of p:MHC and binding of co-stimulatory ligands on DCs to co-receptors on T cells will lead to full activation of T cells. T cells start to proliferate and differentiate into large numbers of daughter effector cells that eliminate the pathogen by cell-mediated mechanisms and in addition, T cells aid the humoral response by helping B cells. Innate and adaptive immune responses are not separate events, but are deeply interconnected by the interface of professional APCs. Lymphocytes require the cells and cytokines of the innate immune system to be activated. Vice versa, T and B cells secrete cytokines that improve the effectivity of the innate immune system.

1.2 Antigen recognition by the TCR and signal transduction

The TCR recognises antigen in complex with MHC molecules. Two classes of MHC molecules exist in the body. Whereas MHC class I molecules are expressed on all nucleated cells, the expression of MHC class II molecules is confined to cells of the immune system. MHC I molecules display intracellular peptides, either processed from self or from non-self (e.g. viral antigens) antigens. Infected cells, which present pathogenic peptides on MHC I are directly lysed by $CD8^+$ CTLs (Germain, 1994). The CD8 co-receptor binds to MHC class I molecules, thereby stabilizing the interaction between the TCR and enabling it to recognize the MHC bound peptide. Similarly, the CD4 co-receptor on T_H cells binds MHC class II

molecules to stabilize the interaction between the TCR and p:MHC class II on the presenting APC (e.g. DC) (Rudolph et al., 2006). Once the TCR binds its specific p:MHC, the supramolecular immunological synapse (IS) forms (Bromley et al., 2001) and the externally sensed signal induces an array of intracellular signalling cascades, which will ultimately activate the T cell to proliferate and differentiate, thereby translating environmental clues into cellular behaviour.

1.2.1 The T cell receptor complex

The TCR is not a single chain receptor, but a multi-component signalling complex. Two types of TCRs exist, which are defined by their component chains: TCR$\alpha\beta$ and TCR$\gamma\delta$. In humans, most mature T cells are $\alpha\beta$T cells and only 5 to 10% are $\gamma\delta$T cells. The N termini of the paired immunoglobulin (Ig)-like polypeptide chains contain the variable regions (V region), which shape the antigen recognition site. The V regions are followed by the constant and the connecting domains, harbouring a disulphide bond covalently connecting the α and β or the γ and δ chains, respectively. Each chain contains a transmembrane domain followed by a short cytoplasmic tail. The cytosolic portion of the TCR chains are not capable of signal transduction (Bentley, 1997). Instead, the non-polymorphic CD3 γ, δ, ε and ζ chains non-covalently associate in different configurations with the TCR polypeptides to build platforms for signal transduction (Meuer et al., 1983a; 1983b; Smith-Garvin et al., 2009). The CD3 complex consists of heterodimers of CD3$\varepsilon\delta$ and CD3$\varepsilon\gamma$ and a homodimer of CD3$\zeta\zeta$. CD3 molecules contain long cytoplasmic tails that comprise various copies of immunoreceptor tyrosine based activation-motifs (ITAMs). ITAMs are found in other immune receptors as well and serve as recruiting platforms for signalling molecules (Reth, 1989). The signature of this motif is two tyrosine residues flanked by a series of amino acids with stereotypic spacing (D/Ex_7D/ExxYxxI/Lx_7YxxI/L; single letter code, x is for any amino acid). Using mutants that lack the key tyrosine residues as well as chimeric proteins, several laboratories have identified the ITAMs to be the minimal requirement to couple the TCR/CD3 complex to the intracellular signalling machinery (Irving and Weiss, 1991; Romeo et al., 1992; Wegener et al., 1992; Letourneur and Klausner, 1992).

1.2.2 TCR proximal signalosome

One of the first events following ligation of the TCR/CD3 complex is thought to be a conformational change within the cytoplasmic tails of CD3 that renders the ITAMs accessible to phosphorylation in a stimulus dependent manner (Xu et al., 2008). Subsequently, Src-family kinases (SFKs), including lymphocyte-specific protein tyrosine kinase (Lck) and FYN oncogene related to SRC (Fyn), are recruited to the TCR complex *via* the co-receptors CD4 and CD8. In the absence of TCR signals, Lck is maintained in an inactive state by the combined action of the tyrosine kinase Csk and the tyrosine phosphatase PEP. Csk phosphorylates an inhibitory tyrosine residue in the C-terminus while PEP dephosphorylates the activation loop tyrosine of Lck. Upon TCR ligation the receptor-like protein tyrosine phosphatase CD45 dephosphorylates Lck in the C-terminus thereby facilitating its activation (Hermiston, 2002). Once activated, Lck and Fyn are able to phosphorylate critical tyrosine residues within the ITAM motifs. Subsequently the Syk-family kinase ζ chain-associated protein kinase of 70 kDa (ZAP-70) is recruited to the doubly phosphorylated ITAMs *via* interaction with its tandem src-homology 2 (SH2) domains. This increases the local concentration of ZAP-70 at activated TCRs. The kinase is fully activated by Lck-mediated phosphorylation of tyrosine residues in the activation loop of its kinase domain (Au-Yeung et al., 2009). The most important substrates of ZAP-70 are the transmembrane adaptor protein linker of activated T cells (LAT) and the cytosolic adaptor protein SH2-domain-containing leukocyte protein of 76 kDa (SLP-76) (Zhang et al., 1998; Wardenburg et al., 1996; Koretzky et al.). LAT and SLP-76 build the framework, also referred to as the TCR proximal signalosome, for further signal propagation and diversification (Lindquist et al., 2003; Fuller et al., 2003) (Fig. 1.1). LAT contains several tyrosine residues, that when phosphorylated serve as interaction sites for phospholipase Cγ1 (PLCγ1), the p85 subunit of phosphoinositide 3-kinase (PI3K) and the adaptor proteins growth factor receptor bound 2 (GRB2) and GRB2-related adaptor downstream of shc (Gads) (Sommers et al., 2004). SLP-76 is recruited by its mutual binding partner Gads (Liu et al., 1999). SLP-76 harbours several phosphorylation-induced interaction sites in its N-terminal domain, which are required to recruit IL-2 inducible kinase (Itk), guanine-nucleotide-exchange factor (GEF) Vav1 and adapter non-catalytic region of tyrosine kinase (Nck) to the complex. In addition, SLP-76 binds PLCγ1 and adhesion and degranulation-promoting protein (ADAP) in a constitutive manner and can inducibly interact with hematopoietic progenitor kinase 1 (HPK1) (Koretzky et al.). Once PI3K gets recruited to the complex it converts phosphatidylinositol 4,5-bisphosphate (PIP_2) into phosphatidylinositol 3,4,5-trisphosphate (PIP_3), which is important for local enrichment of Itk

and Protein Kinase B (PKB/Akt). The binding of PLCγ1 to SLP-76, LAT and Vav1 as well as to its activating kinase Itk, indicates a complicated organization within the complex that is in part also independent of its participant's enzymatic activities. Several laboratories have generated mutant mouse strains and cell lines that support the role of a higher order organization as a prerequisite for sufficient signal propagation from the LAT:Gads:SLP-76 complex (Qi and August, 2007; Miletic et al., 2006; Sommers et al., 2005; Jordan et al., 2008). Formation of the LAT:Gads:SLP-76 complex ultimately leads to the activation of PLCγ1 and subsequent downstream effector pathways as well as to cytoskeletal rearrangements and integrin signalling (Smith-Garvin et al., 2009).

1.2.3 PLCγ1 mediated generation of second messengers

LAT:Gads:SLP-76 complex-mediated activation of PLCγ1 catalyses the generation of the second messengers diacylglycerol (DAG) and inositol-1,4,5-trisphospahte (IP_3) by hydrolysing PIP_2 (Fig. 1.1). While production of DAG initiates two pathways that result in activation of the transcription factors nuclear factor kappa-light-chain-enhancer of activated B cells (NF-κB) and activator protein-1 (AP-1), IP_3 mediates the induction of calcium ion-dependent pathways leading to activation of nuclear factor of activated T cells (NFAT). Both will be further discussed in the following paragraphs.

i. DAG-mediated signalling pathways

Generation of the membrane integral second messenger DAG leads to activation of two distinct pathways. One involves activation of the lymphocyte-specific Protein Kinase C (PKC) isoform PKCθ, which is essential to trigger NF-κB activation and will be discussed in detail in paragraph 1.3.3. The second DAG-induced pathway depends on the small guanine nucleotide binding protein Ras, which is necessary for downstream activation of mitogen activated protein kinases (MAPK). While activation of Ras is mediated by GEFs that facilitate binding of GTP, it is suppressed by GTPase activating proteins (GAPs) that hydrolyse Ras-bound GTP. T cells possess two GEF proteins: Ras guanyl nucleotide releasing protein (RasGRP) and son of sevenless (SOS) (Dower et al., 2000; Ebinu et al., 2000; Egan et al., 1993). RasGRP is recruited to the plasma membrane by binding to DAG, where it is phosphorylated by PKCθ (Ebinu et al., 1998; Roose et al., 2005). In contrast, SOS is constitutively bound to the adaptor protein GRB2, which is inducibly recruited to the LAT:Gads:SLP-76 signalosome, where it locally augments Ras activity. The GEF activity of

SOS is limited by initial RasGRP-dependent RasGTP production, implying a positive feedback loop. Ras activation leads to downstream phosphorylation of the MAPKs extracellular signal-regulated kinase 1 and 2 (Erk1/2). Like the other two major MAPK pathways (the p38 MAPKs and the c-Jun NH2-terminal kinases (JNK) pathways), Erk1/2 activation is part of a hierarchical phosphorylation cascade that involves upstream MAPK kinase kinases (MAPKKKs) and MAPK kinases (MAPKKs) (Dong et al., 2002). Ras activates the MAPKKK Raf1, which in turn phosphorylates the MAPKKs MEK1 and MEK2, leading to Erk1/2 phosphorylation and activation. Erk activity induces the transcription factor Elk1, which regulates c-Fos expression and, thereby, AP-1 (c-Jun:c-Fos) activation (Smith-Garvin et al., 2009).

ii. Ca^{2+} ion-mediated signalling

Calcium-ions (Ca^{2+}) serve as universal second messengers in eukaryotic cells. The concentration of calcium is low in unstimulated T cells. Once the TCR is triggered, highly mobile IP_3 is generated and acts as a ligand for heterotetrameric IP_3-receptors (IP_3Rs) in the membrane of the endoplasmic reticulum (ER). Binding of IP_3 to IP_3Rs causes the release of Ca^{2+} from ER stores into the cytosol. This leads to a transient increase in the local, cytosolic Ca^{2+} concentration. ER store depletion is one prerequisite for a sustained strong Ca^{2+} influx from the extracellular space. In a process, referred to as store-operated Ca^{2+} entry (SOCE), stromal interaction molecules (STIMs) sense ER store depletion and Ca^{2+}-release-activated Ca^{2+} (CRAC) channels are activated, mediating influx of extracellular calcium (Oh-hora and Rao, 2008). Cytosolic Ca^{2+}-ions bind to and modulate the conformation and biochemical property of the protein calmodulin (CaM). In context of TCR induced signalling, Ca^{2+}:CaM acts on the serine/threonine phosphatase calcineurin (CN) and the Ca^{2+}:CaM-dependent kinases (CaMK) (Soderling, 1999; Savignac et al., 2007). CaMKs have diverse functions in different signalling pathways. Whereas CaMKII was identified as a negative regulator during TCR-induced signalling, CaMKIV was found to have a positive regulatory role (Liu, 2009). The Ca^{2+}:CaM-activated CN is able to dephosphorylate proteins of the NFAT family, which comprise three calcium-regulated members in T cells (NFAT1,2,4) (Fig. 1.1). NFAT transcription factors are rendered inactive by hyperphosphorylation, which masks their nuclear localisation sequence (NLS) and exposes their nuclear export sequence (NES). Once CN is activated, it binds NFAT and dephosphorylates critical serine residues. This reveals a NLS and enables NFAT to shuttle to the nucleus where it can bind to promoters and induce gene transcription (Macian, 2005). Although NFAT proteins can bind as

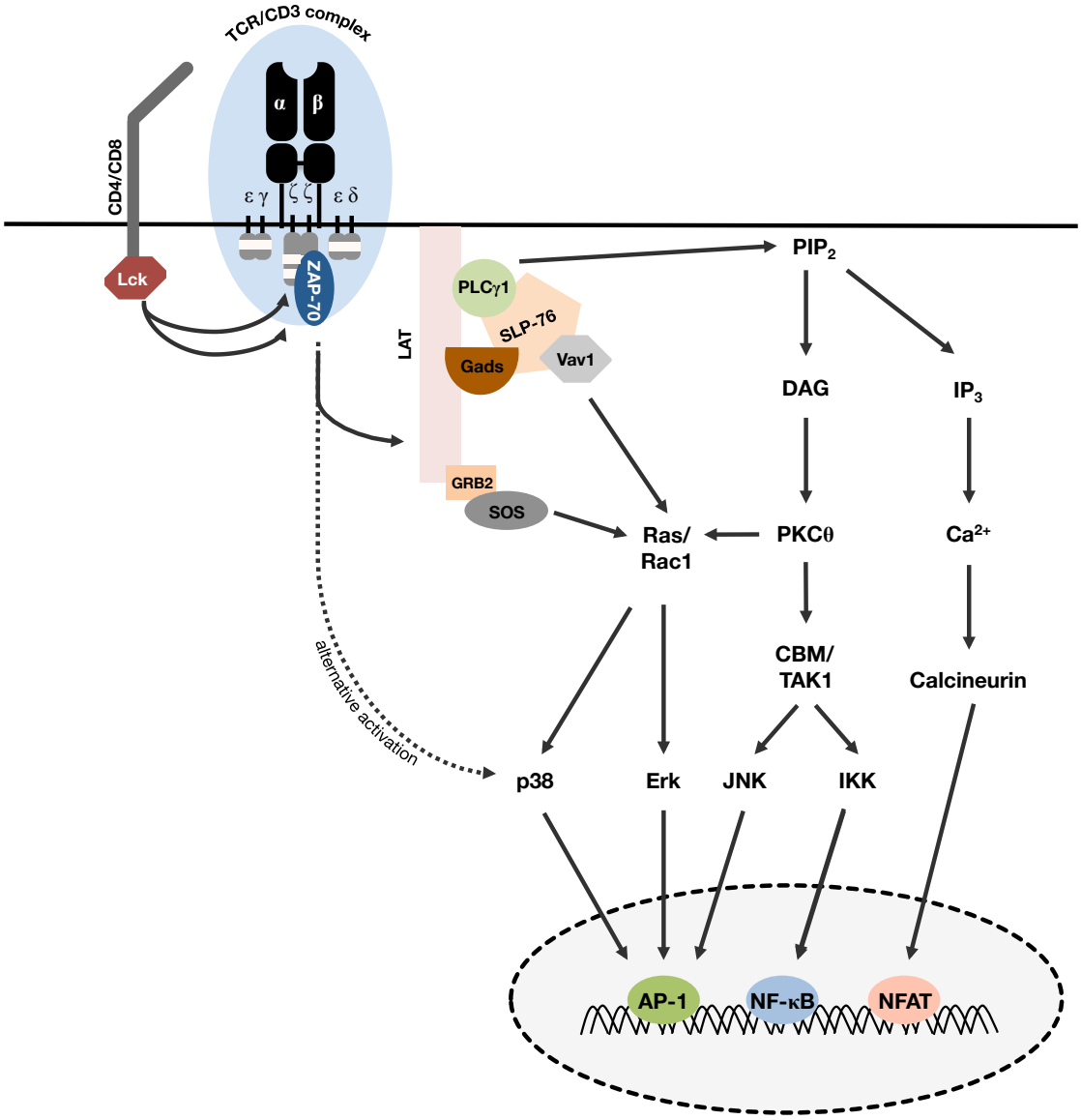

Figure 1.1 TCR-induced signaling pathways. Stimulation of the TCR and engagement of co-receptors lead to activation of src-fmaily kinases, like Lck, which in turn phosphorylate the ITAM motifs in the cytoplasmic tails of the CD3 chains. Subsequently ZAP-70 is recruited and activated *via* binding to the double-phosphorylated ITAMs. In turn, ZAP-70 phosphorylates LAT and SLP-76, leading to the assembly of the proximal TCR signalosome. Phosphorylated LAT is able to interact with SLP-76 *via* the adaptor Gads, inducing recruitment and activation of PLCγ1. Activated PLCγ1 generates the second messengers DAG and IP_3, which in turn activate several pathways. First, IP_3 induces release of Ca^{2+} from the ER leading to activation of NFAT. Second, DAG-mediated activation of PKCθ induces assembly of the CBM complex, leading to NF-κB activation and initiates ERK signalling *via* Ras. In addition, the GEF SOS, recruited to LAT, *via* the adaptor GRB2, facilitates activation of p38 through Rac1. Alternatively, p38 can be activated alternatively *via* ZAP-70 (dashed line). JNK is activated in a TAK1-dependent manner downstream of PKCθ. Activation of Erk, JNK and p38 culminates in AP-1 activity.

homodimers to target gene sequences, there are several examples for cooperative binding with other transcription factors (activators or repressors). The most prominent example is described for the IL-2 promoter, where cooperative binding of NFAT:AP-1 complexes is mandatory for normal induction of IL-2 expression (Macián et al., 2001; Serfling et al., 2007). Once calcium levels decline, CN is inactivated and different kinases phosphorylate NFAT, thereby masking the NLS and exposing a NES. Among those negative regulatory kinases are the glycogen-synthase-kinase 3β (GSK3β), Casein Kinase 1α (CK1α), DYRK1 and 2 and protein kinase A (PKA). These either act in the cytoplasm maintaining NFAT hyperphosphorylated in unstimulated cells or in the nucleus by rephosphorylation of promoter-bound NFAT in stimulated cells.

1.2.4 Activation of the JNK and p38 pathways

In addition to Erk, two other MAPKs, belonging to the family of stress-activated protein kinases (SAPKs), are activated upon TCR engagement: the group of JNKs and the group of p38 MAPKs (Dong et al., 2002).

i. JNK activation

Three members of the JNK family (JNK1-3) have been identified in mammals. Whereas JNK3 is not expressed in T cells, JNK1 and JNK2 expression is low in resting T cells. However expression is strongly induced upon T cell activation. (Rincon and Davis, 2009). JNK1/2 are activated by dual phosphorylation of threonine 180 and tyrosine 182 in the activation loop of the kinase domain by the upstream MAPKKs MKK4 and MKK7. The MAPKKs are also regulated by dual phosphorylation by upstream MAPKKKs. These include the TGFβ-activated kinase (TAK1) (Huang et al., 2009), the mixed lineage kinase (MLK) group and members of the Erk family (Manning and Davis, 2003). Several studies have also identified PKCθ to contribute to JNK activation. The phorbolester 12-myristate 13-acetate (PMA), which activates PKCs, was shown to induce JNK phosphorylation. This is in line with results from PKCθ deficient mice that exhibit reduced c-Jun phosphorylation and concomitantly decreased AP-1 activity (Isakov and Altman, 2002). Moreover, TAK1 activity seems to be required for activation of JNKs (Huang et al., 2009). Downstream substrates of JNK include the transcription factor c-Jun. Phosphorylation of c-Jun by JNKs induces its dimerization with c-Fos, leading to the formation of transcriptionally active AP-1 complexes.

Although some studies associate JNKs with T cell activation, their actual contribution remains controversial. Studies from knockout mice suggest that JNKs are dispensable for IL-2 production and T cell activation (Dong et al., 2002), but seem to play non-redundant roles during T helper differentiation. Whereas JNK1 deficient mice exhibit enhanced T_H2 differentiation (Dong et al., 1998), JNK2 deficiency leads to an impairment of T_H1 polarisation (Yang et al., 1998). The existence of several isoforms of JNK1 and JNK2 adds another layer of complexity, complicating to attribute their relative impact on T cell function.

ii. p38 activation

The p38 pathway is the third MAPK pathway initiated upon TCR triggering. There are four known p38 isoforms (p38α, p38β, p38γ and p38δ), each encoded by a separate gene. All, except p38γ, are expressed in T cells (Hale et al., 1999). p38 proteins can be activated in a classical MAPK signalling cascade manner. In T cells, the formation of the proximal LAT:Gads:SLP-76 signalosome leads to the recruitment and activation of the small Rho-GTPase family members Ras-related C3 botulinum toxin substrate (Rac1) and cell division cycle 42 (CDC42) *via* the GEF Vav1, inducing MAPKKK activity. Several studies, using knockout mice suggest that MKK3, MKK4 and MKK6 act as p38 MAPKKs during classical MAPK activation (Brancho et al., 2003). Similar to JNK, p38 is activated by dual phosphorylation of threonine and tyrosine residues in the activation loop of the kinase domain. Using p38-specific inhibitors, different groups established that p38 needs to autophosphorylate itself in a TAK1-binding protein 1 (TAB1) –dependent manner, to be fully activated (Ge et al., 2002). The requirement for autophosphorylation-dependent activation seems to be cell type specific and can be observed in T cells. Notably, it has become evident that T cells also use an alternative activation pathway, involving ZAP-70 and growth-arrest and DNA damage-inducible 45α (GADD45α). GADD45α seems to have a dual role during TCR-induced MAPK activation. On the one hand, it positively regulates JNK and p38 by facilitating activation of the MAPKKK MTK1, which in turn activates MKK4 and thereby JNK and p38. On the other hand, it was identified as a negative regulator of ZAP-70-mediated phosphorylation of tyrosine 323 of p38, which is required to induce its autophosphorylation on threonine 180 (Lu et al., 2001; Salvador et al., 2005b; 2005a). Prominent downstream targets of p38 include the tumor suppressor p53 and the transcription factors activating-transcription factor 2 (ATF2) and c-Fos. In that way activation of JNK and p38 converge by inducing transcriptional activation of the AP-1 complex. Surprisingly, isoform-specific knockout mice of p38 have shown few abnormalities

despite the body of indirect evidence from studies using inhibitors, transgenic mouse models or protein mutants (Ashwell, 2006).

1.2.5 Co-stimulation by CD28

Several early studies have suggested that binding of p:MHC to the TCR alone is not sufficient for full activation of T cells. This led to the formulation of the two signal hypothesis, which postulates that additional binding of ligands from the surface of APCs to co-stimulatory receptors on the surface of the T cells, are required for T cell activation (Quill and Schwartz, 1987). The best characterised co-stimulatory ligand/receptor complex is the B7/CD28 interaction. CD28 belongs to the Ig-like family of co-stimulatory receptors (Boomer and Green, 2010; Rudd and Schneider, 2003; Rudd et al., 2009). Engagement of CD28 by the B7-family members B7-1 (CD80) and B7-2 (CD86) that are expressed on the surface of activated APCs leads to increased sensitivity to TCR triggering. In addition, co-stimulation strongly enhances IL-2 production and is necessary for full T cell activation *via* amplification of the three major TCR-induced transcription factors NFAT, AP-1 and NF-κB. Consequently, cell survival is increased by elevated expression of anti-apoptotic genes and effector molecules (Thompson et al., 1989; Radvanyi et al., 1996). CD28 is expressed as a disulphide linked homodimer. Its short cytoplasmic tail contains several motifs that are important to facilitate recruitment of signalling molecules upon binding of its ligands. Lck and Fyn can phosphorylate the tyrosine residue in the membrane proximal motif YMNM, which is able to recruit the SH2-domain containing p85 subunit of PI3K and the adaptor proteins GRB2 and Gads (Cai et al., 1995; Schneider et al., 1995; Ellis et al., 2000). The adjacent proline-rich-region was shown to recruit Itk2 *via* its SH3-domain (Marengere et al., 1997), whereas the more distal PYAP motif binds Lck, Grb2 and Filamin-A (Tavano et al., 2006). Although binding and activation of PI3K has been shown, one study using knockin mice suggests that the membrane proximal YMNM-mediated recruitment of PI3K is dispensable for proper IL-2 secretion and T cell activation (Dodson et al., 2009). After CD28 co-stimulation Lck is able to phosphorylate the tyrosine residue in the membrane proximal motif. This enables recruitment of the p85 subunit of PI3K and subsequently, docking and activation of the larger kinase domain-containing subunit p110. PI3K, once activated, induces the production of the D3-lipid PIP_3. D3-lipids serve as docking sites for pleckstrin-homology-domain (PHD)-containing proteins, including phosphoinositide-dependent kinase 1 (PDK1) or Akt. Binding of Akt to PIP_3 induces conformational changes that render Akt

accessible to phosphorylation and activation by PDK1 (Vanhaesebroeck and Alessi, 2000). Upon activation, Akt is released from the membrane into the cytosol, where it can influence different signalling pathways. Accordingly, Akt is able to phosphorylate an inhibitory threonine residue on GSK3β, thus sustaining NFAT activity. In addition, it was shown to phosphorylate activating residues of I-kappa-B-kinase α (IKKα), mammalian target of rapamycin (mTOR) and cAMP-response-element binding protein (CREB), thereby influencing gene expression. PDK1 was proposed to be the crucial component that connects TCR- and CD28-induced NF-κB activation by directly activating I-kappa-B kinase β (Vanhaesebroeck and Alessi, 2000) (discussed in detail in paragraph 1.3.4). Engagement of CD28 also leads to PI3K-independent pathways by binding of the adaptor molecules GRB2 and Gads. GRB2 links CD28 to JNK and p38 activation, possibly through activation of Ras and Rac1 in a Vav1-dependent manner (Bustelo, 2000; Zhang et al., 1999; Su et al., 1994). CD28-initiated signalling is negatively regulated by phosphatase and tensin homolog (PTEN) and inositol-5-phosphate-phosphatase (INPP5D/SHIP1) that function to inactivate the products of PI3K activity. (Shan et al., 2000; Freeburn et al., 2002). Knockout mice of either protein display fatal autoimmune pathologies due to T cell hyper-responsiveness. CD28 co-stimulation provides the means to amplify TCR-induced signalling pathways and to prevent apoptosis by regulating the activity of pro-apoptotic proteins like Bad and Bcl_{XL}. It is still controversial whether CD28 signalling is initiated independent of TCR engagement *in vivo* (Lühder et al., 2003; Tacke et al., 1997). Although anti-CD28 superagonistic antibodies exist that are able activate T cells independently of TCR signals, this effect seems to be rather short-lived and non-physiological (Tacke et al., 1997).

1.3 The transcription factor NF-κB

The identification of the transcription factor NF-κB was a breakthrough discovery in the early 1980s. It was first described as a factor that binds the enhancer sequence 5´-GGGACTTTCC-3 in the κ-light gene locus of B cells, promoting the expression of the κ-light chain during B cell development (Sen and Baltimore, 1986). However, it soon became clear that NF-κB expression is not exclusive to B cells and that the influence on κ-light chain expression is of quantitative and not of qualitative nature. One of the most important early findings was that NF-κB is an inducible factor (Sen and Baltimore, 1986). In the absence of any stimuli, it is sequestered in an inactive form in the cytosol, complexed with an inhibitory protein (Baeuerle and Baltimore, 1988). Activation takes place in response to certain stimuli (e.g. LPS) that induce the release of the inhibitor from the transcription factor, thus enabling

it to migrate to the nucleus where it can bind its target sequences and activate gene transcription. Today, it is known that NF-κB is functional in virtually all cell types and can be activated by various stimuli. Since its initial description, the importance of NF-κB has been demonstrated in thousands of publications, especially manifesting its role in immunology and cancer biology. In context of immune-receptor signalling NF-κB activates transcription of several effector molecules that are necessary for activation, proliferation and differentiation (for instance IL-2, INFγ or TNFα). Many cancer cells abduct NF-κB to increase expression of anti-apoptotic genes leading to enhanced proliferation and survival as well as resistance to classical theraouetic treatment. The following paragraphs will discuss the most important aspects of NF-κB signalling, particularly focussing on its impact on T cell biology.

1.3.1 The family of NF-κB transcription factors

The family of NF-κB transcription factors consists of five members: RelA (p65), c-Rel, RelB, p50 and p52, which are able to homo- or heterodimerize to form the NF-κB complex (Hayden and Ghosh, 2008). Of note, p50 and p52 are generated through proteolytic cleavage of their precursor proteins p105 and p100, respectively. All family members possess a conserved 300 amino acid long Rel-homology-domain (RHD) at their N-terminus, which is necessary for homo- and heterodimerization, interaction with inhibitory proteins and mediates DNA binding. The RHD consists of an amino-terminal domain (NTD) and the dimerization domain (DimD), which is followed by a NLS. RelA, c-Rel and RelB are additionally characterised by the C-terminal transcription activation domain (TAD), which is not present in p50 and p52 (Huxford and Ghosh, 2009). p50 and p52, therefore, rely on forming dimers with RelA, c-Rel or RelB to activate gene transcription. In fact, homodimers of p50 or p52 are found to act as transcriptional repressors. RelB additionally possesses a leucine-zipper-motif (LZ) at its N-terminal region (Vallabhapurapu and Karin, 2009). It was found to preferentially heterodimerize with p100/p52, whereas RelA and c-Rel predominantly dimerize with p50. Whether the LZ of RelB confers specificity for dimerization is not known. A number of posttranslational modifications among the NF-κB proteins including phosphorylation, methylation, acetylation and ubiquitinylation further fine-tune the ability of individual dimers to activate gene transcription (Oeckinghaus and Ghosh, 2009; Liu and Chen, 2011; Harhaj and Dixit, 2011) (Figure 1.2). Furthermore, modifications enable the subunits to recruit and interact with co-factors that are required to access DNA. The combinatorial possibility of 15 individual NF-κB dimers as well as a variety of posttranslational modifications culminates in a multitude of regulatory mechanisms to

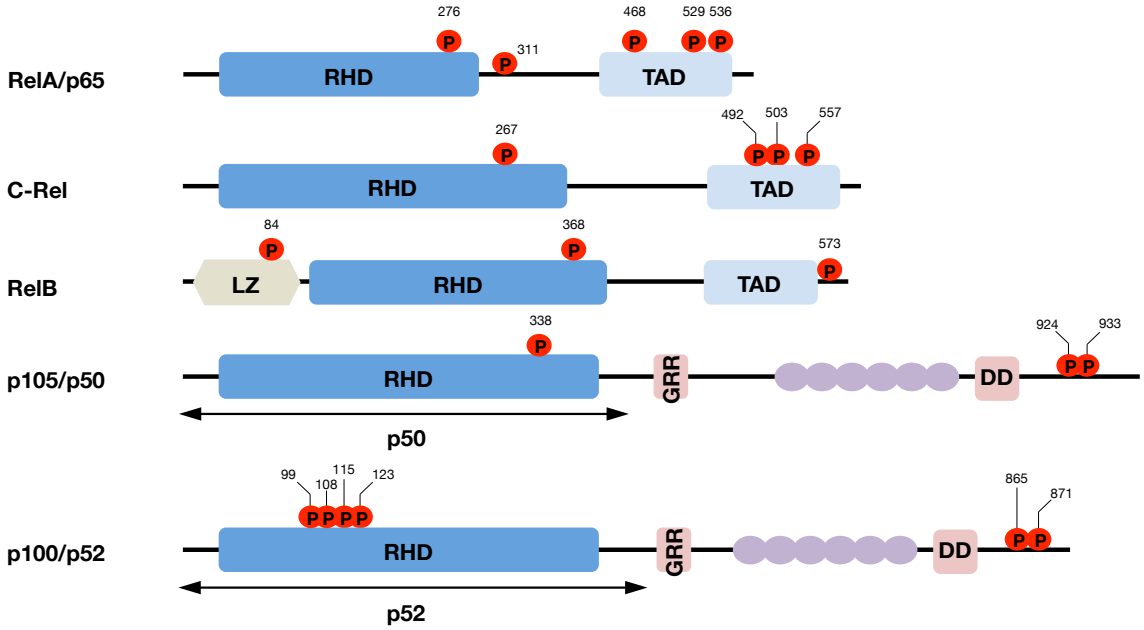

Figure 1.2 The NF-κB family of transcription factors. The NF-κB family consists of five members, which are characterised by the presence of a N-terminal Rel homology domain (RHD). The RHD confers homo- and heterodimerization, interaction with inhibitory proteins and DNA-binding. RelA, RelB and c-Rel also possess a transcription activation domain (TAD), which mediates transcription initiation at κB-site-containing promoters. RelB is additionally characterised by a leucine-zipper (LZ) motif in its N-terminus. p50 and p52 are generated from their precursor proteins p105 and p100, respectively. The N-terminus harbors the RHD of p50 and p52, which is followed by a glycine-rich region (GRR) and multiple ankyrin repeats (violet ovals) and a death domain (DD).
Red circles indicate known phosphorylation sites that alter the function of the respective protein.

control NF-κB activity. By far the most important regulators of NF-κB are the family of inhibitor of kappa B proteins (IκBs)

1.3.2 The IκB family

The best-studied regulators of NF-κB are the IκB proteins. In unstimulated cells IκBs retain the NF-κB dimer in the cytoplasm by masking its NLS. Although the IκBs have been mainly described as potent negative regulators, it has become evident that they can serve different functions (Hayden and Ghosh, 2008). The family of IκBs consists of seven members that can be further subdivided. The group of canonical IκBs consists of IκBα, IκBβ and IκBε, the so called precursor IκBs comprise p105 and p100 and the group of atypical IκB proteins contains Bcl-3 as well as IκBζ . All IκBs are characterised by multiple ankyrin repeats, which enable them to bind to the RHD of NF-κB dimers and interfere with the exposure of the NLS

sequence. It is believed that individual IκBs bind prefentially to a particular subset of NF-κB dimers, but surprisingly few details are known (Oeckinghaus and Ghosh, 2009; Vallabhapurapu and Karin, 2009). The canonical members of the IκB family possess an amino-terminal signal responsive region (SRR), which contains conserved serine residues that are phosphorylated by I-kappa-B kinase beta (IKKβ) (see paragraph 1.3.3) (Fig. 1.3). Phosphorylation initiates K48-linked ubiquitinylation und subsequent degradation *via* the proteasomal pathway. IκBα is the best-studied and prototypic member of the canonical family members and primarily associates with the canonical RelA:p50 dimer. Crystallographic analysis of the IκBα:RelA:p50 complex revealed that IκBα only masks the NLS of RelA, but not p50. In addition, IκBα contains a NES, which mediates immediate export of NF-κB from the nucleus. Hence, under basal conditions, IκBα:NF-κB complexes constantly shuttle between the cytosol and the nucleus. Once IκBα is degraded, this equilibrium shifts and NF-κB will be mainly located in the nucleus. IκBα is resynthesized in a NF-κB-dependent manner, constituting a negative feedback mechanism to block prolonged NF-κB activity.

In contrast to IκBα, the role of IκBβ is less well understood. It shows similar binding to NF-κB dimers and, like IκBα, is also degraded and resynthesized in a stimulus- and NF-κB-dependent manner. In addition to its inhibitory function, IκBβ was reported to augment transcription of a subset of genes (e.g. TNFα) by binding and stabilizing DNA-bound RelA:c-Rel complexes (Rao et al., 2010). IκBε is also degraded and resynthesized under NF-κB-inducing conditions. It is predominantly expressed in cells of the hematopoietic system, indicating that IκBs may have unique roles in different cell types (Basak et al., 2007; Kearns et al., 2006). Surprisingly, cells from mice with triple knockout of the canonical IκB family members exhibit a normal nuclear/cytoplasmic RelA distribution, but a significantly higher basal expression of NF-κB target genes, indicating that modulation of NF-κB transcriptional activity is partly independent of IκB-dependent cytoplasmic sequestration (Tergaonkar et al., 2005).

Under steady state conditions, the IκB/NF-κB–like precursor protein p105 is processed to p50 in a co- and posttranslational fashion (Moorthy et al., 2006; Lin et al., 1998). However, when p105 is bound to NF-κB dimers, it is protected from processing and acta as an IκB protein (Hayden and Ghosh, 2008). A complete IκBα-like degradation is induced by IKKβ-mediated phosphorylation of serine residues in the C-terminal region of p105 (Perkins, 2006). The processing of the IκB-like p100 precursor protein is largely stimulus-dependent and requires the activity of IKKα (Senftleben et al., 2001). IKKα is mainly operative during non-canonical activation of NF-κB (paragraph 1.3.4). Similar to p105, the p100 protein is

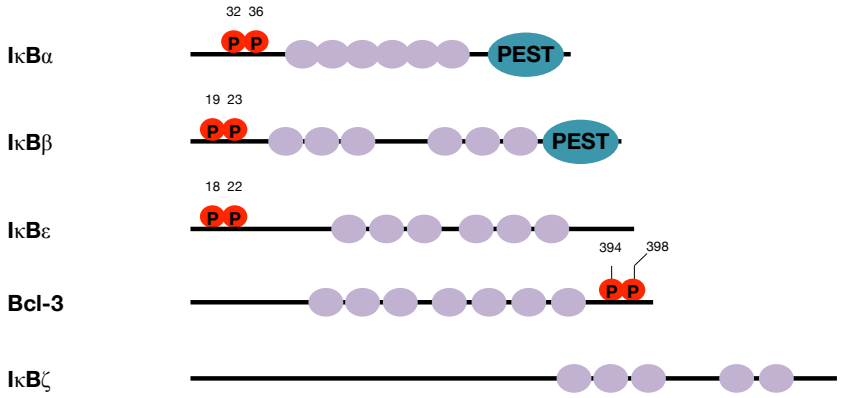

Figure 1.3 The IκB family. IκB proteins are characterised by multiple ankyrin (violet ovals) repeats, which mediate binding to the RHD of NF-κB dimers. Therefore, p105 and p100 can function as an NF-κB protein, when processed to p50 and p52 or as IκB proteins in there full-length form. At their C-terminus IκBα and IκBβ have a proline-, glutamic acid-, serine-, threonine-(PEST) motif, indicative for proteins with a short half life.
Red circles indicate known phosphorylation sites that alter the function of the respective protein.

constantly processed at a low rate to p52, and in its precursor form it acts as an IκB protein. Regulation of RelB by p100 is especially crucial, since it is the only IκB protein that binds RelB (Solan et al., 2002). Whereas RelB is exclusively controlled by p100, p100 can act more broadly, since it was shown to associate with RelA-containing dimers as well. In this respect, it was described to limit RelA-activity in an induced negative feedback following T cell activation (Ishimaru et al., 2006).

The two atypical IκB family members Bcl-3 and IκBζ regulate NF-κB by a distinct mechanism that is not understood yet. Bcl-3 is special in that it contains a TAD. It is found in the nucleus, where it associates with p50 and p52 homo- and heterodimers (Bours et al., 1993). This interaction was suggested to induce release of transcriptionally repressive NF-κB dimers, thereby facilitating recruitment of transcriptionally active RelA-containing complexes (Wulczyn et al., 1992). In contrast, it was shown that induced expression of Bcl-3 inhibits NF-κB activity. These opposing properties may be partially explained by different posttranslational modifications of Bcl-3 (Nolan et al., 1993; Massoumi et al., 2006a; Bundy and McKeithan, 1997). The second atypical IκB protein IκBζ is not constitutively expressed, but its expression is induced after triggering the IL1- or TLR4 receptor (Motoyama et al., 2005). IκBζ is localized to the nucleus where it associates with p50 homodimers as a co-activator for a subset of genes after LPS or IL-1 treatment. In addition IκBζ has been shown to inhibit RelA-containing NF-κB complexes. This is in line with an

observed mild elevation of NF-κB target gene expression in IκBζ knockout mice (Motoyama et al., 2005; Yamamoto et al., 2004).

1.3.3 The IKKs

The induced degradation of IκB proteins by phosphorylation is a prerequisite for NF-κB activation. IκB phosphorylation is mediated by two kinases that either function independently or assembled in a complex with a scaffold protein - the so-called IKK complex. The IKK complex mediates activation of the canonical NF-κB pathway, whereas IKK complex-independent activation leads to non-canonical NF-κB activation (see 1.3.4) (Hayden and Ghosh, 2008; Oeckinghaus and Ghosh, 2009; Huxford and Ghosh, 2009). The IKK complex was initially purified as a high molecular weight complex of 700 to 900 kDa. It was found to contain the two kinases IKK1 and IKK2, IKKα and IKKβ respectively, and an adaptor/scaffold protein termed IKKγ or NEMO (Zandi, 1997; Woronicz et al., 1997; DiDonato et al., 1997; Mercurio et al., 1999). The two kinases display about 50% sequence homology and exhibit molecular weights of 85 and 87 kDa. The 48 kDa sized NEMO is not related to IKKα or IKKβ and does not possess any intrinsic catalytic activity. The exact stoichiometry of the complex is still not resolved, but several studies, suggest a 2:1:1 (IKKγ:IKKα:IKKβ) ratio (Huxford and Ghosh, 2009). Since this cannot account for the high apparent molecular weight of the purified endogenous complex, it was suggested that single complexes oligomerize into higher order structures, consisting of dimers or tetramers of IKK complexes. So far, no *in vitro* reconstitution with purified proteins resulted in a 700 to 900 kDa structure exhibiting catalytic activity. Accordingly, it was recently suggested that the high apparent molecular weight from gel filtration might be due to the elongated structure of NEMO, leaving this issue highly controversial (Xu et al., 2011). The two kinases have a similar domain organization that was predicted to encompass an amino-terminal kinase domain, followed by a ubiquitin-like (UBL) domain, a central leucine zipper and a helix-loop-helix (HLH) motif (Huxford and Ghosh, 2009). The C-terminus was predicted to contain a serine rich region and the NEMO-binding-domain (NBD), which mediates interaction with NEMO (Figure 1.4). In addition, and in contrast to IKKβ, IKKα was predicted to possess a NLS sequence in the kinase domain. This is consistent with a described role of IKKα in the nucleus (Yamamoto et al., 2003). A recently published crystal structure, using *Xenopus laevis* IKKβ, which shares about 74% sequence homology with human IKKβ, describes a domain organization that differs from the previously made predictions. The structure revealed a tretramodular domain organization, encompassing the kinase domain,

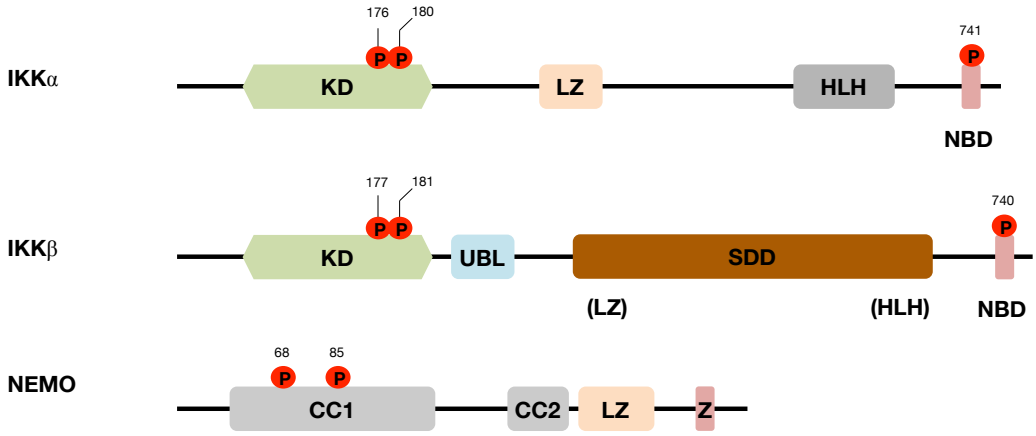

Figure 1.4 The IKK family. IKKα is shown with its predicted domain organization, containing an N-terminal kinase domain, followed by a LZ, a helix-loop-helix (HLH) motif, and the C-terminal NEMO binding domain (NBD). The domain organization of IKKβ is represented according to the crystal structure of *Xenopus laevis* IKKβ. The N-terminal kinase domain is followed by an ubiquitin like domain (UBL), the helical-scaffold/dimerization domain (SDD) and a NBD. Previously predicted motifs for human IKKβ are indicated in brackets. NEMO possesses two coiled-coil (CC1 and CC2) domains, which mediate the interaction with IKKα and IKKβ *via* their respective NBD. The CC2 domain is followed by a LZ and a C-terminal zinc finger (Z) motif. The CC2-LZ region mediates binding to poly-ubiquitin chains and is necessary for NEMO function.
Red circles indicate known phosphorylation sites that alter the function of the respective protein.

the UBL-domain and a helical-scaffold/dimerization domain (SDD) and the NBD. Unexpectedly, the predicted LZ and HLH do not form but appear to be part of the SDD (Figure 1.2). The UBL domain and SDD seem to mediate and restrict the interaction with IκBα. In addition the UBL domain is required for the catalytic activity of the kinase. The SDD was shown to be important for dimerization, which is required during activation, but not to maintain catalytic activity. The study proposes a similar structure and domain organization for related kinases, including IKKα, IKKε and the TANK-binding kinase 1 (TBK1) (Xu et al., 2011).

Phosphorylation of conserved activation loop serine residues in IKKα and IKKβ is mandatory for kinase activity. The phosphorylation sites (S176/S180 in IKKα and S177/S181 in IKKβ (Fig. 1.4)) are reminiscent of the MAPKK consensus motif SXXXS (X can be any amino acid), which is also consistent with the observation that the MAPKKKs TAK1 and NIK are able to phosphorylate IKKs (Hayden and Ghosh, 2008). In addition, it was shown that IKKs can be activated through transautophosphorylation, but the exact mechanism remains elusive. Although IKKα and IKKβ are structurally similar, they exhibit different substrate specificities. Whereas IKKβ can phosphorylate most NF-κB bound IκBs, IKKα preferably displays specificity for p100. This is also reflected in knockout mice. IKKβ is sufficient and necessary

to confer phosphorylation of IκBα and IκBβ in IKKα knockout mice. In contrast, IKKα cannot compensate IKKβ deficiency, although residual IKK activity is observed (Hacker and Karin, 2006). NEMO acts as a scaffold protein with regulatory function within the IKK complex. It was predicted to contain two coiled-coil domains – designated CC1 and CC2 – a helical dimerization domain near the amino-terminal end, a central LZ motif and a Zinc-finger domain (ZF) at its C-terminus (Figure I.2). The N-terminal helical coiled-coil domain interacts with both IKKα and IKKβ *via* their C-terminal NBD. Two NEMO proteins pair through extended coiled coil interactions to form the docking site for a pair of kinase subunits at the N-terminus (Huxford and Ghosh, 2009). Interestingly, the CC2-LZ region of NEMO was shown to bind to free linear ubiquitin chains that act as signalling mediators upon TNF receptor triggering (Rahighi et al., 2009). While IKKα, IKKβ and NEMO are considered to be the essential core components of the IKK complex, other proteins were co-purified with endogenous IKK complex. These include the chaperones Hsp90 and Cdc37 as well as the ELK protein. It is known that Hsp90 stabilizes protein folding of several protein kinases, indicating that Hsp90 might have a non-specific function in IKK-mediated signalling. RNAi-mediated knockdown of ELK was described to interfere with TNFα and IL-1-induced IκB phosphorylation (Ducut Sigala et al., 2004; Chen et al., 2002). While these interactions are stable there may be a multitude of other interacting regulatory proteins, but their binding to the IKK complex may be rather transient and instable.

1.3.4 Induction of canonical and non-canonical NF-κB signalling

Signalling to and activation of NF-κB can be divided into the canonical or classical pathway, which is NEMO-dependent, and the non-canonical or alternative pathway, which is activated in a NEMO-independent fashion. The IKKs and the IκBs are the generic key components for both pathways, but activation of IKKs as well as the composition of NF-κB dimers differ, resulting in initiation of distinct transcriptional programs and functional outcomes. The classical and alternative pathway is initiated by different receptor subsets and requires a different set of signalling molecules upstream of their IKKs (Hayden and Ghosh, 2008).

i. The canonical NF-κB pathway

The key step in the canonical NF-κB pathway is activation of the IKK complex, leading to phosphorylation and degradation of NF-κB-bound IκBs. The canonical pathway is activated

in response to a multitude of stimuli, including cytokines (e.g. TNFα), PAMPs (e.g. LPS) and engagement of antigen receptors (e.g. TCR). Although all stimuli will lead to activation of the IKK complex, the different receptor systems employ specific signalling mediators to do so. Most of our knowledge concerning canonical IKK activation has been gathered by studying TNF-induced signalling. However, some principles like the use of scaffold and adaptor proteins as well as K63-linked ubiquitination can be transferred to other receptor systems, including PRRs and antigen receptors and seem to be a prerequisite for canonical NF-κB signalling (Ruland, 2011). Phosphorylation of serine residues in the activation loop of IKKs is mandatory to induce kinase activity (Hacker and Karin, 2006). However, it has been a long-standing question whether this is facilitated by transautophosphorylation or by upstream IKK kinases (IKK-Ks) (Hayden and Ghosh, 2008; Oeckinghaus et al., 2011). Indeed, evidence for both exists and both might be necessary to induce IKK activity. TAK1 and MEKK3 have been described to act as IKK-Ks. Accordingly, MEKK3 deficient fibroblasts exhibit impaired NF-κB activation after TNFα or IL-1 stimulation. MEKK3 overexpression alone is able to induce IKK activity, indicating that the kinase acts directly proximal of or on the IKK complex (Yang et al., 2001b). In addition, MEKK3 catalytic activity is needed to rescue impaired IKK activity in MEKK3-deficient cells (Blonska et al., 2004). Although this supports an important function for MEKK3, no study has shown that MEKK3 directly phosphorylates the activation loop serine residues of IKKβ under physiological conditions. Therefore, MEKK3 might also serve another function during IKK activation. In contrast to MEKK3, TAK1 overexpression alone does not induce IKK activity, but is dependent on co-overexpression of the TAK1 binding proteins TAB1, TAB2 or TAB3 (Wang et al., 2001; Kanayama et al., 2004; Ishitani et al., 2003; Kishida et al., 2005). Interestingly, single knockouts of TAB1 or TAB2 fail to show a NF-κB defect in response to IL-1 or TNFα (Shim et al., 2005). However, simultaneous RNAi-mediated silencing of TAB1 and TAB2 resulted in impaired NF-κB signalling (Ishitani et al., 2003). Moreover, silencing of TAK1 in Jurkat T cells resulted in impaired IκBα phosphorylation and decreased IL-2 production upon TCR-triggering (Sun et al., 2004). However, the analysis of TAK1-deficent mice did not support a general role for TAK1 in antigen receptor-dependent IKK activation. BCR-triggering resulted in normal IKK activity and TAK1 specifically impinges on TCR-induced NF-κB activation in thymocytes, but not during activation of mature T cells (Liu et al., 2006; Sato et al., 2005; Wan et al., 2006). In conclusion, MEKK3 and TAK1 may act in a cell type specific manner and are possibly required to amplify an initial transautophosphorylation-mediated IKK activation. Transautophosphorylation may occur through recruitment of IKK complexes to macromolecular signalling platforms that may facilitate oligomerization and, thus, proximity-induced transautophosphorylation of IKKs.

Additionally, among different pathways, conserved signalling intermediates involved in activation of the IKK complex are the family of TNFR-associated factors (TRAFs) and receptor-interacting proteins (RIPs). The family of TRAFs consists of seven members. All members are characterised by the presence of the TRAF domain, enabling interaction with signalling mediators. With exception of TRAF1, all TRAFs possess a RING domain, which can function as a ubiquitin ligase (Hacker and Karin; 2006). However, ubiquitin-conjugating activity has only been proven for TRAF2 and TRAF6 (Chen, 2005). Among the best-studied TRAFs are TRAF2, 5 and 6. They have been extensively characterised in context of TNFα/IL-1/Toll-induced NF-κB activation (Tada et al., 2001). Upon TNFα stimulation, TRAF2 or, in its absence, TRAF5 is recruited *via* the adaptor molecule TNFR-associated *via* death domain (TRADD) to the TNFR-complex. Knockout mice from either TRAF do not exhibit any alteration of IKK activation (Tada et al., 2001; Nakano et al., 1999; Yeh et al., 1997). However, cells from double knockout mice are unable to mount a TNFα-dependent NF-κB response. Although it is now established that ubiquitination is necessary for proper IKK activation, the E3-ligase activity of either TRAF2 or TRAF5 is not needed (Devin et al., 2001; Tada et al., 2001). Therefore, it was proposed that TRAF proteins serve as adaptors that recruit E3-ligase activity through recruitment of the cellular inhibitor of apoptosis proteins 1 and 2 (cIAP1 and cIAP2). The TRAF:cIAP1/2 signalosome is able co-recruit RIP1 (Devin et al., 2000), which was shown to be essential for TNFα induced NF-κB activation (Meylan et al., 2004; Ting and Pimentel-Muinos, 1996). Although RIP1 possesses a kinase domain, its kinase activity is dispensable in this context (Lee et al., 2004). Similar to the TRAFs, RIP1 serves as an adaptor that is modified by K63-linked polyubiquitination, most probably by the cIAPs (Oeckinghaus et al., 2011). The polyubiquitin chains on RIP1 were shown to interact with the ubiquitin-binding site of NEMO, thereby recruiting the IKK complex to the receptor, which is thought to induce conformational changes and/or its oligomerization (Ea et al., 2006; Li et al., 2006a; Wu et al., 2006) Interestingly, RIP1-anchored polyubiquitin chains co-recruit and activate TAK1 (*via* TAB2), bringing the IKK complex in close proximity to the proposed IKK-K (Kanayama et al., 2004). Of note, several groups recently characterised a novel E3-ligase complex, called linear ubiquitin chain assembly complex (LUBAC), which was shown to associate with the TNFR (Ikeda et al., 2011; Tokunaga et al., 2011; Gerlach et al., 2011; Haas et al., 2009). LUBAC induces the addition of linear ubiquitin chains to NEMO and RIP1, which was suggested to augment the recruitment of the IKK complex to the receptor. However, none of the studies provide genetic evidence, that this type of ubiquitination is essential for IKK activation.

ii. The non-canonical NF-κB pathway

Whereas receptor-mediated activation of the canonical NF-κB pathway occurs within minutes and is independent of protein synthesis, non-canonical NF-κB signalling requires *de novo* protein synthesis and takes several hours. The non-canonical activation is NEMO- and IKKβ-autonomous, but involves IKKα. It is initiated by a distinct set of receptors belonging to the TNFR-superfamily. These include lymphotoxin β-recepter (LTβR), CD40, receptor activator for NF-κB (RANK) and B cell activating factor receptor (BAFF-R). Non-canonical NF-κB signalling has been implicated in lymphoid organogenesis, B cell development and survival as well as DC maturation and bone metabolism. In addition to IKKα, NF-κB inducing kinase (NIK), which mediates IKKα activation is absolutely required ro initiate non-canoncial NF-κB activation (Xiao et al., 2001; Sun, 2010a). In the absence of any stimuli, NIK exhibits a short half-life and is constantly degraded *via* the proteasome. Upon receptor engagement, NIK is stabilized and activates IKKα. IKKα in turn phosphorylates RelB-bound p100, which induces its limited proteolysis to p52 and enables the RelB/p52 dimer to travel into the nucleus (Derudder et al., 2003; Coope et al., 2002). The control of NIK stability is crucial for positive and negative regulation of the non-canonical NF-κB pathway. A complex consisting of TRA2 and TRAF3, which recruits the E3 Ligase activity of cIAP1 and cIAP2, mediates NIK turnover under basal conditions. Upon receptor engagement, the complex is translocated to the activating receptor, probably followed by conformational changes. As a consequence, the complex is destabilized through degradation of TRAF2 and TRAF3, resulting in liberation and stabilisation of NIK. NIK accumulates in the cytoplasm, where it activates IKKα, leading to non-canonical NF-κB activation (Vallabhapurapu et al., 2008; Sun, 2011). In contrast signal activation, little is known about negative regulation of non-canonical NF-κB. A recent publication suggests that IKKα regulates over-accumulation of NIK in addition to its activating function (Razani et al., 2010). This is likely to control the magnitude of NIK accumulation, but may not be sufficient to shut off non-canonical NF-κB signalling completely.

1.3.5 TCR-induced NF-κB signalling

Activation of NF-κB upon antigen receptor triggering, is essential for proper lymphocyte activation, survival and differentiation. Lack of NF-κB-mediated gene transcription can result in immunodeficiency, whereas an over-activation is associated with autoimmune pathologies and can be causative for development of lymphoid malignancies (Li, 2002). TCR

and CD28 co-receptor stimulation results in activation of the canonical NF-κB pathway. Although some of the characteristics described in paragraph 1.3.4 also apply to TCR-induced signalling, recent studies have established that T cells use a distinct set of signalling molecules to activate the IKK complex. These include the PKC isoform PKCθ and an inducible trimodular complex, composed of caspase recruitment domain (CARD) and membrane-associated guanylatekinase (MAGUK)-containing scaffold protein 1 (CARMA1), CARD-containing adapotor protein B cell CLL/Lymphoma 10 (Bcl10) and the paracaspase mucosa associated lymphoid tissue lymphoma translocation gene 1 (MALT1). The complex is also referred to as the CBM complex (Vallabhapurapu and Karin, 2009; Thome et al., 2010; Blonska and Lin, 2010) (Fig. 1.3). PKCθ is predominantly expressed in T lymphocytes and is the only PKC isoform that was shown to be recruited to the IS upon T cell activation (Monks et al., 1998; Isakov and Altman, 2002). Recruitment and activation of PKCθ is mediated by direct binding to DAG (see paragraph 1.2.3) and phosphorylation by PDK1, whichis activated upon CD28 co-stimulation. Under basal conditions PKCθ is thought to adopt a closed conformation, which is opened upon binding to DAG and subsequent phosphorylation by Lck as well as PDK1 (Villalba et al., 2002). Several studies have established PKCθ as an essential component of TCR-induced NF-κB activation (Schulze-Luehrmann and Ghosh, 2006). However, the connection between PKCθ and IKK complex activation has not been clear until recently. Several studies have now established that the kinase is required for recruitment and assembly of the lymphocyte-specific CBM complex into the IS (Fig. 1.5). The requirement for the CBM complex to induce proper NF-κB signalling and, thus, lymphocyte activation is supported by impaired NF-κB activation in CARMA1, Bcl10 and MALT1 knockout mice (Thome et al., 2010; Blonska and Lin, 2010).

CARMA1 acts as a scaffold protein and is characterised by a N-terminal CARD domain, followed by a coiled-coil domain and an extended linker region. The C-terminus comprises the MAGUK domain, which contains several motifs for protein-protein interactions, typical for scaffold proteins at sites of cell-cell contact. It consists of a PDZ domain (named after the domain-containing PSD-95, Dlg and *Z*O-1 proteins), followed by a SH3 domain and a GUK domain (Dimitratos et al., 1999). The CARD, the SH3 domain and the coiled-coil domain as well as the linker region are all essential for NF-κB activation, whereas the PDZ domain is dispensable (Gaide et al., 2002). While the CARD was shown to be necessary for the inducible interaction with Bcl10, the exact contribution of the GUK- and the SH3 domain to CARMA1 function is not yet understood (Gaide et al., 2002). For other MAGUK proteins it has been proposed that the SH3-GUK domain mediates intramolecular interactions that keep the protein in an auto-repressive conformation (Yaffe,

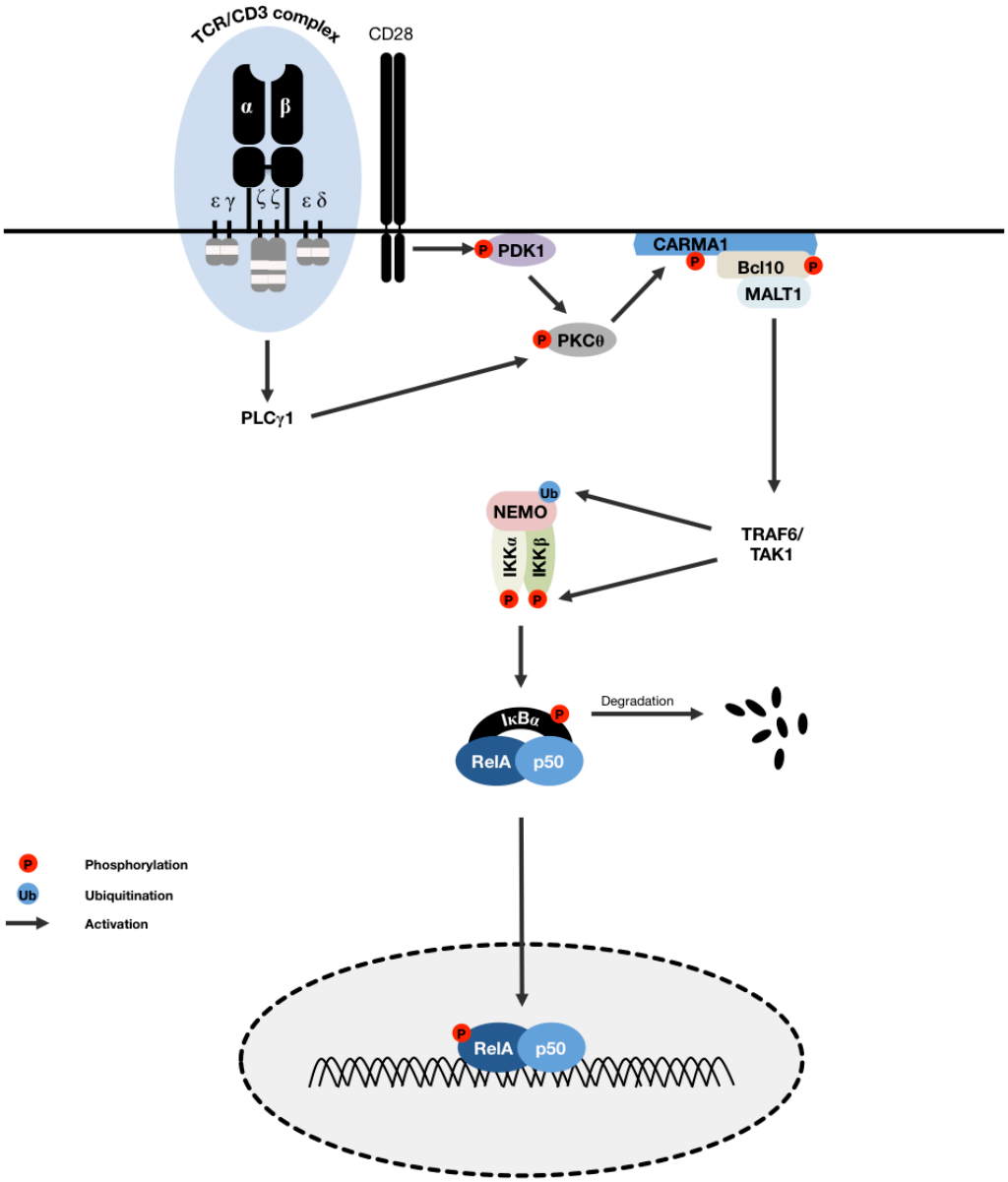

Figure 1.5 T cell receptor induced NF-κB signalling. Stimulation of the TCR leads to the assembly of the proximal TCR signalosome, resulting in the activation of PLCγ1. PLCγ1 mediates generation of the second messenger DAG, leading to recruitment of PKCθ to the plasma membrane. Co-stimulation of CD28 induces the recruitment and activation of PDK1, which activates PKCθ and inducibly associates with CARMA1. PKCθ is now able to phosphorylate CARMA1 in its linker region, possibly provoking a conformational change that induces interaction with preformed Bcl10:MALT1 dimers, which results in the assembly of a macromolecular signalling platform, known as the CBM complex. CBM complex formation in turn leads to recruitment and oligomerization of the E3-ligase TRAF6, stimulating its E3-ligase activity. TRAF6 mediates K63-linked polyubiquitination of NEMO, and Bcl10, inducing the recruitment of the IKK complex to the signalling platform. The IKK complex in turn is activated, presumably through proximity-induced transautophosphorylation. In addition, TRAF6 ubiquitinates itself, leading to the recruitment of TAK1, which may act as an IKK-K to amplify IKK activation. Activated IKKβ phosphorylates IκBα, marking it for degradation *via* the proteasome. The RelA:p50 NF-κB heterodimer is liberated and can shuttle to the nucleus, where it binds to κB-sites and drives gene transcription.

2002; Feng and Zhang, 2009). However, a similar mechanism has not yet been formally shown for CARMA1. CARMA1 function is controlled by phosphorylation of several kinase-specific serine residues in its linker region (Wang et al., 2002; Sommer et al., 2005; Matsumoto et al., 2005)(Matsumoto et al., 2005; Sommer et al., 2005; Wang et al., 2002)(Matsumoto et al., 2005; Sommer et al., 2005; Wang et al., 2002). Upon TCR stimulation, CARMA1 is enriched in lipid rafts, where it is able to interact with PKCθ. PKCθ in turn mediates phosphorylation of the linker region, which evokes a conformational change within CARMA1, enabling it to bind Bcl10. Following TCR triggering, preformed Bcl10:MALT1 complexes are recruited by CARMA1 (Gaide et al., 2002). CBM complex-dependent NF-κB activation is thought to occur through facilitating IKK complex recruitment to and oligomerization at the plasma membrane. IKK activation was shown to be dependent on K63-linked ubiquitination of NEMO. In addition, NEMO possesses an ubiquitin-binding domain, which is thought enable the IKK complex to bind to upstream formed polyubiquitin chains, enabling the IKK complex to be ordered into higher macromolecular structures (Vallabhapurapu and Karin, 2009). The CBM complex may act as a molecular platform that recruits signalling intermediates responsible for NEMO ubiquitination and activation (Blonska and Lin, 2010). K63-linked ubiquitination of NEMO was shown to occur in a CARMA1 dependent manner. Interestingly, phosphorylation of IKK activation loop serine residues in CARMA1- and Bcl10-deficient cells is normal, but kinase activity is completely abolished, indicating that phosphorylation alone is not sufficient (Shambharkar et al., 2007). TRAF2 and TRAF6, which were thought to predominantly act within TNFR/IL-1R-mediated NF-κB activation, were also shown to be involved in TCR-mediated IKK activation (Sun et al., 2004). The study describes an interaction between MALT1 and TRAF6, stimulating its ligase activity towards NEMO and possibly Bcl10. Moreover, TRAF6 autoubiquitination stimulates the recruitment and activation of TAB:TAK1 complexes, which may also participate in the activation of the IKK complex (Sun et al., 2004). The complexity of the CBM-signalosome is even further increased by the finding that caspase-8 is necessary for recruitment of the IKK complex (Misra et al., 2007).

Co-stimulation by CD28 is a prerequisite for full NF-κB activation in T cells. PDK1 appears to be the long missing link between CD28 and IKK complex activation. CD28 stimulation leads to the activation of PI3K, which induces production of PIP_3 to serve as a docking site for PDK1. Binding of PDK1 to PIP_3 induces its activation, possibly through autophosphorylation of a critical threonine residue. This mediates binding of PDK1 to CARMA1 as well as to PKCθ, which in turn is phosphorylated in its activation loop by the former. PDK1-activated PKCθ is now able to phosphorylate CARMA1 in its linker region resulting in CBM complex assembly and NF-κB activation. Thus, PDK1 has a dual function,

by activating and bridging PKCθ towards its substrate (Park et al., 2009; Blonska and Lin, 2010). Of note, CK1α, HPK1 and IKKβ have been shown to phosphorylate non-PKCθ target serine residues in the linker region of CARMA1 that are essential to mediate NF-κB activation (Bidère et al., 2009; Lee et al., 2005; Brenner et al., 2009; Wegener et al., 2006). In summary, lymphocytes activate canonical NF-κB signalling, using lymphocyte-specific kinases and scaffold proteins. An overview of TCR-induced NF-kB activation is shown in Fig. 1.5.

1.3.6 Termination of NF-κB signalling

Although tremendous efforts have been made to understand how NF-κB is activated in various scenarios and contexts, a lot less is known about negative regulation of NF-κB. Immediate activation of NF-κB is required for a successful immune response. However, NF-κB activity has to be tightly controlled to prevent excessive production of inflammatory cytokines that may lead to tissue damage or even death through septic shock. Uncontrolled continuous inflammation enhances the risk for autoimmunity and can promote cancer formation (Karin and Greten, 2005; Ben-Neriah and Karin, 2011). Therefore several negative-regulatory mechanisms have evolved to terminate or modulate the magnitude of NF-κB activity. IκB proteins are the best-characterised negative regulators of NF-κB. Their function has been reviewed in paragraph 1.3.2. Hence, this paragraph will concentrate on the negative regulatory function of ubiquitin-editing enzymes. The role of phosphatases will be discussed separately.

i. Negative regulation of NF-κB by ubiquitin-editing enzymes

The role of ubiquitin-mediated signalling during NF-κB activation upon various inducing conditions is a field of intense investigation. As described in paragraphs 1.3.4 and 1.3.5 addition of K63-linked polyubiquitin chains to signalling molecules is necessary for induction of canonical NF-κB signalling upon various stimuli. K63-linked ubiquitin chains mediate recruitment to and stabilization of downstream signalling proteins into signalling complexes. In addition, they can alter the function and activity of their substrates. Accordingly, counterregulation of ubiquitin signalling is of special interest in this context. Indeed, several deubiquitinases (DUBs) have been found to act as negative regulators (Harhaj and Dixit, 2011). A20 is the best-studied DUB and possesses an E3 ubiquitin ligase domain that surprisingly allows for dual ubiquitin editing function. A20 is expressed in a NF-κB-

dependent manner and can therefore be considered as an induced negative feedback regulator. It was shown to remove K63-linked polyubiquitin chains from RIP1 (see paragraph 1.3.4), NEMO, TRAF6 and MALT1 (Boone et al., 2004; Duwel et al., 2009; Coornaert et al., 2009). Thus, A20 can act in the TNFR-induced as well as in the PRR- and antigen receptor-induced NF-κB pathway. Its activity is controlled by Tax binding protein 1 (TAXBP1), which facilitates interaction with RIP1 or TRAF6. Within the TNFR-pathway, A20 removes K63-linked ubiquitin chains from RIP1. Additionally, A20 functions as an adaptor that recruits the HECT ubiquitin ligase Itch, which promotes K48-linked ubiquitination and degradation of RIP1 (Shembade et al., 2008; Scharschmidt et al., 2004; Wagner et al., 2008). Interestingly, the removal of K63-linked ubiquitin from RIP1 seems to be a prerequisite for its' K48-linked polyubiquitination (Wertz et al., 2004). Consistent with A20s function within different NF-κB pathways, A20-deficient T cells were shown to have prolonged IKK activity and IκBα phosphorylation upon stimulation. Accordingly, T cells from A20-deficient mice exhibit a hyperactivated phenotype and, consequently, A20-deficient mice die early due to hyperinflammation (Lee et al., 2000).

Another important negative regulator of ubiquitin-mediated NF-κB activation is the tumorsuppressor CYLD (cylindromatosis). Unlike A20, CYLD is not expressed in a NF-κB-dependent manner. However its activity is controlled in a stimulus-dependent fashion by phosphorylation and localization (Massoumi et al., 2006b; Reiley et al., 2005). CYLD was shown to deubiquitinate several activators, including TRAF2, TRAF6, TAK1 and NEMO (Trompouki et al., 2003; Sun, 2010b). Whereas A20 and CYLD negatively regulate receptor proximal events, by targeting K63-linked ubiquitination, other E3-ligases mediate inhibition of NF-κB activity by degradative K48-linked ubiquitination of nuclear RelA. Copper metabolism (Murr1) domain containing 1 (COMMD1) was shown to inhibit NF-κB, as an important component of an E3-ligase complex, including elongin b or c and cullin-2 or -5 as well as suppressor of cytokine secretion 1 (SOCS1) (Maine et al., 2007; Natoli and Chiocca, 2008). Another E3-ligase that inhibits NF-κB acitivity in the nucleus is PDLIM2 (PDZ and LIM domain 2). PDLIM2 facilitates incorporation and ubiquitination of RelA in insoluble promyelocytic leukemia nuclear bodies, which are enriched with proteasome activity (Tanaka et al., 2007; Natoli and Chiocca, 2008).

1.3.7 The role of phosphatases in T cell activation and NF-κB signalling

Phosphorylation is a key posttranslational modification, involved in intracellular signal transduction. It can mediate conformational changes (e.g. phosphorylation of CARMA1),

alter the biochemical activity of signalling intermediates (e.g. phosphorylation of IKKs) or can function to establish interaction surfaces for other molecules (e.g. ITAM motifs). The human genome encodes 518 kinases, including 90 protein tyrosine kinases (PTKs) and 428 protein serine/threonine kinases (PSKs). In contrast, there are 107 protein tyrosine phosphatases (PTP) and only a few protein serine/threonine phosphatases (PSPs) (about 30) present. The PSPs are further subdivided into 3 families: the phosphoprotein phosphatases (PPPs), the metal-dependent phosphatases (PPMs) and the aspartate-based phosphatases. The vast majority of phosphorylation reactions occur on serine and threonine residues. Although there are more than 400 known serine/threonine kinases, only 30 PSPs, including seven catalytically active PPPs, are encoded in the human genome (Manning et al., 2002; Shi, 2009). This discrepancy may imply that PPPs act in a broadly unspecific manner to counter-regulate kinase function. However, PPPs are tightly controlled by regulatory subunits that interact with the catalytic cores to modulate substrate specificity, localisation and enzymatic activity. PPPs function, therefore, in multimeric holoenzyme complexes that consist of a catalytic core subunit that associates with one or more regulatory subunits (Virshup and Shenolikar, 2010). Hundreds of regulatory subunits were shown to exist. Accordingly, a plethora of distinct holoenzyme complexes can form that possess the same catalytic core, but exert distinct functions. This concept has been established for protein phosphatase 1 (PP1) and 2A (PP2A), which were shown to account for nearly 90% of phosphatase activity in eukaryotic cells (Moorhead et al., 2007; Virshup and Shenolikar, 2010).

The following paragraphs will briefly discuss the role of PTPs during the initial phase of T cell activation and further review the known PPPs involved in NF-κB signalling in different pathways.

i. The role of phosphatases during T cell activation

The initial steps during T cell activation, leading to the formation of the proximal TCR signalosome, primarily rely on the action of PTKs. Accordingly, most phosphatases involved in these early events belong to the PTP family. About 40 PTPs, are involved in a variety of signalling pathways in T cells. The most important PTPs will be shortly discussed in the following.

The most prominent PTP involved in T cell activation is the transmembrane protein CD45. In resting cells, Lck is kept in an inactive state *via* Csk-mediated mediated phosphorylation of an inhibitory tyrosine residue. Upon T cell activation, CD45 is recruited to the IS and

dephosphorylates the inhibitory site. Although this function as a positive regulator is well established, it was also reported that CD45 could negatively regulate Lck by dephosphorylating the kinase in its activation loop (Hermiston et al., 2003; Maksumova et al., 2005). However, the positive regulatory role seems to dominate since Csk inhibition alone leads to T cell activation (Zikherman et al., 2010). In addition, protein tyrosine phosphatase, non-receptor type 22 (PTPN22) was shown to negatively regulate Lck (Hasegawa et al., 2004). The currently best-understood PTP in lymphocytes is SH2-domain containing phosphatase 1 (SHP1), which mainly acts as a negative regulator of TCR signalling. SHP1 dephosphorylates Lck and ITAM-bound ZAP-70. In addition, SHP1 was reported to dephosphorylate the downstream signalling mediators Vav1 and SLP-76 (Stebbins et al., 2003; Binstadt et al., 1998). In contrast to SHP1, the closely related SHP2 phosphatase positively regulates the Ras-Raf-MEKK-ERK-pathway, through dephosphorylation of an unknown substrate (Frearson and Alexander, 1998). Furthermore, the suppressor of TCR signalling 1 and 2 (Sts1 and 2) phosphatases were shown to negatively regulate proximal TCR signalling events. T cells derived from Sts1- and Sts2 double-deficient knockout mice exhibit hyperphosphorylation of Zap-70, LAT and SLP-76 causing hyperproliferation. Accordingly, double deficient mice have an increased risk of autoimmunity (Carpino et al., 2004; Mikhailik et al., 2007).

ii. The role of protein serine/threonine phosphatases in NF-κB signalling

The best-studied PPP with respect to NF-κB signalling is the serine/threonine phosphatase 2, catalytic subunit A (PP2CA). PP2CA has previously been implicated as a negative regulator of RelA (Yang et al., 2001a; Fu et al., 2003; DiDonato et al., 1997), but these studies lacked evidence for distinct holoenzyme complexes. One study systemically delineated the action of three different PP2CA holoenzymes within the TNFα-induced NF-κB pathway in mouse astrocytes (Li et al., 2006b). First, a holoenzyme consisting of PP2CA and the regulatory subunit PP2R1B was found to associate and dephosphorylate serine 536 in the TAD of RelA, phosphorylation of which is necessary for transcription activation. Second, the authors identified a novel phosphorylation site in the zinc finger domain of TRAF2 (threonine 117), which was shown to be important for NF-κB activation in response to TNFα. Phosphorylation was counteracted by a PP2CA holoenzyme that contains the regulatory subunits PP2R1A and PP2R5C. Accordingly, knock down of either subunit led to a marked increase in NF-κB activity. Third, the authors showed that a PP2CB/PP2R1A holoenzyme was able to interact and dephosphorylate the activation loop serine residues of

Phosphatase	Known holoenzyme composition	Substrate	Activator (+) /Inhibitor (-) of NF-κB	NF-κB-inducing stimulus	Reference
PP1CA	**PP1CA**:**GADD34**: **CUEDC2**	IKKα/β	-	TNFα	Li et al., 2008
PP2CA	PP2CA	RelA (p65) - serine 536	-	TNFα	DiDonato et al., 1997; Yang et al., 2001a; Fu et al., 2003
	PP2CA	MEKK3	-	TNFα	Sun et al., 2010
	PP2CA:**PP2R1B**	RelA (p65) - serine 536	-	TNFα	Li et al., 2006b
	PP2CA:**PP2R1A**: **PP2R5C**	TRAF2 - threonine 117	-	TNFα	Li et al., 2006b
	PP2CA:**PP2R1A**	IKKα/β	-	TNFα	Li et al., 2006b
	PP2CA:**PP2R1A**	CARMA1 - serine 645	-	TCR	Eitelhuber et al., 2011
	PP2CA	NEMO (IKKγ)	+	TNFα	Kray et al., 2005
PP3CA	PP3CA	Bcl-10 - serine 138	+	TCR	Palkowitsch et al., 2011; Frischbutter et al., 2011
PP4C	PP4C	RelA (p65) - threonione 435	not known	-	Yeh et al., 2004
	PP4C:**PP4R1**	IKKα/β	-	TCR	Brechmann and Mock et al., manuscript in preparation
	PP4C	c-Rel	+	-	Hu et al., 1998
PP6C	**PP6C**:**PP6R1**	IκBε	-	-	Stefansson and Brautigan, 2006
WIP1	WIP1	RelA (p65) - serine 536	-	TNFα	Chew et al., 2009
PPM1A/B	PPM1A/B	IKKα/β	-	TNFα	Sun et al., 2009

Table 1.1 Known NF-κB-modulating phosphatases. Known regulatory subunits are highlighted in red.

IKKα and IKKβ (Li et al., 2006b). In addition, PP2CA was more recently reported to dephosphorylate the IKK-K MEKK3, thereby limiting IKK activity (Sun et al., 2010). Indeed, the same authors provided evidence that the metal-ion-dependent phosphatases PPM1A and PPM1B interact with IKKβ and dephosphorylate it in a stimulus-dependent manner upon TNFR engagement (Sun et al., 2009). Interestingly, PP2CA was also implicated to positively regulate NF-κB activity, presumably by removing inhibitory phosphate groups from NEMO (Kray et al., 2005). Another study recently provided evidence that a PP2CA:PP2R1A phosphatase complex is necessary to dephosphorylate a critical serine residue in the linker region of CARMA1 in T cells. Knock down of PP2R1A or chemical inhibition of PP2CA with okadaic acid enhanced CBM complex formation and NF-κB activation (Eitelhuber et al., 2011).

Another study has shown that the PPP PP1c may negatively regulate IKK complex activity. The authors provided evidence that PP1c is recruited to the IKK complex *via* the adaptor protein CUE domain containing 2 (CUEDC2) and the regulatory subunit growth arrest and DNA damage-inducible gene 34 (GADD34). Consistently, knock down of CUEDC2 enhanced IKK activity and IL-6 production in macrophages upon TNFα treatment (Li et al., 2008).

Only few other phosphatases have been linked to the regulation of NF-κB activity. Two publications have implicated a role for the PPP PP6 in regulation of IκBε, but failed to show a functional relevance (Stefansson and Brautigan, 2006; Bouwmeester et al., 2004). A more recent publication has identified the phosphatase WIP1 as a negative regulator of RelA activity (Chew et al., 2009). However, another study, investigating the phenotype of WIP1 knockout mice, reported decreased proliferating capacity of T and B cells, arguing against a general, non-redundant role of WIP1 in regulating NF-κB.

Interestingly, two groups independently reported that the calcium-dependent phosphatase calcineurin (see paragraph 1.2.3) is involved in the positive regulation of NF-κB in T cells by controlling the phosphorylation of an inhibitory serine residue in Bcl-10 (Frischbutter et al., 2011; Palkowitsch et al., 2011).

Recently, we identified a novel NF-κB-regulating PPP phosphatase holoenzyme, containing the catalytic subunit PP4c and the regulatory subunit PP4R1, that regulates IKK complex activity in T cells. We were able to show that PP4R1 acts as an adaptor that directs PP4c phosphatase activity specifically towards the IKK complex in a stimulus-dependent manner. PP4c:PP4R1 is able to dephosphorylate the IKK complex, thereby limiting IKK activity. Notably, this holoenzyme is only functional in expanded T cells, since expression of PP4R1 is absent in resting cells, indicating that the PP4c:PP4R1 holoenzyme is involved in

termination of an immune response. (Brechmann, 2010; Brechmann and Mock et al., manuscript in preparation).

A comprehensive overview of the here discussed NF-κB-modulating phosphatases is given in Table 1.1. Although some of the mentioned studies provide conflicting data concerning redundant roles of different phosphatases in regulating IKK- as well as RelA-activity, these discrepancies may be explained by different experimental setups and redundant roles of different phosphatases in different cell types and signalling contexts.

1.4 Human lymphoid pathologies associated with NF-κB

Given the crucial role of NF-κB, especially in context of an immune response, it is not surprising that deregulation of NF-κB is associated with several lymphoid pathologies. Deregulated NF-κB activity serves mainly pro-oncogenic functions since NF-κB target genes include factors, which promote the hallmarks of cancer, including apoptosis resistance-, migration-, invasion-, and pro-angiogenic factors (Hanahan and Weinberg, 2011). In addition, NF-κB controls the vast majority of pro-inflammatory cytokines, which were shown to favour cancer development under special circumstances (Staudt, 2010; Ben-Neriah and Karin, 2011). Several molecular lesions were identified that drive aberrant NF-κB activity, enabling a malignant cell to evade apoptosis and allow growth independent of paracrine mitogenic factors. In addition, over-activation of NF-κB was associated with increased metastatic capacity, probably through expression of NF-κB-dependent matrix-metalloproteinases (MMPs) (Bond et al., 1998; Levine et al., 2003). This paragraph will focus on the most prominent examples of oncogenic NF-κB activation (for a comprehensive overview see (Lenz and Staudt, 2010; Karin, 2009; Staudt, 2010)).

Several T and B cell malignancies rely on the constitutive activation of NF-κB. The preferential utilisation of the pathway within this cellular compartment may be caused by its crucial role during lymphocyte development and homeostasis (Vallabhapurapu and Karin, 2009). About 90% of human lymphomas arise from the B cell compartment during various stages of B cell development. The most relevant subtype of non-Hodgkin's lymphoma is the diffuse large B cell lymphoma (DLBCL). Recent studies have defined distinct subtypes of DLBCL, according to their gene expression profile and their origin from different stages of B cell development. These include the germinal center-like (GCB) DLBCL, the activated B cell-like (ABC) DLBCL and the primary mediastinal B cell lymphoma (PMBL) (Rosenwald, 2003). Constitutive activation of NF-κB is now considered as a hallmark of the ABC-DLBCL (Lenz and Staudt, 2010; Staudt and Dave, 2005). ABC-DLBCL cells exhibit rapid phosphorylation

and degradation of IκBα and accumulation of RelA:p50 and c-Rel:p50 dimers in the nucleus. Overexpression of an IκBα super-suppressor or treatment with an IKKβ inhibitor sensitize ABC-DLBCL cells towards apoptosis, but have no impact on GCB-DLBCL cells (Davis et al., 2001; Lam et al., 2005). This aberrant NF-κB activation causes increased expression of the transcription factors IRF4 and XBP-1, which normally mediate plasma cell differentiation. Interestingly, accompanying inactivating mutations of the factor Blimp-1, another master regulator that mediates cell cycle arrest in terminally differentiated plasma cells, are frequently observed. As a consequence, malignant cells do not terminally differentiate into plasma cells and escape cell cycle arrest (Shaffer et al., 2009; Staudt, 2010). Another hallmark of the ABC-DLBCL subtype is the NF-κB-dependent expression of IL-6 and IL-10. Both cytokines are secreted in large amounts and signal in an autocrine fashion, inducing STAT3 signalling and thereby favouring cell survival (Yang et al., 2007; Lam et al., 2008). Several mutations within the components of the BCR-driven NF-κB pathway have been identified to cause the constitutive activation of NF-κB in ABC-DLBCL cells. Recently, so-called "*Achilles heel*" RNAi screens, identified several components of the pathway, including CARMA1, A20, CK1α, CD79A and CD79B and MYD88. These were shown to be critical for constitutive NF-κB activation and survival of ABC-DLBCL cells (Davis et al., 2010; Ngo et al., 2011; Staudt, 2010; Bidère et al., 2009; Lenz et al., 2008). Knock down of either of those signalling intermediates sensitized cells towards apoptosis. In fact, several activating and inactivating mutations have now been identified in these proteins. For instance, ~10% of ABC-DLBCL biopsies were shown to contain activating mutations within the coiled-coil domain of CARMA1 (Lenz et al., 2008). These mutated CARMA1 proteins were shown to form signalling-active, cytoplasmic aggregates with several NF-κB pathway components, including Bcl10, MALT1 and the IKK complex. Although the exact mechanism remains elusive, it was proposed that these mutations cause release of CARMA1 from a normally auto-inhibiting conformation, thus allowing its oligomerization with CBM complex components to signalling lattices that activate the IKK complex (Ben-Neriah and Karin, 2011; Staudt, 2010). Nevertheless, these mutations were only found in a small fraction of patients. More recently, somatic mutations in the ITAM containing components of the BCR complex, CD79A (Igα) and CD79B (Igβ), were found in more than 20% of ABC-DLBCL specimens. These mutations mediated increased surface expression of the BCR, leading to auto-clustering and chronic active BCR signalling and, thus, NF-κB activation (Davis et al., 2010). An additional study established a role for the adaptor protein MYD88. MYD88 normally links TLR and IL-1/IL-18 receptor signals to the NF-κB pathways. The authors found recurrent mutations within MYD88 in ABC-DLBCL cell lines as well as in 29% of primary tumor samples. Accordingly, knock down sensitised cells towards apoptosis. In

contrast, overexpression of mutant MYD88 confers survival advantages in NF-κB-independent GCB-DLBCL cell lines. The mutant MYD88 protein promotes survival by spontaneously assembling a complex, containing and activating the kinases IRAK1 and IRAK4, enhanced IL-10, IL-6 and Interferon-β production as well as JAK-STAT signalling. Hence, the found mutations can be considered driver mutations of lymphomagenesis (Ngo et al., 2011). In contrast to these activating mutations, the NF-κB negative regulator A20 was found to be bi-allelicaly inactivated as a frequent pathogenetic event in ABC-DLBCL (Compagno et al., 2009).

Mucosa-associated-lymphoid-tissue (MALT) lymphoma, a form of marginal zone lymphoma, is another tumor entity associated with dysregulated NF-κB activity. Approximately 25% of gastric MALT lymphomas harbor a chromosomal translocation that generates a fusion protein, comprising parts of cIAP2 and MALT1 (Akagi et al., 1999; Dierlamm et al., 1999; Morgan et al., 1999). The cIAP2-MALT1 fusion protein activates NF-κB when overexpressed (Lucas et al., 2001; Uren et al., 2000; Jost and Ruland, 2007). Less frequently, MALT1 and Bcl10 are overexpressed due to a translocation linking them to the immunoglobulin heavy chain locus. At present, the exact mechanism of NF-κB activation through the fusion protein is not known, but it seems to involve the recruitment and activity of TRAF2 *via* the BIR domains of cIAP2 and the MALT1 protease activity. A current model suggests that cIAP2-MALT1 protein oligomerizes, providing a multivalent platform for recruitment of the ubiquitin ligases TRAF2 and TRAF6. The IKK complex gets recruited and subsequently ubiquitinated, possibly helping to retain it in the complex and facilitating its activation by IKK-Ks like TAK1. In addition, cIAP2-MALT1 oligomers might exhibit MALT1 protease activity towards A20, thereby amplifying NF-κB activation (Staudt, 2010).

Multiple myeloma is another prominent example of a neoplastic disorder for which constitutive NF-κB activation has been described, both in cell lines and in patient samples (Ni et al., 2001). In many myeloma cases a diverse array of genetic aberrations target NF-κB regulators. At varying frequencies, multiple myeloma cells harbor gene amplifications or translocations of components of the non-canonical NF-κB pathway, including LTβR, CD40, or NIK as well as deletions or inactivating mutations of components of the canonical NF-κB pathways, including TRAF2, TRAF3 and CYLD. However, all genetic lesions target the activity and/or stabilization of NIK, which leads to activation of non-canonical and canonical NF-κB signalling (Malinin et al., 1997; O'Mahony et al., 2000; Demchenko and Glebov, 2010)

1.4.1 NF-κB and the Sézary syndrome

Cutaneous T cell lymphomas (CTCLs) are a heterogeneous group of skin-associated neoplasms and unlike some B cell lymphomas, CTCLs are rarely curable. Mycosis fungoides (MF) and Sézary syndrome (SS) are the most common variants of CTCL. MF is confined to the skin and is characterised by erythematous patches, plaques, and less frequently, tumors. MF is a slow-progressing disease, defined by indolent clinical behaviour. In contrast, the more aggressive and systemic SS, considered the leukemic subtype of CTCL, is clinically characterised by a triad of generalized erythroderma (defined as affecting <80% of the body surface area), lymphadenopathy and the presence of 5% or more malignant clonal T cells with cerebriform nuclei (known as Sézary cells) (Booken et al., 2008; Diamandidou and Cohen, 1996; Dippel et al., 2003; Klemke et al., 2005; Hwang et al.). Interestingly, malignant MF and Sézary cells exhibit a T_H2 cytokine pattern. Clinical treatment of patients with T_H1 or T_H1-inducing cytokines (IL-12 and IL-2) as well as interferon-α and –β was shown to be beneficial (Kaplan et al., 1990; Rook et al., 1999). SS ultimately results in immunosuppression, due to the clonal expansion of Sézary cells and the collapse of the normal T cell repertoire (Yawalkar et al., 2003). The breakdown of the T cell compartment results in high susceptibility to pathogens that will ultimately result in lethal infections (sepsis). Accordingly, SS patients have an overall low median survival rate of two to four years.

Several publications have established a direct link between aberrant NF-κB activation and the pathogenesis of SS. One report describes a chromosomal rearrangement that results in a truncated version of the NFKB2 gene (encoding p100) in the CTCL cell line Hut78. The truncated p100 protein was shown to be devoid of its C-terminus and to accumulate in the nucleus in the absence of any stimuli (Zhang et al., 1994). These findings were further substantiated by the discovery that p65 in the CTCL cell lines Hut78, MyLa, SeAx and HH exhibited constitutive DNA-binding activity (Izban et al., 2000). DNA binding could be counteracted by chemical inhibition of NF-κB. A more recent study extends this observation to primary Sézary cells and conclusively shows that inhibition of IKKβ is sufficient to drive CTCL cells into apoptosis (Sors et al., 2008;) . Moreover, overexpression of an IκBα super-suppressor led to apoptosis in several CTCL cell lines (Sors et al., 2006), indicating that Sézary cells are oncogenically addicted to constitutive NF-κB activity. A publication from our laboratory uncovered one possible molecular explanation for the selective death response of CTCL cells upon treatment with IKK inhibitors. Targeting of NF-κB with different compounds lead to a marked decrease of ferritin-heavy-chain (FHC) expression (Kiessling et al., 2009). FHC is an iron storage protein whose expression depends on NF-κB.

Downregulation of FHC induced an increase of free intracellular Fe^{2+}-ions, resulting in massive production of reactive oxygen species (ROS) and ROS-dependent cell death *in vitro* and *in vivo*.

Recently we uncovered a role for the PP4c:PP4R1 phosphatase holoenzyme (see paragraph 1.3.6) that controls IKK activity in activated human T cells (Brechmann, 2010; Brechmann and Mock et al., manuscript in preparation). Interestingly, we found PP4R1 expression to be significantly reduced or absent in two CTCL cell lines (Hut78 and HH) as well as in a small cohort of SS patients. Ectopic re-expression of PP4R1 in those deficient cell lines sensitised cells towards apoptosis. Concomitantly, re-expression of PP4R1 suppressed constitutive IKK activity in HH cells. This effect was specific for PP4R1, since control overexpression of PP2CA was not sufficient to induce apoptosis. Therefore, absence of PP4R1 may be one causative factor that drives NF-κB-dependent lymphomagenesis in a subgroup of CTCLs (Brechmann and Mock et al., manuscript in preparation). However, the exact molecular lesions leading to persistent IKK and NF-κB activation in CTCL remain to be uncovered.

Aim of the study

TCR-induced signalling to NF-κB relies on the concerted action of kinases and their phosphorylated substrates, including receptor proximal protein complexes and the NF-κB core components themselves. Hence, phosphorylation events cover every step of NF-κB activation. Although most phosphorylations on target proteins are of transient nature, implying the involvement of phosphatases, the role of phosphatases in NF-κB activation or signal termination has not been thoroughly studied in T lymphocytes to date.

Therefore, a RNAi screening approach, using a NF-κB reporter Jurkat T cell line, was performed to identify NF-κB-modulating phosphatases. Using this approach, we have previously identified and characterised the PP4c:PP4R1 phosphatase holoenzyme. We have shown that PP4c:PP4R1 negatively regulates IKK activity in activated human T cells and that loss of PP4R1 may contribute to survival of a subset of human CTCL cells (Brechmann, 2010; Brechmann and Mock et al., manuscript in preparation). These findings underscored the validity of our screening approach and prompted us to investigate other putative candidate hits, among which PP1α was found as a putative positive regulator of NF-κB. PP1α gained special interest, since it is predominantly expressed in cells of the hematopoietic system, suggesting an important function in this cellular compartment. The present study was therefore conducted to validate PP1α as a positive regulator of NF-κB in T cells with the following objectives: (i) validation of the primary RNAi screen, using different and independent experimental readouts; (ii) biochemical characterisation of the NF-κB pathway in the presence or absence of PP1α; (iii) identification and characterisation of PP1α substrates; (iv) characterisation of the physiological function of PP1α in T cells; (v) evaluation of PP1α as a potential therapeutic target in malignant CTCL cells.

2. Materials

2.1 Chemicals, reagents & consumables

All chemicals and reagents were purchased from Serva (Heidelberg), Fluka (Neu-Ulm), Sigma (München), Roth (Karlsruhe) and Merck (Darmstadt), unless otherwise indicated.

2.1.1 Consumables

Name	Company
96-well plates for qRT-PCR	Applied Biosystems
Amersham HyperfilmTM ECL	GE Healthcare
Amersham™ Hybiond™-N nylon membrane	GE Healthcare
Amersham™ Hybiond™-ECL nitrocellulose membrane	GE Healthcare
Cell culture plates and flasks	TPP/Greiner
Electropuration cuvettes (4 mm)	BioRad
ELISA 96-well plates	costar®
Gaussia-Glow Juice	p.j.k.
Gene RulerTM 1 kb DNA ladder	Fermentas
High Sensitivity" ECL substrate solution: Immobilon Western chemiluminescent HRP substrate	Millipore
LS columns	Miltenyi Biotec
Pipette tips	TipOne
Reaction tubes (1.5, 2 ml)	Eppendorf
Reaction tubes (5, 15, 50 ml)	BectonDickinson/Nunc/TPP
Reaction tubes for PCR	TipOne
Sealing strips	Applied Biosystems

Serological pipettes	Becton Dickinson/Greiner
Sterile filters (0.22 μm, 0.45 μm)	Millipore
Trypan blue	Sigma
Whatman Blotting paper	Biorad/Schleicher & Schuell

2.1.2 Commercial kits and reagents

All kits and reagents were used according to the manufacturers instructions, unless otherwise described.

Name	Company
Cell Line Nucleofector® Kit V	Lonza
Cell Lysis Buffer (10x)	Cell Signalling Technology
CellTiter-Glo® Luminescent Cell Viability Assay	Promega
Dual-Light® System	Applied Biosystems
High Capacity cDNA Reverse Transcription Kit	Applied Biosystems
Human IFNg, IL-2, TNFa ELISA	BD Bioscience
Human IL-8 ELISA	Immunotools
Human T Cell Nucleofector® Kit	Lonza
KOD Hot Star Polymerase Kit	Novagen
Lightshift® Chemiluminescent EMSA Kit	Thermo Scientific
NE-PER Nuclear and Cytoplasmic Extraction Reagents	Thermo Scientific
o-Phenylenediamine dihydrochloride tablets for ELISA	Sigma
PhosSTOP, Phosphatase inhibitor tablet	Roche
Power SYBR® Green PCR Master Mix	Applied Biosystems
Protein A Sepharose beads	Sigma

Protein molecular weight standard	New England Biolabs (NEB
Proteinase Inhibitor Cocktail	Roche
QIAEX II Gel extraction Kit	Qiagen
Qiagen® Plasmid Maxi Kit	Qiagen
Qiagen® Plasmid Mini Kit	Qiagen
QIAquick PCR Purification Kit	Qiagen
RNAqueous®-Micro Kit	Applied Biosystems
Roti®-Quant Bradford assay	Roth
SensoLyte® pNPP Protein Phosphatase Assay	AnaSpec
Signal Boost immunoreaction enhancer kit	Calbiochem (Merck)
Streptavidin-HRP	Jackson ImmunoResearch
Transcriptor High Fidelity cDNA Synthesis Kit	Roche
TRIzol® Reagent	Invitrogen
Western LightningTM Plus-ECL reagent	PerkinElmer

2.1.3 Reagents and kits for T cell isolation

Name	Company
CD4 MicroBeads	Miltenyi Biotec
CD4+ T cell isolation kit II, human	Miltenyi Biotec
CD25 MicroBeads	Miltenyi Biotec
Ficoll	Biochrom

2.1.4 Reagents for treatment of cells

Name	Company
Chloroquine	Sigma
5(6)-Carboxyfluorescein diacetate N-succinimidyl ester (CFSE)	Sigma
Doxycycline	Sigma
Ionomycin	Sigma
Phorbol 12-myristate 13-acetate (PMA)	Sigma
Phytohemagglutinin (PHA)	Sigma
Polybrene	Millipore
Recombinant IL-2	Cell line LBRM-33 5A4; (Gillis et al., 1980)
Recombinant TNFα	BASF
Tautomycetin	Tocris Bioscience

2.2 Buffers and solutions

Buffers and solutions were prepared in sterile double distilled water (ddH_2O). Lysis buffer for lysis of eukaryotic cells were freshly supplemented with Proteinase Inhibitor Cocktail Tablets (Roche) with 1 tablet per 50 ml and 1 tablet of PhosSTOP phosphatase inhibitor cocktail (Roche) per 15 ml of 1x lysis buffer.

Name	Composition
ACK buffer (10x)	41.45 g NH4Cl 5.0 g KHCO3 0.186 g EDTA pH 7.27 ad 500 ml ddH2O

Cell Lysis Buffer (10x)	20 mM Tris-HCl (pH 7.5) 150 mM NaCl 1 mM Na2EDTA 1 mM EGTA 1% Triton X100 2.5 mM sodium pyrophosphate 1 mM β-glycerophosphate 1 mM Na3VO4 1 µg/ml leupeptin
Citrate buffer (ELISA)	6.9 g Citric acid 20.95 g Sodium citrate dihydrate pH 5.0 ad 1 l ddH2O
Coating Buffer (ELISA)	8.4 g NaHCO3 3.56 g Na2CO3 pH 9.6 ad 1 l ddH2O
DNA sample buffer()6x)	30 % (v/v) glycerine 0.36 % (w/v) bromophenol blue (BPB)
FACS Buffer	5% FCS 0.1% NaN3 in PBS
HBS (10x)	1.4 M NaCl 100 mM KCl 500 mM HEPES 20 mM Na2HPO4 22.2 mM Glucose pH 6.5
KCM buffer (5x)	500 mM KCl 150 mM CaCl2 250 mM MgCl2
Kinase buffer	50 mM Tris/HCl pH 8.0 5 mM MgCl2 2 mM MnCl2 0.5 mM DTT
MACS buffer	0.5% BSA 2 mM EDTA in PBS
Nicoletti lysis buffer	0.1% (w/v) sodium citrate pH 7.4 0.1% (v/v) Triton X-100 50 µg/ml propidium iodide
PBS	137 mM NaCl 8.1 mM Na2HPO4 2.7 mM KCl 1.5 mM KH2PO4 pH 7.4

PBS-T	PBS 0.05% (v/v) Tween
Reducing sample buffer (2x)	4% SDS (w/v) 10% 2-mercaptoethanol 20% glycerol 0,004% bromphenol blue 100 mM Tris-HCl
Reducing sample buffer (5x)	10% SDS (w/v) 25% 2-mercaptoethanol 50% glycerol 0.01% bromphenol blue 250 mM Tris-HCl
RIPA buffer	120 mM NaCl 50 mM Tris/HCl pH 7.5 0.5% (w/v) Desoxycholate 1 mM Dithiothreitol
SDS PAGE runnung bufer	25 mM Tris 0.19 M Glycin 1% (w/v) SDS
SDS seperating gel buffer	37.5 mM Tris-HCl pH = 8.8 8-12% (w/v) Acrylamid/Bisacrylamid 37,5:1 0.1% (w/v) SDS 0.03% (w/v) Ammonium persulfate (APS) 0.1% (w/v) Tetramethylethylendiamin (TEMED)
SDS stacking gel buffer	24 mM Tris-HCl pH 6,8 5 % (w/v) Acrylamid/Bisacrylamid 37,5:1 0.1% (w/v) SDS 0.1% (w/v) APS 0.1% (w/v) TEMED
Stripping buffer	15 g glycine 1g SDS 10ml Tween20 pH 2,2 ad 1 l ddH2O
TAE buffer (1x)	40 mM Tris/HCl 20 mM Acetic acid 1 mM EDTA pH 8.3
TBE buffer (10x)	890 mM Tris base 890 mM Boric acid 20mM EDTA pH 8.0
TBS	20 mM Tris/Cl pH 7.2 150 mM NaCl
TBS-T	1x TBS 0,1% (w/v) Tween-20

Transfer buffer (wet blot transfer)	25 mM Tris 192 mM Glycine 20% (v/v) Methanol
TSB solution	10 mM MgCl2 10 mM MgSO4 5% (v/v) DMSO 10% (v/v) PEG 6000 in LB medium

2.3 Culture Reagents

Unless otherwise indicated, all media for culture of eukaryotic cells were supplemented with 10% heat-inactivated FCS (v/v) and 1% (v/v) penicillin/streptomycin. For selection of stably transduced Jurkat, Hut78 or HH cells, respective media were supplemented with 1 µg/ml puromycin. All media were stored at 4°C and prewarmed to 37°C before use:

2.3.1 Reagents for bacterial culture

Media for *E. coli* were autoclaved and stored at 4°C. Autoclavation of liquids was carried out at 125°C for 30 min. To ensure plasmid propagation LB medium and LB agar plates were supplemented with 50-100 µg/ml ampicillin or 30 µg /ml kanamycin.

Medium	Constituents
Luria Broth (LB) Medium	10g tryptone
	5 g yeast extract
	10 g NaCl
	pH 7.0
	ad 1 l ddH2O
LB Agar	20g Agar in 1 l LB Medium

2.3.2 Reagents for eukaryotic cell culture

Culture media

Name	Company
Dulbecco's Modified Eagle Medium (DMEM)	Sigma
Iscove's Modified Eagle Medium (IMDM)	Gibco
Roswell Park Memorial Institute (RPMI) 1640 medium	Sigma
X-Vivo 15 Medium	Lonza

Cell culture supplements

Reagent	Company
Fetal Calf Serum (FCS)	Biochrom/Gibco
Penicillin/Streptomycin	Sigma
Puromycin	Sigma
Trypsin/EDTA	Sigma/Gibco

2.4 Biological material

2.4.1 Bacteria

For plasmid propagation the *E. coli* strain DH5α was utilised.

Name	Company
DH5α	Invitrogen

2.4.2 Eukaryotic cell lines

Name	Description
Gluc-J16	Reporter T cell line derived from J16-145 with stable genomic integration of a NF-kB-dependent Gaussia luciferase. cassette (Brechmann and Mock et al., 2011)
HEK293T (CRL-11268)	Human embryonic kidney cell line (Pear et al., 1993).
HEK293FT	subclone of HEK293T.
HH (CRL-2105)	Human CTCL derived from a patient with Sézary syndrome (Starkebaum et al., 1991)
Hut78 (TIB-161)	Human CTCL cell line derived from a patient with Sézary syndrome (Gootenberg et al., 1981).
JE6.1 (TB-152)	Human lymphoblastoid cell line derived from acute T cell leukemia cell line (Schneider et al., 1977).
J16-145	Subclone of the human lymphoblastoid cell line J16.
JE6.1 shContr.	Jurkat T cell line stably transduced with a Doxycycline-inducible non-targeting shRNA expression cassette.
JE6.1 shPP1α #47	Jurkat T cell line stably transduced with a Doxycycline-inducible PP1α-targeting shRNA expression cassette.
JE6.1 shPP1α #34	Jurkat T cell line stably transduced with a Doxycycline-inducible PP1α-targeting shRNA expression cassette.
JE6.1 shPP1α #50	Jurkat T cell line stably transduced with a Doxycycline-inducible PP1α-targeting shRNA expression cassette.

2.5 Materials for molecular biology

2.5.1 qRT-PCR primers

Primers for SYBR Green qRT-PCR were designed using the online primer designing tool Primer-BLAST (http://www.ncbi.nlm.nih.gov/tools/primer-blast/). In General all primers were designed to span exon-exon junctions with primer efficiencies between at least 1.7 and 2.0. All primers for qRT-PCR were synthesized by MWG Biotech or Sigma.

Gene	Primer	Sequence (5' -> 3')
A20	forward	TGCGGCACCCTTGGAAGCAC
	reverse	TGCGCTGGCTCGATCTCAGTT
CD25	forward	CACTCGGAACACAACGAAACA
	reverse	TGTGGCTTCATTTTCCCATG
CD69	forward	GCTCTTTGCATCCGGAGAGTGGA
	reverse	ACAGCACACAGGACAGGAACTTGG
HPRT1	forward	TGACACTGGCAAAACAATGCA
	reverse	GGTCCTTTTCACCAGCAAGCT
IL-2	forward	AAGTTTTACATGCCCAAGAAGG
	reverse	AAGTGAAAGTTTTTGCTTTGAGCTA
IL-8	forward	GAATGGGTTTGCTAGAATGTGATA
	reverse	CAGACTAGGGTTGCCAGATTTAAC
IFNG	forward	TTCAGCTCTGCATCGTTTTGG
	reverse	TCCGCTACATCTGAATGACCTG
NFKBIA	forward	CGCCCAAGCACCCGGATACA
	reverse	AGGGCAGCTCGTCCTCTGTGA
PP1CA	forward	TGGCCAAGTTCCTCCACAA
	reverse	GCCGCTTGGCAAAGAACTC
RelA	forward	CGGGATGGCTTCTATGAGG
	reverse	CTCCAGGTCCCGCTTCTT

2.5.2 PCR primers for gene cloning

For cloning of HA-tagged human PP1CA as well as FLAG-tagged PP1CA, the primers listed below were used. Amplicons were BamHI/NotI-digested and ligated into derivatives of the pEF4 expression vector (Invitrogen) containing 5'-HA or 5'-FLAG-epitope tags (pEF4:HA/pEF4:FLAG) (see 2.5.7). PCR primers were synthesized by MWG Biotech or Sigma.

Primer	Sequence (5' -> 3')	Target vector
PP1CA_BamHI forward	CGCGGATCCGCGGGCTCCGACAGCGAGAAGCTCAA	pEF4:HA / pEF4:Flag
PPP1CA_NotI reverse	ATAGTTTAGCGGCCGCCTATTTCTTGGCTTTGGCGGAA TTG	pEF4:HA / pEF4:Flag

2.5.3 DNA oligonucleotides for electromobility shift assay

Electromobility shift assays (EMSAs) were performed using the following DNA oligonucleotides, which were biotinylated at their 5' – ends. To retrieve double stranded DNA, sense and antisense DNA oligonucleotides were mixed in equal amounts and incubated for 5 minutes at 95°C in a heat block. After incubation, the heat block was turned off and the oligonucleotide mixture was cooled down to room temperature. DNA oligos were purchased from Sigma. Biotinylation of 5'-ends was performed by Sigma.

Binding transcription factor	strand	Sequence (5' -> 3')
NF-κB	sense	GGATCCTCAACAGAGGGGACTTTCCGAGGCCA
	antisense	TGGCCTCGGAAAGTCCCCTCTGTTGAGGATCC
NF-Y	sense	TTTTCTGATTGGTTAAAA
	antisense	TTTTAACCAATCAGAAA

2.5.4 siRNA for gene transcript silencing

siRNAs were dissolved in RNase-free H_2O with a final concentration of 20 µM and 10 µl aliquots were stored at -80°C until use.

siRNA	targeted gene	Sequqnece (5' -> 3')	Company
siContr.	non-targeting	UUCUCCGAACGUGUCACGUTT	Qiagen
siCYLD	CYLD	GAUUGUUACUUCUAUCAAATT	Applied Biosystems
siCARMA1#1	CARMA1	ACUCGAGAUCGAUCAGCUATT	Qiagen
siPP1CA #1	PPP1CA	CAUCUAUGGUUUCUACGAUTT	Applied Biosystems
siPP1CA #2	PPP1CA	CGAGAGCAACUACCUCUUUTT	Applied Biosystems
siPP1CA #3	PPP1CA	CGACCUUCUGCGACUAUUUTT	Applied Biosystems
siRelA	RelA	CCAUCAACUAUGAUGAGUUTT	Applied Biosystems

2.5.5 shRNAs for gene transcript silencing

All shRNA sequence clones targeting PP1CA were obtained as glycerol stocks from Open Biosystems. As a negative control a non-targeting shRNA control vector was used. All shRNA sequence clones were used from pGIPZ shRNAmir lentiviral vectors. shRNA cassettes were cloned into the pTRIPZ inducible shRNAmir vector from Open Biosystems according to the manufacturers instructions.

Clone ID	target gene	shRNA sequence (5' -> 3')
V2LHS_262414 (#14)	**PP1CA**	TGCTGTTGACAGTGAGCGACGCATCTATGGTTTCTACGATTAGTGAAGCCA CAGATGTAATCGTAGAAACCATAGATGCGGTGCCTACTGCCTCGGA
V3LHS_635636 (#36)	**PP1CA**	TGCTGTTGACAGTGAGCGATACGACCTTCTGCGACTATTTTAGTGAAGCCA CAGATGTAAAATAGTCGCAGAAGGTCGTAGTGCCTACTGCCTCGGA

V3LHS_635635 (#35)	**PP1CA**	TGCTGTTGACAGTGAGCGACAGCGAGAAGCTCAACCTGGATAGTGAAGCCACAGATGTATCCAGGTTGAGCTTCTCGCTGTTGCCTACTGCCTCGGA
V3LHS_635634 (#34)	**PP1CA**	TGCTGTTGACAGTGAGCGACGCGGCCATAGTGGACGAAAATAGTGAAGCCACAGATGTATTTTCGTCCACTATGGCCGCGATGCCTACTGCCTCGGA
V3LHS_635633 (#33)	**PP1CA**	TGCTGTTGACAGTGAGCGACGGCTACGAGTTCTTTGCCAATAGTGAAGCCACAGATGTATTGGCAAAGAACTCGTAGCCGTTGCCTACTGCCTCGGA
V3LHS_318050 (#50)	**PP1CA**	TGCTGTTGACAGTGAGCGACTCAAGATCTGCGGTGACATATAGTGAAGCCACAGATGTATATGTCACCGCAGATCTTGAGGTGCCTACTGCCTCGGA
V3LHS_318046 (#46)	**PP1CA**	TGCTGTTGACAGTGAGCGCCGGCTACGAGTTCTTTGCCAATAGTGAAGCCACAGATGTATTGGCAAAGAACTCGTAGCCGTTGCCTACTGCCTCGGA
V3LHS_318047 (#47)	**PP1CA**	TGCTGTTGACAGTGAGCGCCGCGGCCATAGTGGACGAAAATAGTGAAGCCACAGATGTATTTTCGTCCACTATGGCCGCGATGCCTACTGCCTCGGA
V3LHS_318051 (#51)	**PP1CA**	TGCTGTTGACAGTGAGCGCCCAGGTGGTAGAAGACGGCTATAGTGAAGCCACAGATGTATAGCCGTCTTCTACCACCTGGTTGCCTACTGCCTCGGA
	non-targeting	*not available*

2.5.6 Enzymes

All restriction endonucleases were purchased from Fermentas or New England Biolabs (NEB). KOD DNA polymerase was purchased from Novagen®. T4 DNA ligase as well as calf intestinal phosphatase (CIP) were obtained from Fermentas. All enzymes were used according to the manufacturer's instructions.

2.5.7 Vectors

Vector	Description	Origin/Reference
pEF4:HA	Derivative of the pEF4 eukaryotic expression vector with a 5' single HA tag	Invitrogen/ J. Hoffmann, DKFZ
pEF4:HA-PP1CA	pEF4:HA derivative encoding for HA-tagged human PP1CA full-length protein	This study
pEF4:Flag	Derivative of the pEF4 eukaryotic expression vector with a 5' single FLAG tag	Invitrogen/ J. Hoffmann, DKFZ
pEF4:Flag-PP1CA	pEF4:Flag derivative encoding for Flag-tagged human PP1CA full-length protein	This study
8xNF-κB-pGluc	pGluc basic derivative with a Gaussia reporter cassette under control of the mouse c-fos promoter and eight kB sites	Brechmann, 2010 / Arnold et al., 2001
8xNF-κB-pGL	pGL derivative with a firefly reporter cassette under control of the mouse c-fos promoter and eight kB sites	Arnold et al., 2001
pfosLacZ	pSDK derivative encoding for b-galactosidase under control of the mouse c-fos promoter	Arnold et al., 2001
pTRIPZ inducible shRNAmir (empty vector)	Lentiviral inducible shRNAmir expression vector	Open Biosystems

pTRIPZ shPP1CA #14	Derivative of pTRIPZ inducible shRNAmir with shRNA cassette targeting PP1CA retrieved from pGIPZ vector (Clone ID: V2LHS_262414)	Open Biosystems / This study
pTRIPZ shPP1CA #36	Derivative of pTRIPZ inducible shRNAmir with shRNA cassette targeting PP1CA retrieved from pGIPZ vector (Clone ID: V3LHS_635636)	Open Biosystems / This study
pTRIPZshPP1CA #35	Derivative of pTRIPZ inducible shRNAmir with shRNA cassette targeting PP1CA retrieved from pGIPZ vector (Clone ID: V3LHS_635635)	Open Biosystems / This study
pTRIPZ shPP1CA #34	Derivative of pTRIPZ inducible shRNAmir with shRNA cassette targeting PP1CA retrieved from pGIPZ vector (Clone ID: V3LHS_635634)	Open Biosystems / This study
pTRIPZ shPP1CA #33	Derivative of pTRIPZ inducible shRNAmir with shRNA cassette targeting PP1CA retrieved from pGIPZ vector (Clone ID: V3LHS_635633)	Open Biosystems / This study
pTRIPZ shPP1CA #50	Derivative of pTRIPZ inducible shRNAmir with shRNA cassette targeting PP1CA retrieved from pGIPZ vector (Clone ID: V3LHS_318050)	Open Biosystems / This study
pTRIPZ shPP1CA #46	Derivative of pTRIPZ inducible shRNAmir with shRNA cassette targeting PP1CA retrieved from pGIPZ vector (Clone ID: V3LHS_318046)	Open Biosystems / This study
pTRIPZ shPP1CA #47	Derivative of pTRIPZ inducible shRNAmir with shRNA cassette targeting PP1CA retrieved from pGIPZ vector (Clone ID: V3LHS_318047)	Open Biosystems / This study
pTRIPZ shPP1CA #51	Derivative of pTRIPZ inducible shRNAmir with shRNA cassette targeting PP1CA retrieved from pGIPZ vector (Clone ID: V3LHS_318051)	Open Biosystems / This study

2.6 Antibodies

2.6.1 Antibodies for immunoblot analysis

Primary antibodies for immunoblot analysis were diluted, as indicated in the table, in TBS-T, containing 5% BSA and 0,02% NaN_3. Secondary, horseradish peroxidase (HRP)-conjugated, antibodies were diluted 1:10000 in TBS-T, containing 1% non-fat, dry milk.

Alternatively, for detection of phospho-proteins, secondary antibodies were diluted 1:10000 in Signal Boost enhancer solution for secondary antibodies (Calbiochem).

(i) primary antibodies for immune-blotting (IB) and immune-precipitation (IP)

Name	Species and Isotype	Antigen	Dilution	Company
Anti-β-Actin	Rabbit, polyclonal	**β-actin**	1:8000 (IB)	Sigma
Anti-cRel	Rabbit, polyclonal	**c-Rel**	1:1000 (IB)	SCBT
Anti-ERK1 (MK12)	Mouse, IgG1	**Erk1**	1:1000 (IB)	BD Bioscience
Anti-FLAG (M2)	Mouse, IgG1	**Flag epitope**	1:1000 (IB), 2 µl (IP)	Sigma
Anti-HA (12CA5)	Mouse, IgG2b	**HA epitope**	100 µl hybridoma supernatant (IP)	selfmade
Anti-HA (3F10)	Rat, polyclonal	**HA epitope**	1:1000 (IB)	Roche
Anti-IkBα	Mouse, IgG1	**β-actin**	1:1000 (IB)	CST
Anti-IkBβ	Mouse, IgG2a	**IkBβ**	1:1000 (IB)	SCBT
Anti-IkBε	Rabbit, polyclonal	**IkBε**	1:1000 (IB)	CST
Anti-IKKα	Rabbit, polyclonal	**IKKα**	1:1000 (IB)	CST
Anti-IKKβ (10A9B6)	Mouse, IgG1	**IKKβ**	1:500 (IB)	Imgenex
Anti-IKKγ (FL-419)	Rabbit, polyclonal	**IKKγ**	1:1000 (IB), 5 µl (IP)	SCBT
Anti-p-ERK1/2	Mouse, IgG2a	**phospho-Erk1 (T202/Y204) and phospho-Erk2 (T180/Y182)**	1:2000 (IB)	SCBT
Anti-p-IkBα (5A5)	Mouse, IgG1	**phospho-IkBα (S32/S36)**	1:1000 (IB)	CST

Anti-p-IKKα/β (S180/S181)	Rabbit, polyclonal	**phospho-IKKα (S180) and phospho-IKKβ (S181)**	1:1000 (IB)	CST
Anti-p-IKKα/β (S176/S177)	Rabbit, polyclonal	**phospho-IKKα (S176) and phospho-IKKβ (S177)**	1:1000 (IB)	CST
Anti-p-P65 (s536)	Rabbit, polyclonal	**phospho-P65 (S536)**	1:1000 (IB)	CST
Anti-p-P38 (T180/Y182)	Rabbit, polyclonal	**phospho-P38 (T180/Y182)**	1:2000 (IB)	CST
Anti-PP1α	Mouse, IgG1	**PP1α**	1:2000 (IB)	Invitrogen
Anti-p105/p50	Goat, polyclonal	**p105/p50**	1:1000 (IB)	CST
Anti-p38	Rabbit, polyclonal	**p38**	1:1000 (IB)	CST
Anti-p65	Rabbit, polyclonal	**p65**	1:1000 (IB)	CST
Anti-Tubulin (B-5-1-2)	Mouse, IgG1	**Tubulin**	1:10000 (IB)	Sigma

(ii) secondary HRP-conjugated antibodies for immune-blot analysis

Name	Species and Isotype	Antigen	Dilution	Company
Anti-IgG1-HRP	Goat, polyclonal	**Mouse-IgG1**	1:10000 (IB)	SCBT
Anti-IgG2a-HRP	Goat, polyclonal	**Mouse-IgG2a**	1:10000 (IB)	SCBT
Anti-IgG2b-HRP	Goat, polyclonal	**Mouse-IgG2b**	1:10000 (IB)	SCBT
Anti-Goat-IgG-HRP	Sheep polyclonal	**Goat-IgG**	1:10000 (IB)	SCBT
Anti-Rabbit-IgG-HRP	Goat, polyclonal	**Rabbit-IgG**	1:10000 (IB)	SCBT
Anti-Rat-IgG	Goat, polyclonal	**Rat-IgG**	1:10000 (IB)	SCBT

2.6.2 Antibodies for T cell stimulation

Name	Species and Isotype	Antigen	Company
Anti-CD3 (OKT3)	Mouse-IgG2a	**CD3**	SCBT
Anti-CD28 (CD28.2)	Mouse-IgG1	**CD28**	Beckton Dickinson
Anti-Mouse	goat-polyclonal	**Mouse-IgG**	Southern Biotechnology

2.7 Instruments

Instrument	Company
ABI 7500 Standard qPCR	Applied Biosystems
Agarose gel electrophoresis apparatus	GIBCO BRL
Analytical and precision balances	Mettler
Bacteria culture incubator/shaker CH-403	Infors AG
Centrifuges **- Biofuge Fresco 17** **- Biofuge A** **- Megafuge 3.0R** **Sorvall Evolution RC**	Heraeus
Chemiluminesence detector Chemi-Smart 5100	Vilber Lourmat
CO2-cell culture incubator Stericult	Forma Scientific
Developing system for Roentgen films Curix 160	Agfa-Gevaert
Electrophoresis power suply PS500	Renner
Electroporation System Gene Pulser II	Bio-Rad
FACS Canto II	Beckton Dickinson
Freezer **- -20°C** **- -80°C**	Liebherr Forma Scientific
Gel documentation system	Bio-Rad

GeneAmp PCR-System 9700	Applied Biosystems
Laminar chambers	Baker Company
Orion L Microplate Luminometer	Berthold Detection Systems
Microplate reader 680	Bio-Rad
Microscopes: **- Fluorescence microscope Labovert FS** **- Light microscope ID 02**	Leica Zeiss
Microwave oven HMG 730G	Bosch
Mini-PROTEAN Tetra Electrophoresis System	Bio-Rad
Mini Trans-Blot Cell	Bio-Rad
Neubauer counting chamber	Brand
NanoDrop ND-1000	Peqlab
pH-meter Calimatic	LHD Labortechnik
Spectrophotometer BioPhotometer	Eppendorf
Thermocycler DNA Engine DYAD	MJ Research
Thermal Cycler C1000	Bio-Rad
Thermostated hot block 5320	Eppendorf
Waterbaths	Köttermann

2.8 Software

Instrument	Company
7500 Software (Version 2.0.1)	Applied Biosystems
4Peaks (Version 1.7)	Mekentosj

Bio-1D	Vilber Lourmat
Chemi-Capt	Vilber Lourmat
EnzymeX 3	Mekentosj
FACSDIVA	Beckton Dickinson
Microsoft office:mac 2008 (Version 12.3.1)	Microsoft
Microsoft office:mac 2011 (Version 14.1.3)	Microsoft
Papers2 (Version 2.0.9)	Mekentosj
Photoshop CS4 Extended (Version 11.0)	Adobe
Simplicity 4.10	Berthold Detection Systems
Mac OS X 10.6.8	Apple Inc.
7500 Software (Version 2.0.1)	Applied Biosystems

3. Methods

3.1 Methods in Molecular Biology

3.1.1 Cultivation and storage of bacteria

Bacteria were cultured under aerobic conditions at 37°C in a rotary shaker at 180 rpm. For propagation of plasmids, LB media were supplemented with ampicillin (100 µg/ml), kanamycin (30 µg/ml) or zeocin (25 µg/ml) and inoculated with cells of a single colony of transformed bacteria. For long term bacteria strain storage, 1 ml freshly saturated bacterial culture was pelleted at 3000 g for 5 minutes. The supernatant was discarded and the bacterial pellet was resuspended in 1⁄4 volume of LB. Then 1⁄4 volume of 100% glycerol was added and the cell suspension mixed. Bacteria were stored at -80°C

3.1.2 Generation of KCM-competent bacteria

For the generation of transformation competent *E. coli* cells, 100 ml LB medium without antibiotics were inoculated with 1 ml overnight culture of *E. coli*. The culture was grown until an OD_{600} value of 0.5-0.6 was reached. The bacterial suspension was incubated on ice for 10 minutes and then harvested at 1,500 g and 4°C for 15 minutes. The supernatant was removed and the bacterial pellet was resuspended in 7.5 ml TSB solution. After incubation on ice for 1 h the bacteria were shock-frozen with liquid nitrogen, and aliquots of 100 µl were stored at -80 °C until use.

3.1.3 Transformation of KCM-competent bacteria

100 µl aliquots of KCM-competent bacteria were thawed on ice. Subsequently 100 µl of 1x KCM, containing a suitable amount of plasmid DNA (100 – 500 ng) or 20 µl of a ligation sample were added to the bacterial suspension. The transformation sample was incubated on ice for 20 minutes, followed by 10 minutes of incubation at room temperature (RT). For

regeneration, 800 µl of pre-warmed LB medium without antibiotics was added and cells were incubated at 37°C for 45 minutes in a rotary shaker. After regeneration, bacteria were centrifuged at 2000 g for 2 minutes. The supernatant was discarded and the bacterial pellet was resuspended in 200 µl of LB Medium. The suspension was spread onto LB-Agar plates, containing appropriate antibiotics and were incubated at 37°C overnight.

3.1.4 Plasmid preparation on analytical scale (miniprep)

For analytical plasmid isolation 5 ml of LB medium, supplemented with an appropriate antibiotic, were inoculated with a single bacterial colony and the culture was grown at 37°C in a shaker overnight. The next day the plasmid DNA was isolated using the Qiagen® Plasmid Mini Kit according to the manufacturer's instructions.

3.1.5 Plasmid preparation on preparative scale (maxiprep)

For the production of larger amounts of plasmid DNA, 100-250 ml of LB medium, containing appropriate antibiotics, were inoculated and the cultures were grown at 37°C in a shaker overnight. The preparation of plasmid DNA was carried out with the Qiagen® Plasmid Maxi Kit according to the manufacturer's instructions.

3.1.6 Photometric determination of DNA concentrations

DNA concentrations were determined using a Biophotometer (Eppendorf) or a NanoDrop ND-1000. DNA concentrations can be approximately calculated by the following formula: OD_{260} = 1 refers to 50 µg/ml DNA (layer thickness of the cuvette: 1 cm). The ratio OD_{260}/OD_{280} characterises the purity of DNA with values between 1.7 and 2.0 for pure DNA.

3.1.7 Isolation of total cellular RNA

For the isolation of total cellular RNA from small amount of cells (1 to $5x10^5$ cells), the RNAqueous®-*Micro Kit* (Applied Biosystems) was used according to he manufacturer's protocol. For isolation of total cellular RNA from larger amounts of cells (0.1 to $1x10^7$ cells) phenol-chloroform extraction was performed using TRIZOL© reagent. Cells were centrifuged at 2000 rpm for 5 minutes. Afterwards, the supernatant was discarded and up to $1x10^7$ cells were lysed with 750 µl of TRIZOL reagent at RT for 5 minutes. Subsequently 150 µl of

chloroform was added and the mixture was inverted for 15 seconds, followed by a 2 minutes incubation at room temperature. For phase separation, the TRIZOL/chloroform mixture was centrifuged at 12000 g for 15 minutes. The mixture separates into a lower red phenol-chloroform phase, an interphase and a colourless upper aqueous phase. The RNA remains exclusively in the upper phase. The aqueous phase was transferred into a fresh Eppendorf tube and mixed with an equal amount of 100% isopropanol, followed by 10 minutes incubation at RT. Subsequently, the mixture was centrifuged at 12000 g for 10 minutes to precipitate the RNA. After centrifugation, the supernatant was discarded and the RNA pellet was washed with 75% ethanol. After washing, the RNA pellet was air-dryed and subsequently resuspended in DEPC-treated water. RNA concentrations were photometrically determined using Nanodrop ND-1000. RNA was stored at -80°C.

3.1.8 Reverse transcription of RNA into cDNA

To produce cDNA from total RNA, the High Capacity Reverse Transcription Kit (Applied Biosystems) was used according to the manufacturer's protocol. For one reverse transcription reaction , 2 µg total RNA were used. One reaction mix contained the following components:

Components	volume / amount
10x RT Buffer	2.0 µl
25x dNTP (100mM)	0.8 µl
10x RT Random Primers	2.0 µl
Reverse Transcriptase	1.0 µl
Rnase Inhibitor	1.0 µl
Nuclease free H2O	3.2 µl
total cellular RNA	2.0 µg/10 µl
Nuclease free H2O	x µl
total	20 µl

Reverse transcription reactions were performed using the conditions below. Synthesized cDNA was diluted 1:20 in sterile ddH_2O and stored at –20°C. cDNA was used for quantification of gene expression by SYBR-based qRT-PCR.

Step	Time; Temperature	
Annelaing	25°C	10 min
Elongation	37°C	120 min
Denaturation	85°C	5 min

For cloning of individual genes, total RNA was extracted from Jurkat T cells and reverse transcribed using the Transcriptor High Fidelity cDNA Synthesis Kit (Roche). The recombinant Transcriptor High Fidelity Transcriptase possesses enhanced proof-reading capability for high accuracy of reverse transcription of RNA. 2 µg of total RNA in a volume of 10 µl were mixed with 1 µl anchored oligo$(dT)_{18}$ primers (50 pmol/µl) and filled up with 0.4 µl ddH_2O. To denature the template-primer mixture, samples were heated for 10 minutes at 65°C. Subsequently samples were stored on ice and the following components were added to a final volume of 20 µl.

Components	volume
Transcriptor High Fidelity Reverse Transcriptase, 5x Reaction Buffer	4.0 µl
Protector RNase Inhibitor	0.5 µl
dNTP mix /10mM)	2.0 µl
DTT (100mM)	1.0 µl
Transcriptor High Fidelity Transcriptase (10U)	1.1 µl
Template-primer mix	11.4 µl
total	20 µl

All reagents were mixed and reverse transcription was performed under the following conditions

Step	Temperature; Time	
Elongation	50°C	30 min
Denaturation	85°C	5 min

3.1.9 Polymerase chain reaction (PCR)

The polymerase chain reaction (PCR) enables amplification of DNA fragments *in vitro* (Mullis et al., 1986). Short oligonucleotide fragments which anneal to the complementary strands of the DNA template in an inverse orientation determine the ends of the amplified DNA fragment. In the presence of dNTPs thermo stable DNA polymerases extend these forward- and reverse-primers along the denatured single stranded DNA generating a complementary DNA strand.

Cloning and mutagenesis of tagged human PP1α was performed, using the KOD Hot Start Polymerase Kit (Novagen). KOD Hot Start DNA Polymerase is a pre-mixed complex of the high fidelity KOD DNA Polymerase and two monoclonal antibodies that inhibit the DNA polymerase at ambient temperatures (Mizuguchi et al., 1999). The KOD DNA polymerase possess a 3'→5' proofreading capacity, which replaces mismatched 3'- terminal nucleotides from primer-template complexes. Primers were designed with 40% to 60% GC content, no internal secondary structure and complementarities at the 3'-end. PCR reactions were prepared on ice. PCR was performed according to the manufacturer's recommendations under the following conditions.

Component	Volume/Amount	Final concentration
KOD buffer (10x)	5.0 µl	1x
25 mM MgSO4	3.0 µl	1.5 mM
dNTPs (2mM)	5.0 µl	0.2 µM (each)
KOD Hot Start NA Polymerase (1 U/ml)	1.0 µl	0.02 U/µl
Forward primer (100 µM)	0.25 µl	0.75 µM
Reverse primer (100 µM)	0.25 µl	0.75 µM
ddH_2O	34.5 µl	x µl
Template DNA	1 µl (30-50 ng)	30-50 ng/50µl
total volume	20 µl	

The following cycle conditions were applied.

Step	Temperature; Time		Cycles
Polymerase activation	95°C	2 min	1
Denaturation	95°C	20 s	35
Annealing	Lowest primer Tm °C	10 s	
Elongation	70°C	20s/kb	
Storage	4°C	∞	

3.1.10 Quantitative Real Time-PCR (qRT-PCR)

Quantitative real-time PCR (qRT-PCT) relies on the quantification of incorporated fluorescent DNA-intercalating reporter dyes, like SYBR Green, which can be detected by a CCD camera during conventional PCR. Thereby DNA amplification products are already detected during synthesis, allowing relative and absolute quantification of transcripts without the danger of measuring saturated signals, which often limits analysis of semi-quantitative RT-PCR. Incorporation of SYBR Green was detected using the ABI Prism 7500 standard (Software: 7500 2.0.3) qRT-PCR cycler, which allows for measurements in a 96-well format. Master mixes for triplicate measurements were prepared according to the following table.

Component	Volume
Template cDNA	1 µl
Forward primer (5 µM)	5.1 µl
Reverse primer (5 µM)	5.1 µl
Power SYBR© Green Master Mix (2x)	42.5 µl
ddH_2O	30.3 µl
total volume	85 µl

Reactions were carried out in triplicates with a final volume of 25 µl per reaction in a 96 well plate. The Power SYBR® Green PCR Master Mix contains 300 µl 110x SYBR Green buffer, 360 µl 25 mM MgCl2, 240 µl dNTP(10 mM each), 15 µl U/µl Hot Gold Star Taq polymerase and 30 µl U/µl uracil-N-glycosylase.

Relative gene expression levels were determined through cycle theshold values (C_t) by normalisation to the house-keeping genes hypoxanthine phosphoribosyltransferase 1 (HPRT1) or glyceraldehyde-3-phosphate as reference genes. Results are presented as fold

expression compared to transcript levels of unstimulated control cells, which were set to 1. Fold expression was calculated using the $\Delta\Delta C_t$ method (Pfaffl, 2001) according to the following formula:

$$\text{relative mRNA expression} = 2^{-(C_t \text{ of gene of interest} - C_t \text{ of HPRT1/GAPDH})}$$

To accurately evaluate results, two control samples were used on every plate. The „no-template“ control serves to exclude unspecific primer-dimer-amplification products and is prepared like a normal triplicate master mix, but without template. The no-RT-control uses purified RNA, instead of cDNA to control for genomic DNA-contamination during RNA isolation.

3.1.11 Enzymatic manipulation of DNA

(i) Digestion of DNA with restriction endonucleases

For the sequence-specific cleavage of DNA molecules the samples were incubated with restriction endonucleases under appropriate reaction conditions. The amount of enzyme and DNA, the choice of buffer, temperature and duration of the reaction were adjusted according to the manufacturer’s instructions.

(ii) Dephosphorylation of linearized vector DNA

Restriction of vector DNA with a single enzyme may lead to subsequent religation. Therefore, 5’ termini of vector DNA were dephosphorylated using Antarctic Phosphatase™ (NEB) according the manufacturers recommendations.

(iii) Ligation of DNA fragments

For the ligation of linearised vectors with DNA-fragments the T4 DNA ligase was used. This enzyme catalyses the formation of phosphodiester bonds between adjacent 3’-OH and 5’-P ends in double-stranded DNA. For ligations of cohesive ends a molar ratio between 1:5 and 1:10 (vector vs. insert DNA) was chosen.

3.1.12 Agarose gel electrophoresis

DNA samples were separated, characterised and purified by agarose gel electrophoresis. For preparation of agarose gels 1% agarose (w/v) was dissolved in 1x TAE buffer by boiling

and supplemented with 6 µl ethidium bromide/100 ml solution. Prior to loading DNA samples were mixed with 6x DNA loading buffer. Additionally, 5-10 µl of a DNA molecular weight standard (Gene Ruler™ 1 kB DNA ladder, Fermentas) was loaded. The voltage was set to 5 V/cm electrode distance and electrophoresis was performed in a horizontal gel chamber filled with TAE buffer. DNA fragments stained with ethidium bromide were visualized by UV-excitation at l = 312 nm.

3.1.13 Extraction of DNA from agarose gels

DNA fragments and linearized vectors were isolated from agarose gels and purified using the QIAEX II Gel extraction Kit (Qiagen). Alternatively, double-stranded DNA fragments from PCR or other enzymatic reactions were purified using the QIAquick PCR Purification Kit (Qiagen).

3.1.14 DNA sequencing

DNA sequencing was conducted by GATC Biotech according to the dideoxy method (Sanger et al., 1977).

3.2 Methods in mammalian cell culture

3.2.1 General culture conditions

All used cell lines were cultured at 37°C in an atmosphere with a relative humidity of 90% and a CO_2 content of 5%. FCS was heat-inactivated at 56°C for 30 minutes before use. Unless otherwise stated, all used media were supplemented with 10% heat inactivated FCS and 1% penicillin/streptomycin. Cell lines were harvested at 1500 rpm for 5 minutes at 4°C. Primary human T cells were harvested at 1500 rpm for 10 minutes at $°C. All cell culture work was carried out under sterile conditions using a laminar flow hood.

3.2.2 Culture of adherent cells

The epithelial cell lines HEK293FT and HEK293T were maintained in DMEM medium allowing them to grow at a confluence of up to 80%. Cells were split in ratios of 1:3 to 1:12 depending on further use. Therefore, culture medium was removed, cells were carefully

washed with 10 ml of sterile PBS. Subsequently, the supernatant was discarded and 2 - 5 ml Trypsin/EDTA, depending on the flask size were added for 5 minute at 37°C. Detached cells were resuspended in fresh DMEM medium and seeded with a confluence of 15 – 25 % into fresh culture flasks or plates.

3.2.3 Culture of suspension cell lines

For the culture of suspension cell lines or primary human T lymphocytes the following media were used.

Cell line	Cell culture medium
JE6.1; J16-145; Gluc-J16; JE6.1 shContr.; JE6.1 shPP1α; JE6.1 shPP1α #34; JE6.1 shPP1α #47; JE6.1 shPP1α #50	IMDM
HUT78; Hut78 shPP1α #47; HH; HH shPP1α #47	RPMI
Primary human CD4+ T cells	X-vivo 15 medium (supplemented with 25 U/ml IL-2, when T cells were activated)

Culture media were replaced every three days. All suspension cells were cultured up to a density of 4 – 5 x 10^5/ml before they were split.

3.2.4 Thawing and freezing of eukaryotic cells

1–1.5 x 10^7 cells were harvested by centrifugation and resuspended in 1ml freezing medium, containing 90% (v/v) FCS and 10% (v/v) DMSO. 1 ml of cell suspension was transferred into a cryo-tube and immediately stored at -80°C or -140°C for long-term storage. For thawing, cryo-tubes were incubated at 37°C in a water bath until the suspension was completely thawed. Subsequently, cells were transferred into 10 ml of sterile 1x PBS to dilute the DMSO. Cells were centrifuged at 1500 rpm for 5 minutes and afterwards resuspended in 10 to 15 ml prewarmed RPMI, IMDM or DMEM, depending on the cell line.

3.2.5 Determination of the cell density and viability

The cell density was determined using a Neubauer chamber slide. If necessary, cells were diluted prior counting. To assess viability, cell suspensions were diluted with trypan blue solution to 0.05% (w/v) trypan blue and counted in a Neubauer chamber. Cell density was calculated according to the following formula:

$$\text{cell number/ml} = \text{mean cell number per square} \times \text{dilution factor} \times 10^4$$

3.2.6 Ficoll gradient isolation of lymphocytes from human blood

Primary human mononuclear cells were isolated from 500 ml total blood or buffy coats according to the following protocol. 1 ml heparin was added to 500 ml whole blood to inhibit coagulation. Buffy coats were adjusted to 200 ml with PBS. 15 ml Ficoll were filled in 50 ml Falcon tubes and slowly overlaid with 35 ml blood, followed by centrifugation (650 x g, 20 min, 20°C, with slow acceleration and without break). Peripheral blood mononuclear cells (PBMCs) were collected from the interphase and washed once with 1x PBS, followed by centrifugation (460 x g, 10 min, 20°C). The cell pellet was resuspended in 50 ml RPMI medium supplemented with 10% (v/v) FCS. PBMCs were transferred into cell culture flask and cultured for up to 60 minutes (37°C/5% CO_2) to deplete adherent monocytes and macrophages. Non-adhering lymphocytes were washed from the cell culture flask with medium. Lymphocytes were used subsequently for the purification of $CD4^+$ T cells *via* magnetic-activated cell separation (MACS).

3.2.7 Magnetic-activated cell separation of $CD4^+$ T Lymphocytes

$CD4^+$ T lymphocytes were purified from a mixed lymphocyte population (3.2.6) using magnetic-activated cell separation (MACS). Cells can be separated by MACS either by positive or negative selection. In a first step, $CD25^+$ T cells were removed by positive selection. For that, the PBMC suspension was incubated with a limiting amount (2µl/10^7 cells) of bead-coupled anti-CD25 monoclonal antibodies. After a subsequent washing step, the cell suspension was loaded onto a column in a magnetic field. The magnetic beads retain the $CD25_+$ cells in the column, while the remaining cell types flow through. Outside of the magnetic field, $CD25^+$ cells were eluted from the column. In a second step, $CD4^+CD25^-$ T cells were isolated from the $CD25^+$-depleted fraction using the CD4 Isolation kit II and additionally depleted from $CD25^+$ cells with 6 µl of anti-CD25 MACS beads per 10^7 cells.

Alternatively, bulk $CD4^+$ T cells were isolated from total PBMCs by positive selection using CD4 MicroBeads (Miltyenyi Biotec) according to the manufacturer's protocol. Briefly, PBMCs were resuspended in 80 µl of buffer per $1x10^7$ total cells. 20 µl of CD4 MicroBeads conjugated to anti-CD4 monoclonal antibodies were added per $1x10^7$ total cells. The suspension was mixed and incubated for 15 minutes at 4°C. Subsequently, cells were washed by addition of 2 ml of buffer per $1x10^7$ cells, followed by centrifugation at 300 g for 10 minutes. Finally, up to $1x10^8$ cells were resuspended in 2 ml of buffer. Magnetic separation of bead-labelled $CD4_+$ cells was performed as described before. Isolated T cells were rested overnight in X-Vivo 15 medium and diluted to a concentration of $2x10_6$ cells/ml.

3.3 Cell biological methods

3.3.1 Transient transfection by electroporation

Electroporation is a method for the direct transfer of macromolecules (*i.e.* DNA) into target cells by perforating the plasma membrane with a short electric pulse. For transient transfection of Jurkat T cells circular DNA plasmids were used ranging from 5 to 15 µg. Per electroporation 1 x 10^7 cells were harvested washed once in PBS and then resuspended in 400 µl prewarmed RPMI medium without FCS or antibiotics. The cell suspension was mixed with the plasmid sample and subsequently transferred into an electroporation cuvette. Electroporation was performed with the Gene Pulser System (BioRad), using 950 µF and 250 V. Then, cells were transferred into 5 ml of prewarmed IMDM medium without antibiotics. 24 to 48 hours after electroporation cells were used for subsequent analyses.

3.3.2 Nucleofection and siRNA-mediated gene silencing

For siRNA-mediated gene transcript knock down, Jurkat T cells as well as primary human T cells were transiently transfected by nucleofection using the Cell Line Nucleofector Kit V and the Human T Cell Nucleofector Kit (Amaxa), respectively, according to the manufacturer's instructions. $2x10^6$ Jurkat T cells or $1x10^7$ primary human CD4 T cells were resuspended in 100 µl kit-specific nucleofection solution containing 1µM siRNA. Subsequently, cells were transferred into nucleofection cuvettes. Nucleofection was performed with program X-01 for Jurkat T cells or program U-14 for primary human $CD4^+$ T lymphocytes using the Amaxa Nucleofector I. After nucleofection, Jurkat T cells were transferred into 6 well plates, containing 5 ml of prewarmed IMDM supplemented with FCS, but without antibiotics and

cultured for 72 hours before further use. Transfected primary human $CD4^+$ T cells were transferred into 3 ml of X-vivo 15 medium in a 12 well plate format and cultured for 48 to 72 hours before used for further analyses.

3.3.3 Transfection of HEK293T cells by the $Ca_3(PO_4)_2$ method

Cells were grown to 70-80% confluence in 10 cm cell culture dishes. 5-20 μg plasmid DNA were mixed with 1 ml 1x HBS and 50 μl 2.5 M $CaCl_2$ were carefully added. After addition of CaCl2, mixture were shortly vortexed and incubated for 10 to 15 minutes at RT. Subsequently, the mixture was added drop-wise to the cells. To assess transfection efficiency, one cell sample was transfected with an expression vector encoding green fluorescent protein (GFP). 24 hours after transfection efficiency was determined by fluorescence microscopy. After additional 24 hours cells were harvested, lysed and lysates used for further analyses.

3.3.4 Production of recombinant retroviruses

HEK293FT cells (packaging cells) were seeded with a cell density of $1.5x10^6$ cells/ml in 5 ml of DMEM medium in T25 flasks. After reaching a confluence of up to 70%, cells were pre-treated with 25 μM chloroquine. After 1 hour of incubation with chloroquine, cells were transfected with the $Ca_3(PO_4)$ method, using 600 μl 1x HBS and 30 μl 2.5 M $CaCl_2$. Cells were transfected with 6.3 μg TRIPZ shRNAmir expression vector, 4.3 μg of psPAX2 (encoding for gag, pol, and env proteins) and 2.3 μg of pMD2.G2 (encoding for VSV-G) for pseudotyping. 12 hours after transfection the medium was replaced with 4 ml fresh DMEM medium and virus production was continued for additional 24 hours.

3.3.5 Viral transduction of target cells

Two days post transfection of packaging cells, supernatants were collected and centrifuged at 1500 rpm for 5 minutes at 4°C to remove cell debris. Next, cleared supernatants were passed though a 0.45 μm filter. $1x10^5$ target cells (Jurkat T cells) were harvested and resuspended in 200 μl IMDM or RPMI medium, containing 8 μg/ml polybrene, transferred into a 24 well and pre-incubated for 45 minutes at 37°C. 1 ml of viral supernatant was added to each well and cells were infected by spin occulation. Therefore, cells were centrifuged at 2500 rpm for 2 hours at 30°C. After spin occulation, cells were cultured for

additional 12 hours in the presence of the viral supernatant. Subsequently, cells were washed three times with fresh IMDM medium, supplemented with 10% FCS and 1 % penicillin/streptomycin, finally resuspended in 1 ml of fresh medium and transferred into 24 well plates. 48 hours after transduction, stably transduced Jurkat T cells were selected by puromycin resistance (1 µg/ml). Medium with fresh puromycin was replaced every 48 hours. Puromycin was removed when 100% of non-transduced control cells were trypan blue positive.

3.3.6 CFSE labelling of primary human CD4$^+$ T cells

For CFSE labelling, 50 ml reactions tubes were coated with RPMI/10% FCS (v/v). Primary human CD4$^+$ T cells were transferred to pre-coated tubes and harvested by centrifugation at 1500 rpm at 4°C for 10 minutes. Cells were washed once with 20 to 40 ml PBS, followed by centrifugation at 1500 for 10 minutes. Then, cells were resuspended in PBS at a cell density of 2x10^7 cells/ml. CFSE (stock solution: 5 mM) was diluted to a concentration of 0.4 µM in PBS. One volume of CFSE solution was added to one volume of cell suspension (final CFSE concentration: 0.2 µM). Cells were incubated on a rotator in the dark at 20°C for 10 minutes. Then, the reaction was stopped by addition of ice-cold RPMI/10% FCS (v/v) and incubated on ice for 5 minutes. Afterwards, cells were washed twice with RPMI/10% FCS (v/v) and finally resuspended in X-vivo 15 medium at a density of 3x10^6 cells/ml and left untreated overnight. To determine proliferation, cells were distributed in 96-well round bottom plates at a density of 0.75x10^5 cells/100 µl per well. Cells were either left untreated by addition of 100 µl medium, or stimulated *via* the TCR using agonistic antibodies at a final concentration of 0.2 µg/ml anti-CD3, 0.5 µg/ml anti-CD28 and 2 µg/ml GAM in a final volume of 200 µl. CFSE dilution was assessed by flow cytometry (Beckton Dickinson) at 4 to 6 days after stimulation.

3.3.7 Apoptosis analysis

Apoptotic cell death was examined by DNA fragmentation according to the method of Nicolletti (Nicoletti *et al*., 1991). Cells were collected by centrifugation at 1500 rpm for 5 minutes, washed with 200 µl PBS and centrifuged again at 1500 rpm for 5 minutes. Then, cells were lysed in 200 µl of Nicoletti lysis buffer, containing propidium iodide and stored overnight at 4°C in the dark. The propidium iodide stained DNA fragments were quantified

by flow cytometry (Becton Dickinson). Specific DNA fragmentation was calculated according to the following formula:

(% experimental DNA fragmentation – % spontaneous DNA fragmentation) /
(100 – % spontaneous DNA fragmentation) x 100%.

3.4 Biochemical and immunological methods

3.4.1 *In vitro* stimulation of Jurkat and primary human CD4$^+$ T cells

Jurkat T cells and primary human T cells were stimulated with agonistic soluble anti-CD3 (OKT3), anti-CD28 (CD28.2) and goat and mouse monoclonal antibodies (TCR stimulation), using final concentrations between 0.01 to 1.0 µg/ml. Alternatively, cells were stimulated with PMA (10ng/ml) and Ionomycin (10 µM) to induce PKC activation and Ca^{2+} influx, mimicking TCR stimulation. Stimulation *via* TNFR1 was performed using 50 ng/ml recombinant TNFα. For biochemical experiments 0.5 to 1x10^7 cells were harvested by centrifugation at 1500 rpm at 4°C, resuspended in 4 ml fresh medium and 5-fold concentrated stimulation medium was added. Stimulations in 96-well plates were performed in a final volume of 200 µl. 1 to 2x10^5 Gluc-J16, Jurkat or primary human T cells were resuspended in 100 µl fresh medium and 100 µl 2-fold concentrated stimulation medium was added. Stimulations were stopped by transferring cells into 15 ml or 1,5 ml reaction tubes, depending on the stimulation volume, which were pre-filled with ice-cold PBS. Subsequently, cells were centrifuged at 1500 rpm at 4°C for 5 minutes. Then, the supernatant was removed, cells were washed with ice-cold PBS and centrifuged at 1500 rpm at 4°C. The supernatant was drawn off and cells were lysed as described below.

3.4.2 Cell lysis and protein quantification

Cells were pelleted by centrifugation, the supernatant was drawn off and cells were washed once with ice-cold PBS. Subsequently, cells were pelleted, the supernatant was removed and cells were resuspended in 20 µl of ice-cold lysis buffer per 1x10^6 cells. Lysates were incubated on ice for at least 20 minutes. Whole cell lysates were cleared from insoluble cell content by centrifugation at 16000 g at 4°C in a table top centrifuge for 15 minutes . Protein concentration of whole cell lysates was determined using the Roti-Quant® Bradford assay

according to the manufacturers' instructions. 0 to 2 µg/ml bovine serum albumin was used as a standard, with dilution series done in lysis buffer. 1 µl of sample was mixed with 1 ml of Roti-Quant® Bradford reagent and incubated for 5 minutes in the dark. After incubation, absorbance at 595 nm was measured in a photometer, and concentrations were determined according to the standard curve. Subsequently, lysates were adjusted to equal protein levels. For polyacrylamide gel electrophoresis (PAGE), lysates were mixed with an appropriate amount of 2x or 5x reducing SDS sample buffer (Laemmli et al., 1970) and heated to 95°C for 5 minutes. Alternatively, lysates were subjected to immunoprecipitation (see paragraph 3.4.4)

3.4.3 Preparation of nuclear and cytoplasmic cell extracts

Nuclear and cytoplasmic extracts were prepared using the NE-PER Nuclear and Cytoplasmic Extraction kit (Thermo Scientific) according to the manufacturers instructions. After extraction, protein concentration was determined as described previously (see paragraph 3.4.2). For storage of nuclear extracts, glycerol ((20% (v/v)) was added and samples were stored at -80°C. Cytoplasmic extracts handled like whole cell lysates (see paragraph 3.4.2).

3.4.4 Immunoprecipitation

For immunoprecipitation (IP) cleared whole cell lysates were adjusted to a volume of 500 µl in 1.5 ml Eppendorf tubes. Then, lysates were incubated with a 50% slurry of protein A-beads at 4°C on a rotator for 1 hour to pre-clear lysates from unspecifically adsorbing proteins. After incubation, samples were centrifuged at 2000 rpm and 4°C in a table top centrifuge for 2 minutes. Subsequently, the pre-cleared lysates were transferred to a new Eppendorf tube and the desired antibody was added, followed by 1 hour of incubation on a rotator at 4°C. After incubation 50 µl of a 50% slurry of protein A-sepharose beads were added and samples were incubated for at least 3 hours or overnight. The matrix was washed at least 5 times with 1 ml of ice cold lysis buffer to remove unspecifically bound proteins. Beads were resuspended in 50 µl of lysis buffer together with 50 µl 2x or 12.5 µl of 5x reducing sample buffer and heated at 95°C for 5 minutes. Purified proteins were detected by SDS-PAGE and immunoblotting (see paragraph 3.4.4 and 3.4.5)

3.4.5 SDS polyacrylamide gel electrophoresis (SDS-PAGE)

For analysis, proteins were separated using discontinuous SDS-PAGE (sodium dodecyl sulphate – polyacrylamide gel electrophoresis) under reducing conditions (Laemmli et al., 1970). SDS is an anionic detergent, which denatures proteins and concomitantly confers to them a net negative charge. Approximately 1.4 g SDS bind per gram protein and, thus, migration of SDS-protein complexes through polyacrylamide gels in an electric field largely depends on their molecular mass. For separation of proteins 8-12% polyacrylamide separating gels and 5% polyacrylamide stacking gels were used.

The polymerisation was started by adding 0.1% (v/v) TEMED and 0.1% (v/v) ammonium persulphate (APS) and the polymerizing solution was used immediately. The separating gel was covered with isopropanol. After 15 minutes the isopropanol was removed by washing with water, the gel surface was dried and the stacking gel was added. Electrophoretic separation was conducted at a constant current od 25-30 mA/fel for 1.5-2.0 hours. To approximate apparent molecular weights of analysed proteins, an appropriate molecular weight marker was employed. Following SDS-PAGE, the polyacrylamide gels were subjected to immunoblotting (see paragraph 3.4.6).

3.4.6 Immunoblot analysis

After SDS-PAGE, separated proteins were analysed by immunoblot (IB) analysis. Therefore, proteins were electrophoretically transferred onto a nitrocellulose membrane *via* Wetblotting at 100V (~300 mA) under cooling conditions for 1.5 to 2 hours. In order to analyse different proteins at the same time, blots were horizontally cut according to the apparent molecular weight, estimated by the utilised marker. Afterwards, membranes were blocked with 5% (w/v) non-fat dry milk in TBS-T on a rotary shaker at 20°C for 1 hour. After incubation, membranes were washed 3 times with TBS-T for 10 minutes each. For detection of specific proteins, membranes were incubated with primary antibodies (see paragraph 2.6.1) at 4°C overnight. Then, membranes were washed 6 times with TBS-T on a rotary shaker at 20°C, 10 minutes each. Next, membranes were incubated with required secondary HRP-conjugated antibodies (see paragraph 2.6.1) at 20°C for 1 hour. Subsequently, membranes were washed 3 times with TBS-T for 10 minutes each time. Finally, protein bands were detected with ECL substrate solution in a Vilber Lourmat chemiluminescence detection system (Software, Chemi-Capt 5000) and bands were quantified using the Bio-1D software. For detection of further proteins, the membrane was incubated with stripping buffer to denature primary and secondary antibodies, followed by rigid washing of the membrane

with TBS-T. Then, the membrane was blocked for 1 hour and the procedure was continued as described above.

3.4.6 *In vitro* kinase assay

In vitro kinase assays were performed as described previously (Brenner et al., 2005). Endogenous IKK complex was immunoprecipitated with anti-NEMO antibodies. Immunoprecipitates were washed 3 to 5 times with lysis buffer, followed by one wash step with kinase buffer. Then, beads were resuspended in 100 µl kinase buffer and split in equivalent 50 µl aliquots. One part was used to control for protein input, while the other part was subjected to *in vitro* kinase reaction. 5 µg of recombinant GST:IκBα together with 10 µCi [$_{32}$P-γ]ATP were added to the reaction mix to serve as a specific substrate of IKK kinases. The kinase assay reaction was conducted at 30°C for 30 minutes. Subsequently, proteins were electrophoretically separated by SDS-PAGE. Afterwards, the gel was dried and subjected to autoradiography.

3.4.7 Electromobility shift assay (EMSA)

EMSAs were performed, using the Lightshift® Chemiluminescent EMSA Kit (Thermo Scientific) according to the manufacturers' instructions. The assay makes use of biotinylated dsDNA oligonucleotides (see paragraph 2.5.3). To assess binding activity of transcription factors, nuclear extracts of stimulated Jurkat or primary human $CD4^+$ T cells were prepared (see paragraph 3.4.3), and 0.5 to 1 µl of nuclear extract was added to the reaction mixture.

3.4.8 *Gaussia* luciferase reporter assay

0.5-2x10^5 GLuc reporter cells were stimulated in 96 well plates for 5 hours. For each sample, 20 µl of supernatant was subjected to a *Gaussia* luciferase assay (p.j.k.) according to the manufactures' instructions. Luciferase activity was measured in 96-well plates using a Orion L microplate Luminometer (Berthold Detection Systems) with an integration time of 3.0 sec. In parallel, cell viability was determined (see 3.4.10) and normalized Gluc activity was calculated as the ratio between Gluc activity and cell viability counts.

3.4.9 Cell viability assay

Cell viability was assessed in a 96-well format using the CellTiter-Glo® Luminescent Cell Viability Assay (Promega). The assay determines the number of viable cells by measuring the intracellular content of ATP. The amount of ATP correlates with the amount of metabolically active cells. Cells were resuspended in medium and 50 µl of the cell suspension was added to 50 µl of the CellTiter-Glo® reagent (1:1 diluted with medium). Then, plates were incubated for 20 minutes at 37°C in the dark. Luminescence was measured using an Orion L Microplate Luminometer (Berthold Detection Systems) (integration time 1.0 sec).

3.4.10 Transient reporter assay

For transient reporter assays $1x10^7$ Jurkat T cells or $2x10^5$ HEK293T cells were co-transfected with NF-kB- or AP-1-specific transcriptional reporter plasmids (pGL8xNF-κB-fos or p3xAP-1-Luc) and pfos-LacZ as described previously (Arnold et al., 2001). Jurkat T cells were co-transfected with 8 µg of reporter plasmid and 1 µg of pfos-LacZ. HEK293T cells were co-transfected with 2µg of reporter plasmid and 0.2µg of pfos-LacZ. Transfection efficiency was normalized to LacZ expression. 24-48 h post transfection cells were left untreated or treated (see paragraph 3.4.1), lysed and luciferase activity was measured using the *Dual-Light® System* (Applied Biosystems) and an Orion L Microplate Luminometer (Berthold Detection Systems) according to the manufactures' instructions.

3.4.11 Enzyme-linked immunosorbent assay (ELISA)

To determine cytokine concentrations in the supernatant of stimulated cells, cells were stimulated in a 96-well format (see paragraph 3.4.1) overnight. Subsequently, the supernatant was collected, and the levels of secreted IL-2, IL-8 and IFNγ were measured using enzyme-linked immunosorbent assays (ELISA), according to the manufacturers' instructions. 96-well half area plates were coated with capture antibody (diluted in coating buffer, 50 µl per well) overnight at 4°C. After coating, plates were washed 3 times with PBS-T and unspecific binding sites were blocked with 100 µl PBS/10% FBS per well for 1 hour at 20°C. Plates were washed 3 times and 50 µl of sample or standard was added per well and incubated for 1 hour at 20°C. After incubation, plates were washed 3 times with PBS-T. Subsequently, 50 µl biotinylated detection solution (diluted in PBS/10% FCS, 1:2000 streptavidin-HRP (Jackson-Immunoresearch)) was added and incubated at 20°C for

1 hour. Subsequently, plates were washed 5 times with PBS-T. Finally, 50 µl substrate solution (citrate buffer, 0.5mg/ml o-phenylendiamine, 0.1% (v/v) H_2O_2) were added and incubated for an appropriate period of time before the reaction was stopped by addition of 25 µl 3M H_2SO_4. For end-point reading, the absorbance signal was measured at 490 nm, using the Microplate Reader Model 680 (Biorad).

3.5 Computational and statistical analysis

3.5.1 Statistical normalization

Statistical analysis of the primary RNAi screen and data pre-processing were conducted using the *cellHTS2* Bioconductor/R software package (in collaboration with D. Nickles, DKFZ) (Boutros et al., 2006; Pelz et al., 2010). For each 96-well two reporter signals were measured: channel 1 was representative of overall cell viability and cell numbers, whereas channel 2 was based on measurement of NF-kB-driven Gluc activity (see also 5.1.5). Computational analysis of raw data from each channel revealed in part considerable interplate variations as well as systematic intraplate effects (positional effects, such as column, row, or edge effects). Therefore, values were statistically normalized using the stringent *B* score algorithm that is suitable to standardize for intraplate and plate-to-plate variability (Birmingham et al., 2009; Brideau et al., 2003; Malo et al., 2006). *B* score normalization yielded accurate and similar distributions of median normalized signal intensities between replicates and across different plates as assessed by box plot analysis (Boutros et al., 2006; data not shown). In addition to statistical normalization, pre-processed data from either channel were combined in order to calculate values for NF-kB-specific Gluc activity normalized to cell numbers (channel2/channel 1; biological normalization). Subsequently, mean Gluc activity of two biological replicates for each siRNA transfection was determined. Mean values, in turn, were transformed into the statistical *z* score for hit selection and post-screen analysis.

3.5.2 Candidate selection by analysis of statistical normality

For identification of candidate phosphatases (hits) quantified RNAi phenotypes (*i.e.* mean values of normalized NF-kB activity) were scored for statistical significance. To this end, normalized measurements were transformed into the statistical *z* score (Boutros et al., 2006). Data transformation helps to further minimize data variability and allows for the

analysis of statistical normality which is instrumental in defining appropriate thresholds for hit selection. Using a quantile-quantile (QQ) plot analysis (Ramadan et. al., 2007) *z* scores assigned to individual phosphatase siRNAs (sample quantiles) were plotted against values from a theoretical normal distribution (theoretical quantiles) (Fig. 5.5 A). *z* score deviations from normally (randomly)-distributed values indicated statistically significant RNAi phenotypes. For hit selection *z* scores > +1.5 and < -1.5 were defined as cut-offs values (Fig. 5.5 A and B).

3.5.3 Student's t-test

The unpaired Student's *t*-test (independent two-sample t-test; unequal sample sizes and unequal variance) was used for statistical analysis of data sets, including ELISA, reporter gene assays and gene expression analysis. A p value * ≤ 0.05 was considered statistical significant. Individual p value thresholds are indicated in figure legends.

4. Results

Signalling to NF-κB upon TCR-triggering and co-receptor engagement is mediated by the concerted action of various signalling proteins, including kinases, ubiquitin-editing enzymes, scaffold and adaptor proteins. Phosphorylation is the major reversible post-translational modification used to facilitate signal transduction and considerable effort has been made to identify kinases involved in signal transduction to NF-κB. In contrast, little is known about the function of phosphatases as signalling modulators in the NF-κB pathway, despite their well established role in regulation of other transcription factors (e.g. NFAT). To evaluate the importance of phosphatases on TCR-induced NF-κB activation, we have performed a semi-large scale RNA-interference (RNAi) screen in Jurkat T cells. The detailed screening procedure is published (Brechmann, 2010) and, thus, is only shortly summarised in the following paragraph.

4.1 RNAi screen and data analysis

For RNAi-screening, a NF-κB reporter cell line (from here on referred to as Gluc-J16), based on Jurkat T cells that harbour a NF-κB responsive Gaussia-luciferase (Gluc) reporter gene was used (Brechmann , 2010). Gluc contains a natural N-terminal secretion sequence that mediates quantitative secretion of native Gluc protein in an active form. Stimulation of Gluc-J16 cells with agonistic antibodies against CD3 and CD28 or PMA and Ionomycin as well as TNFα results in NF-κB-dependent synthesis of Gluc, which is subsequently secreted into the surrounding medium (Brechmann, 2010). Therefore, the strength of luciferase activity can be measured in the supernatant of stimulated cells and directly reflects the strength of NF-κB activity.

For RNAi-screening, a commercially available small interfering RNA (siRNA) library, targeting 298 known or predicted phosphatase and phosphatase-associated gene transcripts, was used (Brechmann, 2010). Each targeted transcript was covered by three independent siRNA oligos, which were transfected independently and in biological duplicates into Gluc-J16 cells in a 96-well format. In addition, several siRNAs, targeting known NF-κB regulators in T cells, such as CYLD (negative regulator) CARMA1 and RelA (positive regulators) and non-targeting control siRNA oligos were used. 72 hours after transfection, cells were equally split and either kept unstimulated or stimulated *via* the TCR, using agonistic anti-CD3 and anti-CD28 antibodies and goat-anti-mouse (GAM) crosslinking antibodies (from here on referred to as anti-CD3/CD28). After stimulation, luciferase activity was measured in the

supernatants. In addition, cell viability was assessed. Data analysis was carried out with the cellHTS2 software package (Boutros et al., 2006; Petz et al., 2010). The raw luciferase as well as the viability data set was normalized using the iterative B score algorithm, which compensates systemic inter- and intraplate variations (Birmingham et al., 2009). After B score normalisation, the ratio of processed luciferase and viability values was calculated for each individual siRNA transfection to obtain values for NF-κB-specific Gluc-activity, normalised to cell viability (Brechmann, 2010). Afterwards, the mean Gluc activity of two biological replicates was calculated and transformed into the statistical z score for hit selection. The z score specifies the number of standard deviations of a sample from the population mean and therefore provides a specific measure for the biological effect of an individual siRNA (Birmingham et al., 2009). Positive and negative z scores indicate increased or and reduced reporter activity, respectively.

4.2 RNAi screen identifies protein phosphatase 1, catalytic subuit alpha (PP1α) as a positive regulator of NF-κB signalling in T cells

Primary RNAi screening identified several tentative candidate phosphatases involved in regulation of NF-κB activity upon TCR stimulation. To be further considered as a hit, at least two independent oligos per targeted gene had to exceed a z score ≥ 1.5 for negative regulators and ≤ -1.5 for positive regulators. Several siRNAs, targeting phosphatases, known to be involved in TCR-induced signalling were found to score above the threshold criteria. A comprehensive summary of the screening results is given in Brechmann, 2010.

As shown in Fig. 4.1 A, RelA, CARMA1 and CYLD siRNAs consistently scored above the given threshold criteria. In detail, siRNAs targeting the negative regulator CYLD reproducibly surpassed a z score of 1.5, indicating enhanced NF-κB-driven activity. In contrast, siRNAs targeting the positive regulators CARMA1 or RelA consistently scored below a z score of 1.5, underscoring the validity of the here applied screening and analysis strategy.

Albeit the assumption that phosphatases may primarily counteract the activating function of kinases and, thus, signalling to NF-κB, the RNAi screen also identified protein phosphatase 1, catalytic subunit alpha (PP1α) as a positive regulatory phosphatase. Two siRNA oligos, targeting PP1α, scored below a z score of -1.5 (siPP1α#1 z score: -2.08; siPP1α#3 z score: -2.11), indicating PP1α as a putative positive regulator of NF-κB activity (Fig 4.1 A). To validate the primary RNAi screening result, Gluc-J16 cells were transiently transfected with the PP1α-specific siRNA oligos, used for primary RNAi screening along with a non-targeting

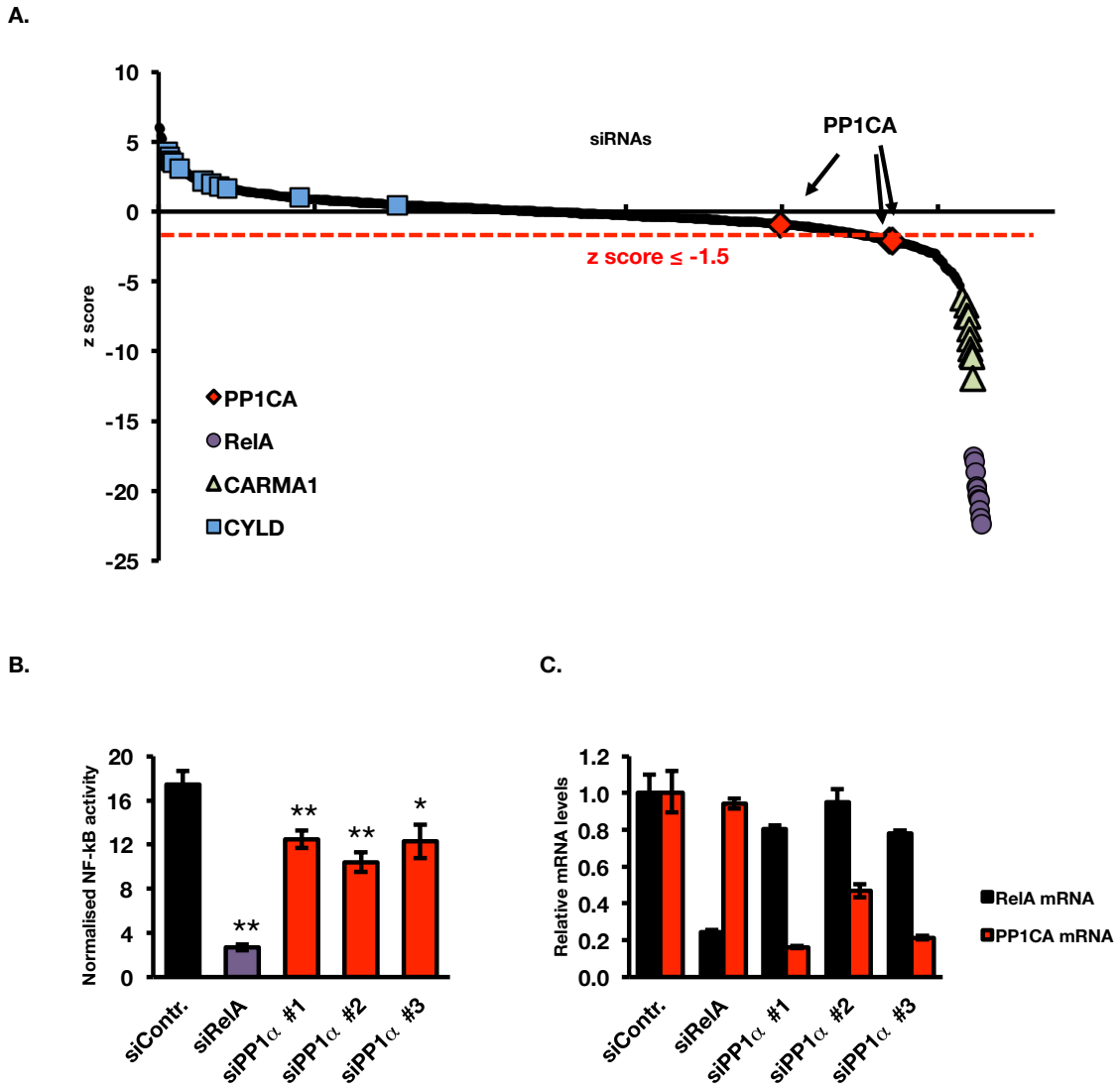

Figure 4.1 Results of RNAi screen and validation of PP1α as a positive regulator of TCR-induced NF-κB signalling. (A) Results of RNAi screen, depicting z score distribution of individual phosphatase-specific and control siRNAs. The positions of siRNA oligos for PP1α, RelA, CARMA1 and CYLD are depicted. The Red dashed line indicates the z score threshold of -1.5. **(B)** Validation of primary screening results. Gluc-J16 cells were transfected with non-targeting (siContr.), RelA-targeting (siRelA) or three independent PP1α-targeting (siPP1α #1,#2,#3) siRNAs. 72 hours after transfection, cells were stimulated with 0.5 µg/ml anti-CD3/28 and luciferase activity was assessed in the supernatant. In parallel, cell viability was determined using Cell Titer Glo©. Luciferase activity was normalised to cell viability. **(C)** Relative mRNA levels of RelA and PP1α were determined by qRT-PCR to control for knock down. Values are normalised to siContr.. Results are representative for 3 independent experiments (B and C). Given is the mean +/- SD of triplicate stimulation; *, $p \leq 0.05$; **, $p \leq 0.005$

control siRNA and a siRNA targeting RelA (Fig. 4.1 B). 72 hours after transfection, cells were stimulated *via* the TCR and luciferase activity was measured in the supernatant of cells.

In line with the primary screen, all PP1α-targeting siRNAs (siPP1α #1 – 3) reduced NF-κB-driven reporter activity by 30 to 40%. As expected, knock down of RelA almost abolished luciferase activity (Fig 4.1 A). In addition, knock down efficiency of individual siRNA oligos were assessed by qRT-PCR (Fig. 4.1 C). PP1α-specific oligos #1 and #3 reduced PP1CA mRNA by 80% or more, while oligo #2 was less efficient (Fig. 4.1 B). Probably, due to its lower knock down efficacy oligo #2 may have resulted in a less pronounced phenotype during RNAi screening and, thus, did not score under the given criteria (Fig. 4.1 A). Importantly, knock down of RelA had no effect on PP1α expression and *vice versa* (Fig. 4.1 C). In summary, transient knock down of PP1α in Gluc-J16 cells confirmed the result of the primary RNAi screen.

4.3 Ectopic expression of PP1α increases stimulus-independent and TCR-dependent NF-κB activity

Ectopic expression of proteins, for example using HEK293T cells, is a standard procedure to characterise protein function in an investigated signalling pathway. HEK293T cells are easy to transfect and overexpression of some NF-κB pathway components themselves can induce NF-κB activation independent of an additional stimulus. The primary RNAi screen and subsequent validation experiments indicated PP1α as a putative positive regulator of NF-κB signalling. Therefore, in complementation of these loss-of-function data, PP1α was ectopically expressed in HEK293T or in Jurkat T cells to determine its impact on NF-κB activation.

To this end, HEK293T cells were transiently transfected with increasing amounts of an expression plasmid, encoding haemagglutinin (HA)-tagged human PP1α or an empty vector (Mock) as control (Fig. 4.2 A). NF-κB activity was determined by co-transfecting a NF-κB luciferase reporter plasmid. HA-PP1α expression was controlled by immunoblot analysis (Fig. 4.2 A, lower panel). After transfection, cells were cultured for 24 hours to allow sufficient expression of exogenous HA-PP1α. Subsequently, luciferase activity was determined.

Compared to Mock-transfected cells, expression of HA-PP1α induced reporter activity in a dose-dependent manner, indicating that forced PP1α expression can lead to NF-κB activation.

In a second approach, HA-PP1α was ectopically expressed in Jurkat T cells. Therefore, cells were transfected with a NF-κB reporter plasmid, together with an empty (Mock) or the HA-PP1α-encoding expression plasmid (Fig. 4.2 B). 24 hours after transfection, cells were

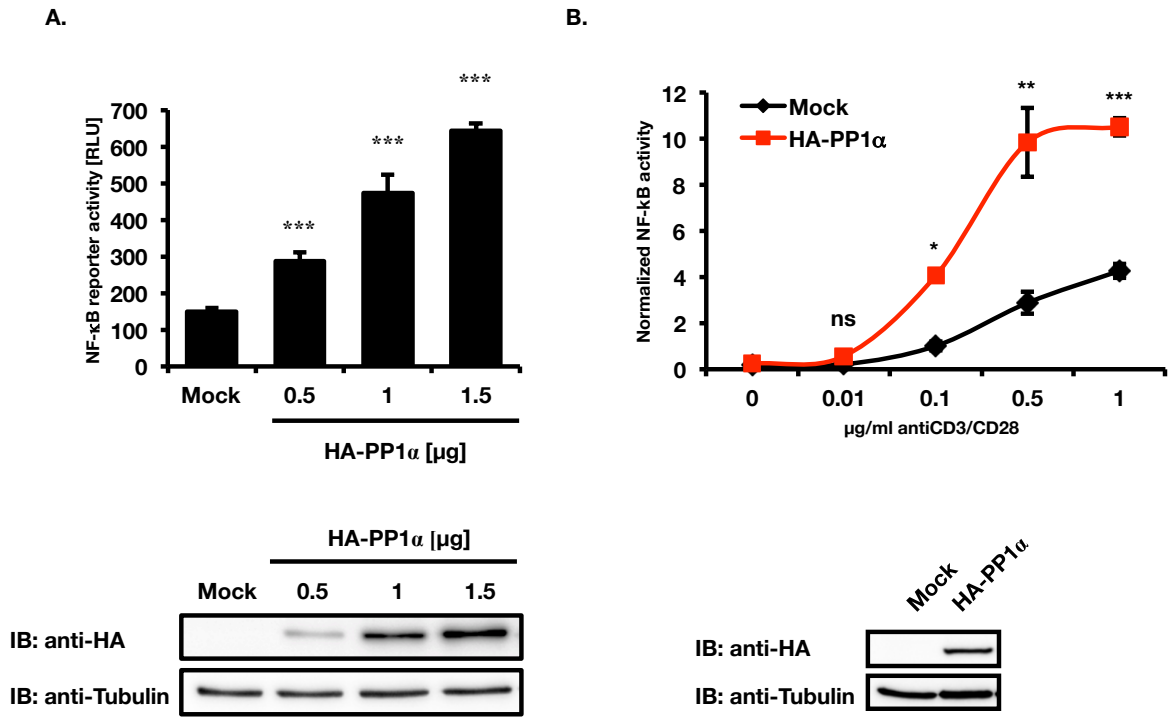

Figure 4.2 Ectopic expression of PP1α augments NF-κB reporter gene activity. HEK293T cells **(A)** or Jurkat T cells **(B)** were transiently transfected with empty vector (Mock) or expression plasmid, encoding haemagglutinin (HA)-tagged human PP1α. To determine NF-κB activity, cells were co-transfected with a NF-κB reporter plasmid. 24 hours after transfection, NF-κB activity was assessed in whole cell lysates (WCL) of cells. **(B)** Cells were stimulated *via* the TCR using increasing concentrations of anti-CD3, anti-CD28, as indicated and NF-κB activity was determined in WCLs. **(A and B)** WCLs were subjected to SDS-PAGE followed by immunoblot analysis with indicated primary antibodies. Given is the combined mean +/- SD of duplicate transfections, each measured in triplicate (A) of three stimulations, each measured in triplicate (B). *, $p \leq 0.05$; **, $p \leq 0.005$; ***, $p \leq 0.0005$

stimulated with increasing concentrations of anti-CD3/CD28 to monitor TCR-induced NF-κB activation in response to TCR-triggering. In addition, expression of HA-PP1α was controlled by immunoblot analysis (Fig 4.2 B, lower panel).

Upon stimulation, HA-PP1α expressing cells showed significantly elevated luciferase activity compared to Mock transfected cells (Fig. 4.2 B, upper panel). However, in contrast to HEK293T cells, basal NF-κB activity was not induced by exogenous PP1α expression in Jurkat T cells.

In summary, these data further corroborate a role of PP1α in NF-κB activation. Importantly, in Jurkat T cells, enhanced NF-κB activity was dependent on stimulation, suggesting that PP1α is actively engaged downstream of the TCR or CD28.

4.4 Transient knock down of PP1α attenuates secretion of NF-κB-dependent cytokines in T cells

The preceding loss- and gain-of-function experiments implicated a positive-regulatory role of PP1α on NF-κB activation in T cells. However, reporter gene assays are limited in respect to explore the physiological function of a protein. In T cells, NF-κB controls transcription of various cytokines upon TCR engagement. The genes encoding the T cell cytokine IL-2 and the chemokine IL-8 contain several κB-binding sites in their promoter regions that are required to drive gene expression. To verify a physiological role of PP1α in T cell-intrinsic NF-κB-dependent function, the influence of PP1α knock down on IL-2 and IL-8 cytokine secretion was investigated.

Therefore, Jurkat cells were transiently transfected with non-targeting control or two independent PP1α-targeting siRNAs (Fig. 4.3, top panels). To test for technical variation, each siRNA oligo was transfected in replicates. 72 hours after transfection, cells were stimulated *via* the TCR and secretion of cytokines was monitored using ELISA. In parallel, knock down of PP1α was analysed by immunoblot analysis.

Transfection of PP1α-specific siRNAs conferred potent protein knock down, which was consistent between replicate transfections of the same oligo. As expected, loss of PP1α correlated with a significant decrease in IL-8 and IL-2 secretion by 40 to 50% (Fig. 4.3 A and B). This phenotype was highly reproducible and did not differ between replicate transfections.

To further extend these findings in non-malignant cells, IL-2 secretion was monitored in PP1α-silenced primary human T cells. Therefore, $CD4^+$ T cells were isolated from peripheral blood of healthy donors and transiently transfected with two independent PP1α-specific or non-targeting control siRNAs. Knock down of PP1α was controlled by qRT-PCR (Fig. 4.3 C, right panel). 48 hours after transfection, T cells were stimulated *via* the TCR and the RNAi-phenotype was determined by measuring IL-2.

In line with the phenotype in Jurkat T cells, PP1α knock down in primary T cells correlated with a significant decrease in secreted IL-2 compared to control transfected cells (Fig. 4.3 C, left panel). Knock down was potently conferred by PP1α-specific oligos, resulting in 20% or less residual PP1α mRNA (Fig. 4.3 C, right panel).

Collectively, these results provide further evidence for a physiological function of PP1α in T cells and suggest that regulation of NF-κB activity by PP1α directly affects cytokine

secretion.

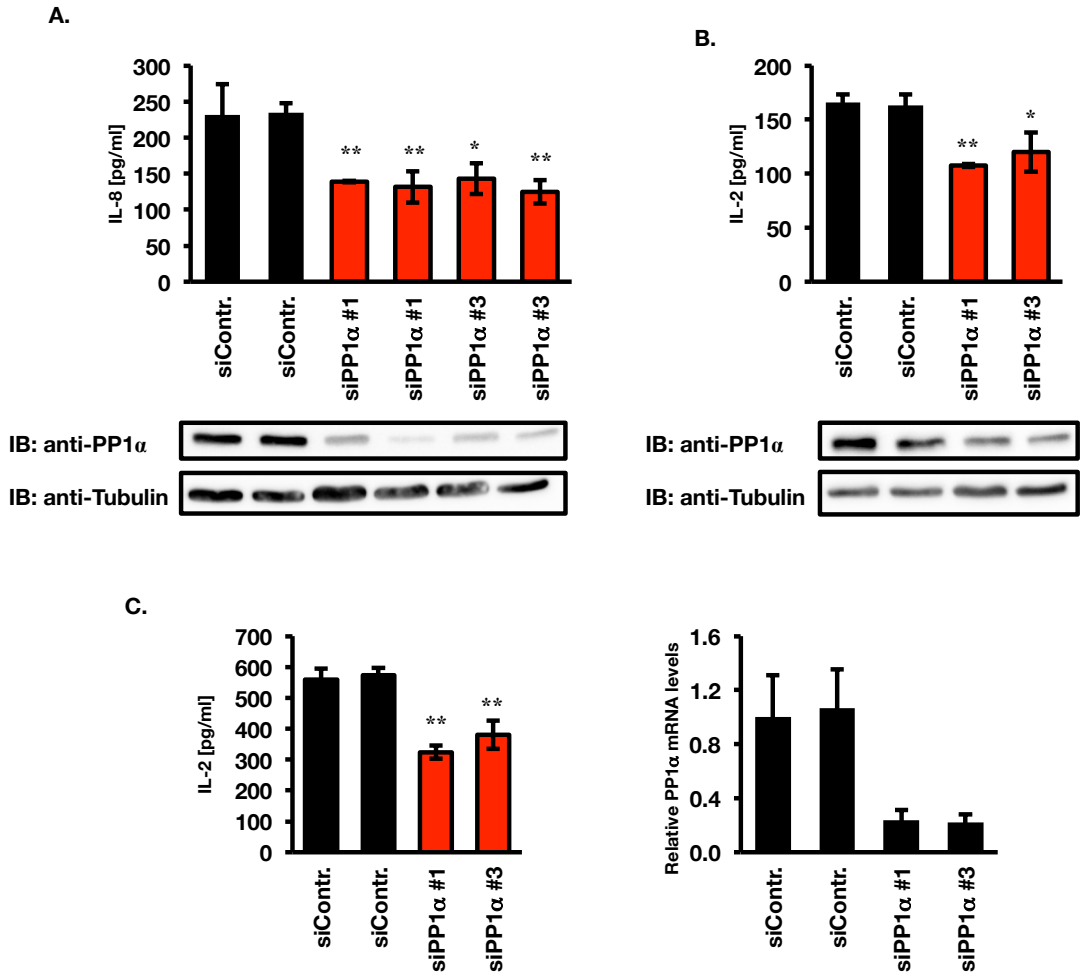

Figure 4.3 Knock down of PP1α attenuates cytokine secretion. (A and B) Jurkat T cells were transiently transfected with non- (siContr.) or two independent PP1α-targeting (siPP1α #1, #3) siRNAs. 72 hours after transfection, cells were stimulated with 0.5 µg/ml anti-CD3/CD28 for 12 hours. Subsequently, cytokine levels were measured by ELISA. Knock down of PP1α was controlled by subjecting WCLs to SDS-PAGE, followed by immunoblot analysis using primary antibodies as indicated. Error bars: +/- SD of three independent stimulations, measured in technical replicates **(C)** Primary human $CD4^+$ T cells were isolated from peripheral blood of healthy donors and subsequently transfected with non-targeting control (siContr.) or two independent PP1α-targeting (siPP1α #1, #3) siRNAs. 48 after transfection, cells were stimulated with 0.5 µg/ml anti-CD3/CD28 for 12 hours and IL-2 levels were measured by ELISA (mean +/- SD of three independent stimulations, measured in technical replicates) . Knock down of PP1α was controlled by qRT-PCR (right panel) and mRNA levels normalised to siContr. (mean +/- SD of technical triplicates).*, $p \leq 0.05$; **, $p \leq 0.005$

4.5 Transient knock down of PP1α reveals no overt differences in phosphorylation of NF-κB signalling mediators

Due to the correlation of RNAi-mediated knock down of PP1α and attenuated NF-κB activity as well as decreased cytokine secretion, it is possible that PP1α directly influences signal transduction to NF-κB. A central hub within the canonical NF-κB signalling pathway is the IKK complex, which mediates phosphorylation-induced degradation of IκB proteins, thereby liberating NF-κB dimers to translocate to the nucleus and drive gene transcription. Hence, it was sought to determine whether PP1α interferes with activating phosphorylation events within the TCR-induced NF-κB signalling pathway.

Therefore, Jurkat T cells were transiently transfected with non- or PP1α-targeting siRNA. 72 hours after transfection, cells were stimulated *via* the TCR for up to 90 minutes. To follow the dynamic activation of the NF-κB pathway over time, samples were taken at different time points after stimulation (Fig. 4.4). Cells were subsequently lysed and whole cell lysates (WCL) were subjected to SDS-PAGE, followed by immunoblot analysis, using phospho-site specific antibodies against IKKα/β, IκB and p65. In parallel, to control for pathway specificity, activation of MAPK signalling was monitored by analysis of Erk1/2 and p38 phosphorylation. Membranes were reprobed with pan-specific antibodies against the respective proteins to control for equal loading and to allow an estimation of the strength of phosphorylation reactions.

As depicted in Fig. 4.4, activation loop phosphorylation of IKKα (S180) and IKKβ (S181), indicative for IKK activation, peaked after 25 minutes of stimulation and occurred to a similar extent in control and PP1α-silenced cells upon TCR-triggering. Accordingly, phosphorylation of p65 (S536), critical for the transcription activating function of NF-κB also peaked upon 25 minutes of stimulation and was unaffected by PP1α knock down. Interestingly, degradation of IκBα was mildly attenuated, while phosphorylation of the resynthesized IκBα protein after 90 minutes of stimulation was slightly reduced in PP1α-silenced cells. However, IκBα resynthesis, which occurs in a NF-κB-dependent manner, was not altered. Importantly, phosphorylation of the MAPKs Erk1 and Erk2, as well as p38 was not influenced by reduced PP1α levels, indicating that the strength of TCR stimulation was comparable between control cells and PP1α-silenced cells.

As assessed by phospho-immunoblotting, signalling to NF-κB did not seem to be generally altered in the absence of PP1α. Yet, a mild influence on IκBα phosphorylation and degradation was reproducibly found among independent experiments. However, low cell

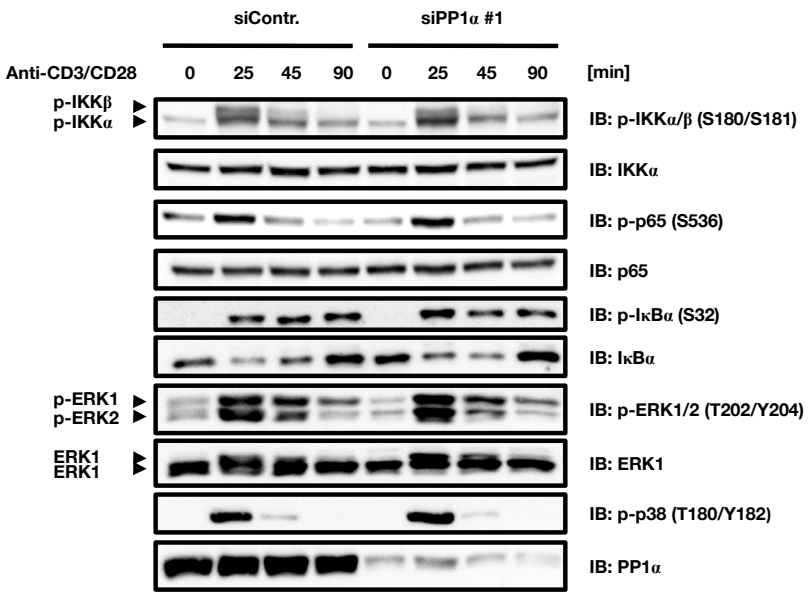

Figure 4.4 Transient knock down of PP1α does not reveal overt difference in the phosphorylation of NF-κB signalling components. Jurkat T cells were transiently transfected with non- (siContr.) or PP1α-targeting (siPP1α #1) siRNA. 72 hours after transfection, cells were stimulated with 0.5 µg/ml anti-CD3/CD28 for the indicated periods of time. Subsequently cells were lysed and equal amounts of protein were subjected to SDS-PAGE, followed by immunoblot analysis. Phosphorylation of signalling proteins was deteceted by using the phospho-site specific primary antibodies as indicated. The membrane was reprobed with antibodies targeted against total protein to control for equal loading.

numbers, and fluctuating cell viability upon transient transfection, hampered phospho-immunoblot analysis and, thus, required further investigation.

4.6 Generation of cell lines with inducible PP1α knock down

So far, validation and initial characterisation of PP1α function was based on transient transfections *via* nucleofection, a commercially available electroporation method under optimised buffer conditions. Although knock down and overexpression were quantitatively achieved, the number of cells receiving siRNA or DNA constructs within the cell population is limited and does not allow for rigid biochemical analysis of signalling pathways. In addition, nucleofection can alter cellular behaviour and lowers cell viability, further complicating the analyses of PP1α function. To circumvent these obstacles, Jurkat T cell lines that harbour a stably integrated non- or PP1α-targeting small hairpin RNA (shRNA) expression cassette were generated. To avoid adaptation effects due to long-term silencing

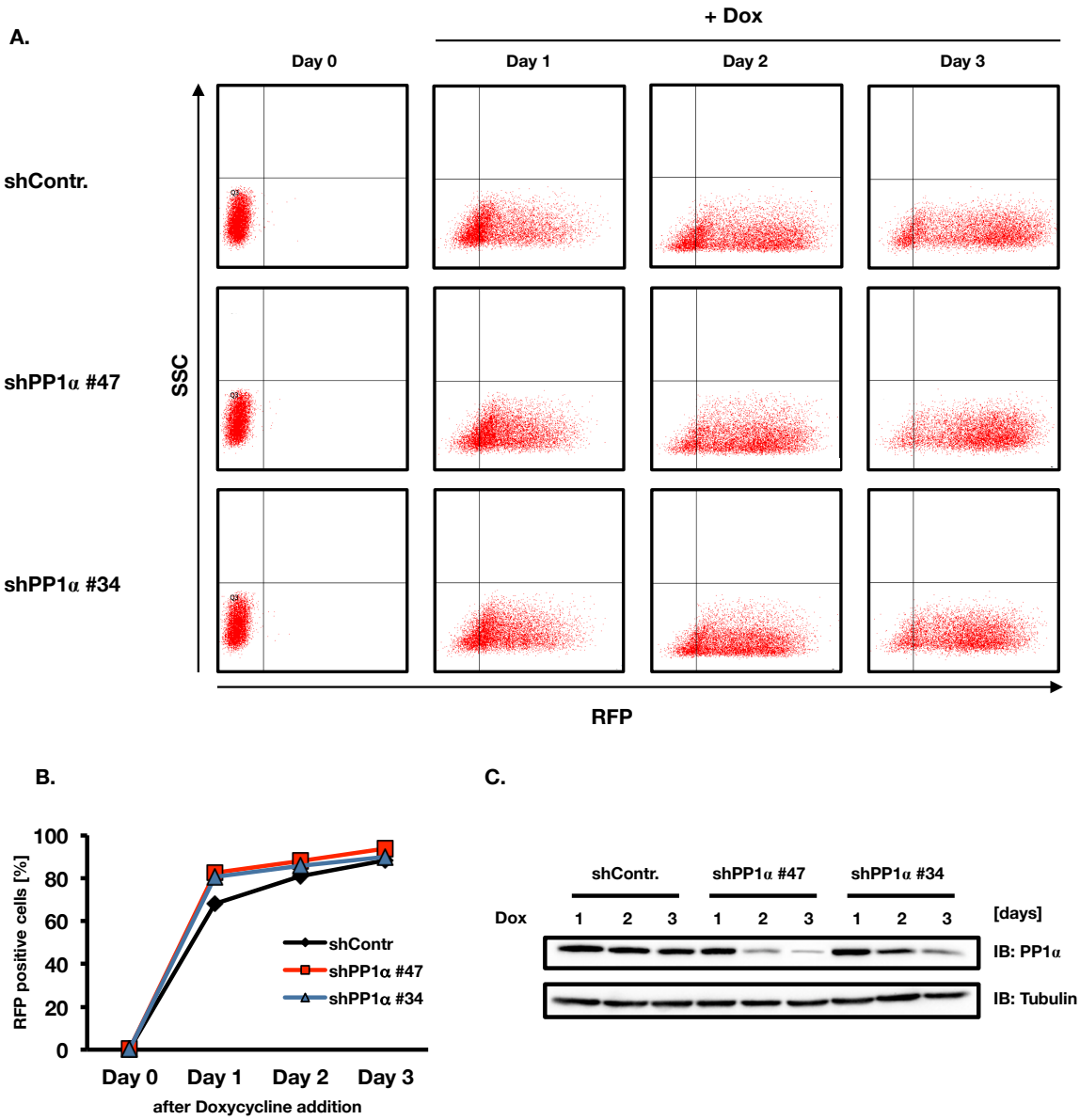

Figure 4.5 Characterisation of inducible shRNA expression in stably selected Jurkat T cells. **(A)** Indicated cell lines were treated with 2 µg/ml Doxycycline. Induction of RFP expression was measured daily using flow cytometry. **(B)** Percentage of viable, RFP positive cells. **(C)** Inducible PP1α-silencing was controlled by acquiring WCLs of Dox-treated cells daily. Subsequently, equal amounts of protein were subjected to SDS-PAGE, followed by immunoblot analysis with indicated primary antibodies. Equal loading was controlled by reprobing the membrane with anti-Tubulin antibody.

of proteins, a Doxycycline (Dox)-inducible shRNA expression system was used. For convenience, Dox-induced shRNA expression is accompanied by co-expression of red-fluorescent protein (RFP), which allows tracking of induced expression by flow cytometry. In addition, the lentiviral constructs contain a puromycin resistance cassette, enabling

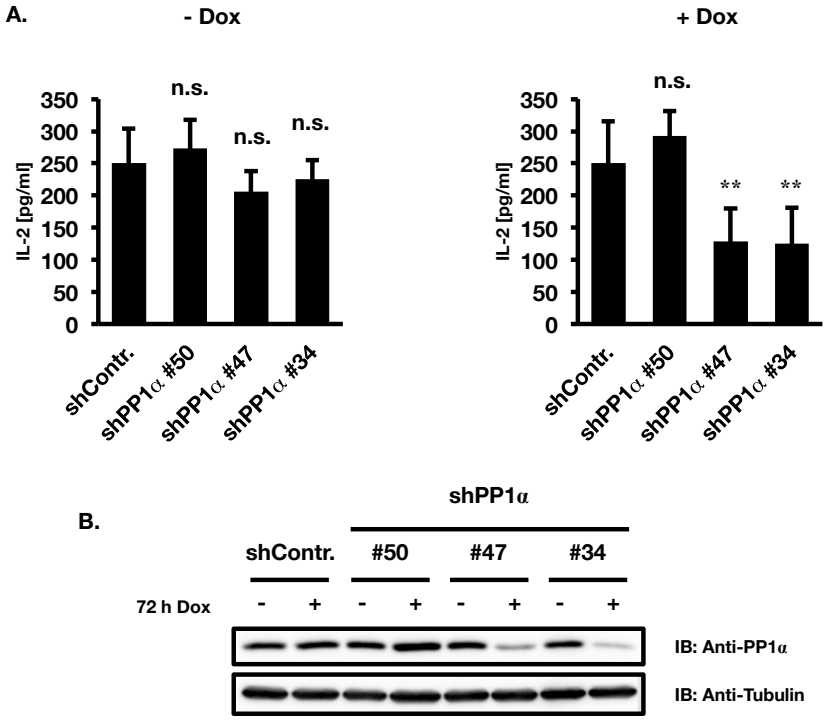

Figure 4.6 Inducible PP1α knock down attenuates secretion of IL-2. (A) Indicated cell lines were cultured in the absence (left panel) or presence (right panel) of 2 µg/ml Dox for 72 hours. Cells were stimulated with 0.5 µg/ml anti-CD3/CD28 for 12 hours. Subsequently, secretion of IL-2 was measured by ELISA. Mean +/- SD of three independent stimulations and replicate technical measurements is shown. **(B)** Induced knock down of PP1α protein was controlled by subjecting WCL of cells in (A) to SDS-PAGE, followed by immunoblot analysis using primary antibodies as indicated. **, $p \leq 0.005$

selection of cells that stably incorporated the inducible expression cassette into their genome. Overall, nine independent shRNA expression constructs and one non-targeting control shRNA construct were used for generation of stable Jurkat cell lines. For the purpose of this thesis, the characterisation of only three cell lines, one control cell line (shContr.) and two shPP1α expressing cell lines (shPP1α #47, and shPP1α #34) are shown (Fig. 4.5). For characterisation, stably selected cell lines were treated with Dox and analysed for RFP expression by flow cytometry (Fig. 4.5). A single application of Dox resulted in robust RFP expression on day one, which increased over time (Fig. 4.5 A) and resulted in 90% of RFP positive cells after three days (Fig. 4.5 B). Of note, Dox treatment did not influence cell viability (data not shown). In parallel, samples of Dox-treated cells were taken every 24 hours and expression of PP1α was determined by immunoblot analysis. The extend of PP1α protein knock down in shPP1α expressing cell lines occurred in a time-dependent manner (Fig. 4.5 C) and inversely correlated with RFP positivity. To exclude differential TCR stimulation-dependent behaviour, cells were analysed for CD3 and CD28

surface expression by flow cytometry (data not shown). CD3 and CD28 surface expression did not differ between cell lines and importantly was not altered upon Dox application (data not shown). In conclusion, stable cell lines, in which PP1α protein expression can be inducibly silenced, were successfully generated.

To test whether inducible knock down of PP1α would also suppress IL-2 secretion, as seen by transient silencing, the two cell lines shPP1α #47 and shPP1α #34 and two cell lines that did not decrease PP1α protein levels upon Dox treatment, shContr. and shPP1α #50, were analysed by ELISA (Fig. 4.6 A). All cell lines were cultured in the absence or the presence of Dox. Three days after Dox application, cells were stimulated *via* the TCR and IL-2 secretion was measured using ELISA. In parallel, PP1α protein levels were assessed by immunoblot analysis (Fig. 4.6 B).

As shown, all cell lines used produced comparable amounts of IL-2 in the absence of Dox, indicating that the stable incorporation of the shRNA expression cassette did not alter expression of IL-2. In contrast, Dox-induced PP1α silencing suppressed IL-2 secretion by 40 to 50 % (Fig. 4.6 A, right panel). Importantly, decreased IL-2 levels were confined to cells with reduced PP1α protein expression (Fig. 4.6 B) and did not per se correlate with Dox treatment, assigning the phenotype specifically to PP1α function.

In conclusion, the previous results were confirmed with an independent PP1α loss-of-function model. Moreover, the used shRNA sequences differ from the previously used siRNA sequences, further excluding off-target effects and supporting a specific influence of PP1α on TCR-mediated signalling.

4.7 Knock down of PP1α attenuates IKK activity

Since transient knock down by siRNA was not applicable to biochemically characterise PP1α function within the TCR-induced signalling pathway, the inducible shRNA expression system was used for further experiments. Therefore, the phosphorylation status of several NF-κB pathway components upon TCR-engagement was analysed. In addition, the kinase activity of the endogenous IKK complex was determined by an *in vitro* kinase assay.

To this end, PP1α silencing or control shRNA expression was induced, as described above. After 72 hours of initial Dox application, cells were stimulated *via* the TCR over a period of 90 minutes. The dynamic activation of pathway components was monitored by obtaining samples of stimulated cells after defined periods of stimulation. To investigate IKK kinase activity, the endogenous IKK complex was immunoprecipitated from WCLs, using anti-NEMO antibodies. IKK activity was directly measured by applying a fraction of the

immunoprecipitates to an *in vitro* kinase assay using recombinant GST-IκBα as a substrate. In parallel, an equivalent portion of immunoprecipitated protein was subjected to SDS-PAGE to control for equal complex purification by immunoblot analysis. In addition, the phosphorylation pattern of various signalling proteins was determined in WCLs.

As seen in Fig. 4.7 A, PP1α-silencing correlated with a decrease in IKK kinase activity, visualised by autoradiography of ^{32}P-IKK and ^{32}P-GST-IκBα. Though, the initial IKKα/β autophosphorylation was comparable between PP1α sufficient and deficient cells, in the latter autophosphorylation declined more rapidly (Fig. 4.7 A and B). In contrast, phosphorylation of IKKα/β as assessed by immunoblot analysis of WCLs was unchanged in PP1α-silenced cells (Fig 4.7 A and C), indicating that the activity of IKK-Ks was not affected. Overall, the phosphorylation of GST-IκBα was less pronounced in the absence of PP1α (Fig 4.7 A and B), indicating that IKK kinase activity towards its substrate was decreased. Although phosphorylation of IκBα as assessed by phospho-immunoblot analysis seemed unaffected (Fig. 4 A), normalisation of phosphorylated to total IκBα protein levels revealed a reduction of substrate phosphorylation, again indicating that IKK kinase activity was reduced in of PP1α-silenced cells compared to control cells (Fig 4.7 C). In contrast, phosphorylation of p65 itself and the MAPKs p38 and Erk1 and Erk2 occurred to an equal extent in both cell lines (Fig. 4.7 A, quantification data not shown), implying that the strength of TCR stimulation between cell lines was comparable and could not account for the observed differences in IKK activity.

The experiments used to assess PP1α function were either based on endpoint measurements after several hours of stimulation or were covering only a time frame of up to 90 minutes. To gain an extended picture about the influence of PP1α on the NF-κB pathway, long-term kinetics of up to 6 hours were performed.

To this end, non- or PP1α-targeting shRNA expression was induced as previously described. 72 hours after Dox treatment, cells were stimulated *via* the TCR over a period of 6 hours, during which lysates of stimulated cells were prepared after different time points of stimulation. Subsequently, samples were subjected to SDS-PAGE and the phosphorylation status of NF-κB pathway signalling components was determined by phospho-immunoblot analysis (Fig. 4.8)

As shown in Fig. 4.8 A and B, phosphorylation of IKKα/b peaked after 0.5 hours of stimulation and was comparable in shContr. and in PP1α-silenced cells (Fig. 4.8 A and B), again indicating that the activity of upstream kinases, responsible for IKK phosphorylation,

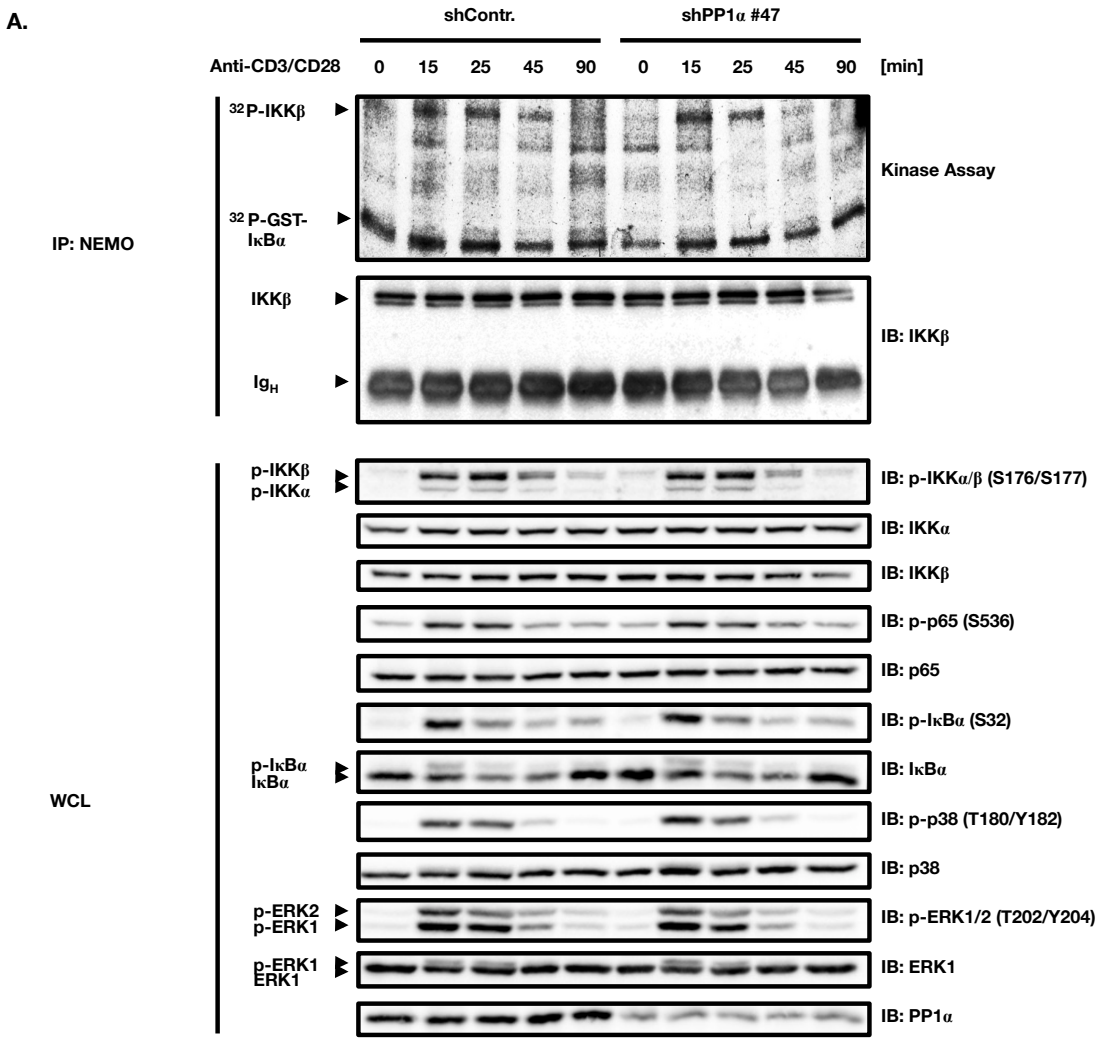
A.
shContr.
shPP1α #47
Anti-CD3/CD28
0 15 25 45 90 0 15 25 45 90 [min]
IP: NEMO
32P-IKKβ
32P-GST-IκBα
Kinase Assay
IKKβ
IgH
IB: IKKβ
WCL
p-IKKβ
p-IKKα
IB: p-IKKα/β (S176/S177)
IB: IKKα
IB: IKKβ
IB: p-p65 (S536)
IB: p65
IB: p-IκBα (S32)
p-IκBα
IκBα
IB: IκBα
IB: p-p38 (T180/Y182)
IB: p38
p-ERK2
p-ERK1
IB: p-ERK1/2 (T202/Y204)
p-ERK1
ERK1
IB: ERK1
IB: PP1α

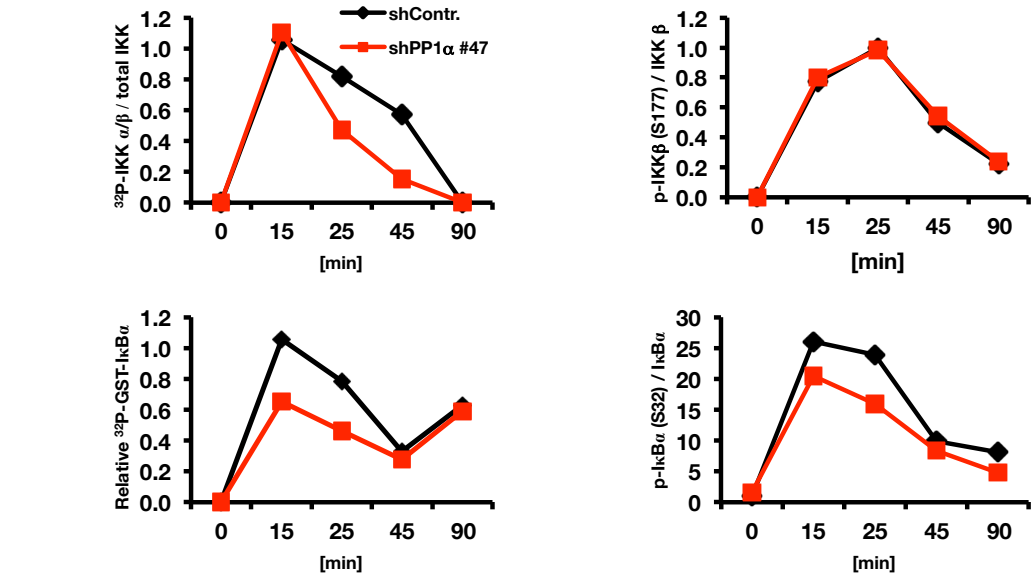
B.
32P-IKK α/β / total IKK
shContr.
shPP1α #47
[min]
Relative 32P-GST-IκBα
[min]
C.
p-IKKβ (S177) / IKK β
[min]
p-IκBα (S32) / IκBα
[min]

Figure 4.7 PP1α alters the kinetics of IKK kinase activity. (A) Indicated cell lines were treated with 2 µg/ml Dox to induce non-targeting shRNA expression in control cells (shContr.) or PP1α-silencing (shPP1α #47). 72 hours later, cells were stimulated with 0.5 µg/ml anti-CD3/CD28 for the indicated periods of time. Subsequently, cells were lysed and the IKK complex was immunoprecipitated using anti-NEMO antibody. To determine IKK activity, a fraction of the immunoprecipitate was subjected to a kinase assay in the presence of [γ-^{32}P]-ATP and recombinant GST-IκBα as substrate. An equal portion of immunoprecipitate and WCLs were subjected to SDS-PAGE, followed by immunoblot analysis using indicated primary antibodies. **(B)** Quantification of IKK autophosphorylation activity was carried out by quantifiying relative band intensities. The ^{32}P-IKK band and total immunoprecipitated IKKβ band intensities of control cells at 15 minutes of stimulation was set to 1. ^{32}P-IKK intensities were normalized to total IKKβ intensities, to obtain specific values for kinase activity per precipitated protein. Relative amount of ^{32}P-GST-IκBα was assessed by measuring respective intensities. Intensities in unstimulated cells were considered as background and set to 0, whereas the intensitiy in control cells at 15 minutes of stimulation was set to 1. **(C)** Relative quantification of of IKKβ (S177) and IκBα (S32) phosphorylation was performed by measuring intensities of the respective immunoblot. Intensities of p-IKKβ (S177) at 25 and p-IκBα (S32) at 15 minutes of stimulation in control cells were set to 1. Subsequently values were normalized to intensities of total IKKβ and IκBα to obtain values indicative for phosphorylation per total protein. Kinase assay, immunoblot analysis and quantifications are representative of three independent experiments.

is not likely to be influenced by PP1α. However, phosphorylation of IκBα was again slightly decreased by 20 to 30% (Fig. 4.8 A and B), confirming the previous finding. IKK phosphorylation was not altered, however kinase activity, measured by phosphorylation of IκBα was reduced in PP1α-silenced cells. In contrast, stimulation-dependent IκBα degradation and resynthesis occurred to a similar extent in the early phase of TCR-induced signalling (up to 2 hours). However, IκBα levels remained decreased at later time points after stimulation in PP1α-silenced cells. In line with the preceding experiment, p65 phosphorylation in the TAD domain was not observed to be influenced by the absence of PP1α.

Collectively, these results demonstrate and verify an influence of PP1α on IKK kinase activity, although kinetics and magnitude of IKK activation loop phosphorylation were unaffected. The slight changes in phosphorylation and degradation of IκBα require additional experimental attention, probably applying more sophisticated techniques not applicable at present. In summary, PP1α seems to have only a subtle influence on the early cytoplasmic events of signalling to NF-κB.

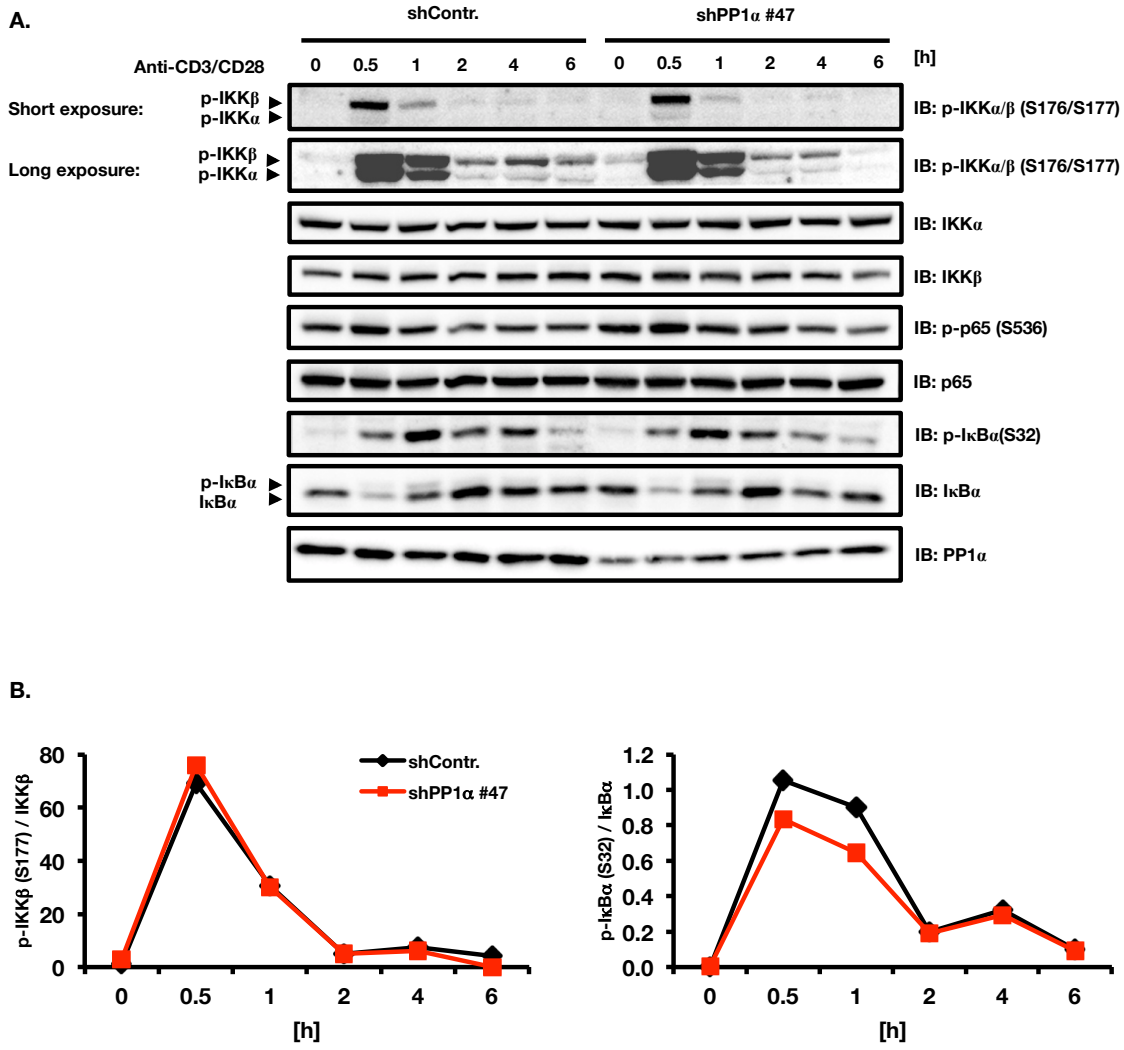

Figure 4.8 PP1α-silencing decreases IκBα phosphorylation. (A) Indicated cell lines were cultured in the presence of 2 µg/ml Dox to induce expression of non-targeting shRNA in control cells (shContr.) or PP1α-silencing (shPP1α #47). 72 hours later, cells were stimulated with 0.5 µg/ml anti-CD3/CD28 for the indicated periods of time. Subsequently, WCL were subjected to SDS-PAGE, followed by immunoblot analysis using indicated primary antibodies. **(B)** Quantification of relative IKKβ and IκBα phosphorylation normalized to total protein was performed as described in Fig. 4.7. Immunoblot analysis and quantifications are representative of 3 independent experiments.

4.8 PP1α does not affect TNFα induced signalling to NF-κB

In macrophages, PP1 has been described as a negative regulator of IKK activity in response to TNFα stimulation (Li et al., 2008). Such a role has not been observed in the present study. Nevertheless, the idea of an ambiguous signalling function of PP1α downstream of different receptor systems in the same cell type is an appealing concept. Therefore, we sought to

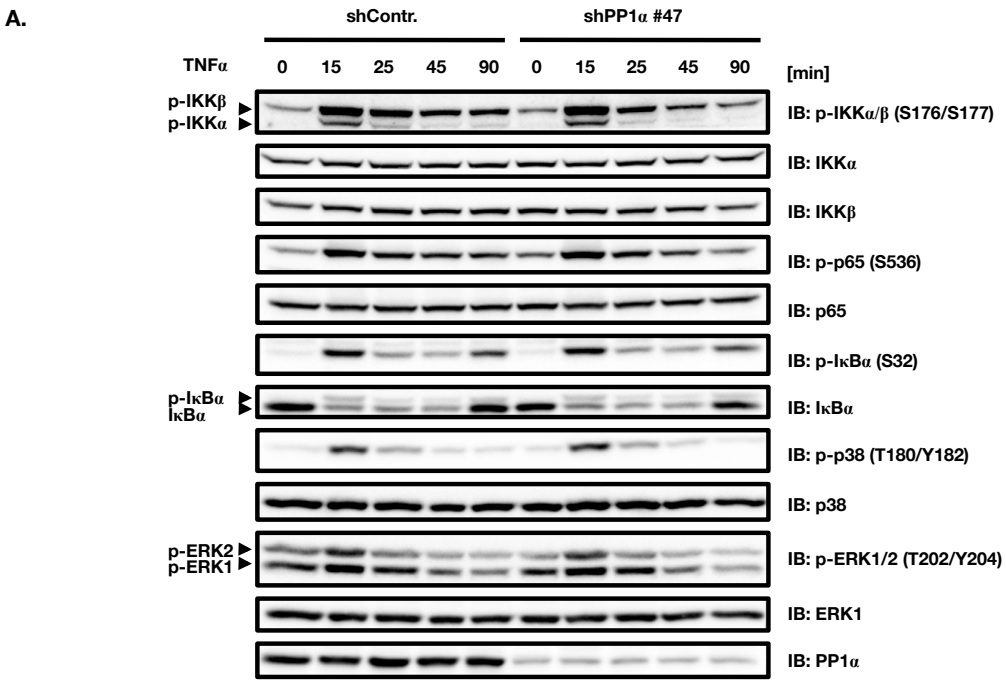
A.
shContr.
shPP1α #47
TNFα
0 15 25 45 90 0 15 25 45 90
[min]
p-IKKβ
p-IKKα
IB: p-IKKα/β (S176/S177)
IB: IKKα
IB: IKKβ
IB: p-p65 (S536)
IB: p65
IB: p-IκBα (S32)
p-IκBα
IκBα
IB: IκBα
IB: p-p38 (T180/Y182)
IB: p38
p-ERK2
p-ERK1
IB: p-ERK1/2 (T202/Y204)
IB: ERK1
IB: PP1α

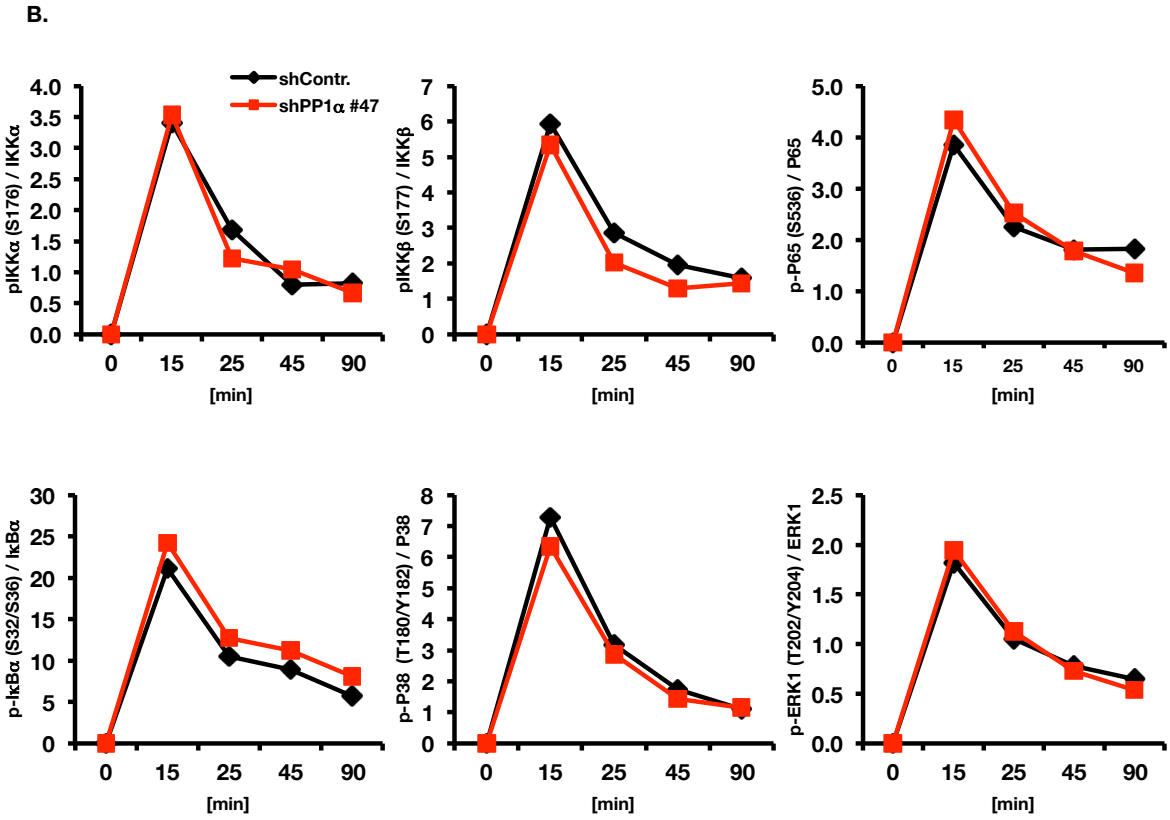
B.
shContr.
shPP1α #47
pIKKα (S176) / IKKα
pIKKβ (S177) / IKKβ
p-P65 (S536) / P65
p-IκBα (S32/S36) / IκBα
p-P38 (T180/Y182) / P38
p-ERK1 (T202/Y204) / ERK1
0 15 25 45 90
[min]

Figure 4.9 PP1α does not influence TNFα-induced signalling to NF-κB. (A) Indicated cell lines were cultured in the presence of 2 µg/ml Dox to induce expression of non-targeting shRNA in control cells (shContr.) or PP1α-silencing (shPP1α #47). 72 hours later, cells were stimulated for the indicated periods of time with 50 ng/ml recombinant TNFα. Subsequently, WCLs were prepared and subjected to SDS-PAGE, followed by immunoblot analysis using indicated primary antibodies. **(B)** For quantification of phosphorylation, band intensities were normalized to intensities of total protein, as described before. Intensities in unstimulated cells were set to 1. Shown immunoblot analysis and quantifications are representative of 3 independent experiments.

determine whether PP1α impinges on IKK activity after TNFR stimulation in T cells.

Knock down of PP1α or non-targeting shRNA expression was induced as described above. 72 hours later, cells were stimulated *via* TNFR1 by application of recombinant TNFα over various periods of time and activation of NF-κB and MAPK signalling was analysed as before.

As shown in Fig. 4.9, phosphorylation of the investigated signalling proteins collectively peaked after 15 minutes of TNFα stimulation and subsequently declining to basal levels. Intriguingly, the phosphorylation pattern was unchanged between PP1α-sufficient and -silenced cells (Fig. 4.9 A). Also normalisation of phospho-signals to total protein levels did not reveal overt differences (Fig. 4.9 B). Moreover, the previously observed decrease in IKK kinase activity after TCR engagement, was not apparent after TNFα stimulation (Fig. 4.9 B), suggesting that PP1α neither plays a negative nor a positive regulatory role in TNFR-induced NF-κB signalling in T cells. In line with these data, TNFα-induced NF-κB-dependent luciferase reporter acitivity was not altered in PP1α-silenced Gluc-J16 cells (Frey, 2009; data not shown), indicating that the phosphatase acts exclusively within the TCR-induced NF-κB pathway.

4.9 PP1α modulates *bona fide* NF-κB target gene expression

So far, the here performed experiments were not able to give any indication to the mechanism of PP1α function in TCR-induced NF-κB signalling. Although cytokine production and NF-κB reporter gene activity were affected in the absence of PP1α, the signalling cascade leading to NF-κB activation, despite a small reduction in IKK activity, seemed functional. However, these data only provided limited information about the transcriptional activity of NF-κB. To gain an extended picture of the kinetics of TCR-induced NF-κB-mediated gene expression in PP1α-silenced *versus* non-silenced cells, NF-κB responsive genes were subject of further analyses.

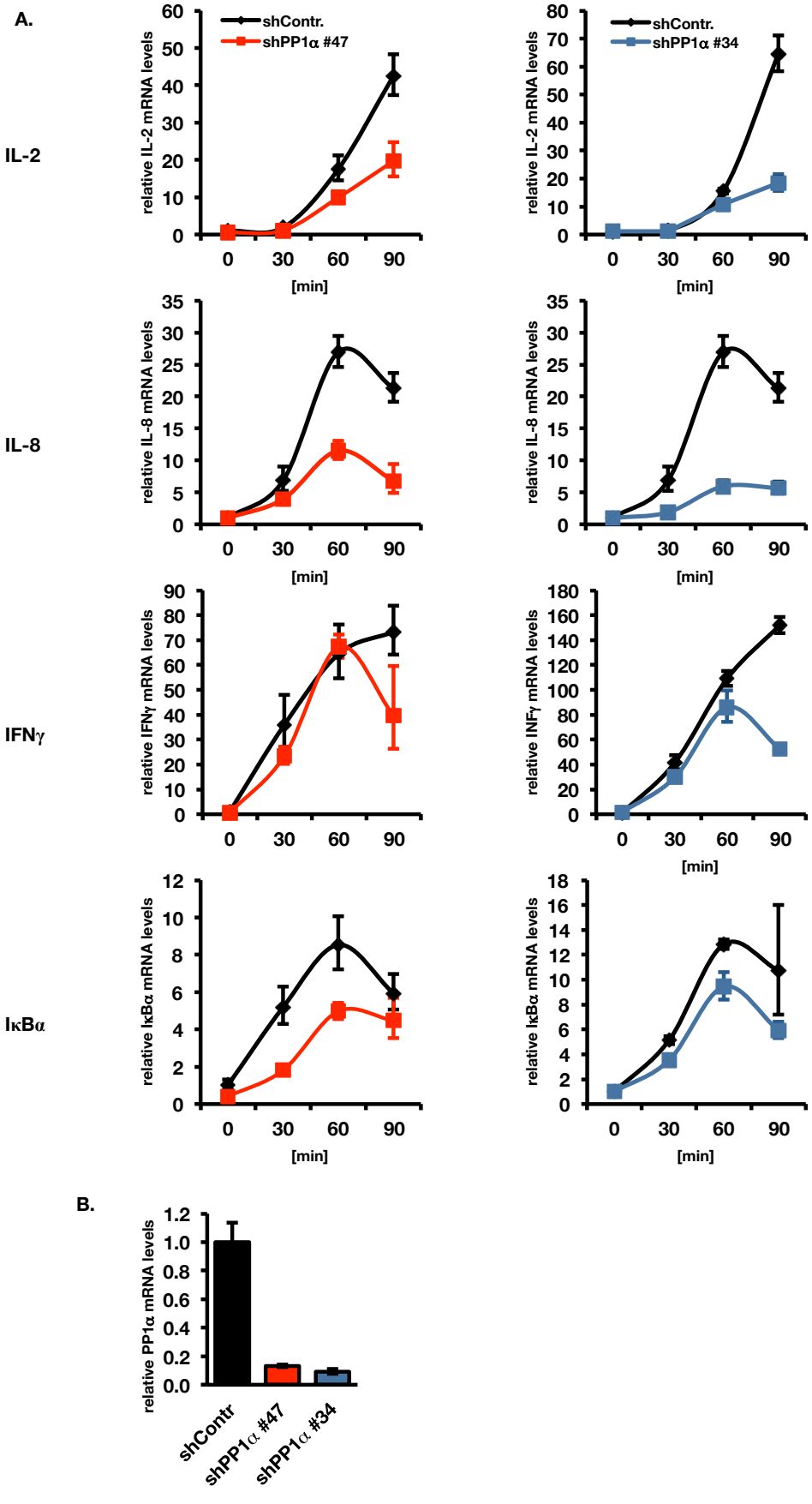
A.
IL-2
IL-8
IFNγ
IκBα
shContr.
shPP1α #47
shPP1α #34
relative IL-2 mRNA levels
relative IL-8 mRNA levels
relative IFNγ mRNA levels
relative INFγ mRNA levels
relative IκBα mRNA levels
[min]
0 30 60 90
B.
relative PP1α mRNA levels
shContr
shPP1α #47
shPP1α #34

Figure 4.10 PP1α influences transcription of *bona fide* NF-κB target genes. (A) Non-targeting and PP1α-targeting shRNA was induced in the indicated cell lines (shContr., shPP1α #47 and #34, respectively) by culturing cells in the presence of 2 µg/ml Doxycycline for 72 hours. Subsequently, cells were stimulated with 0.5 µg/ml anti-CD3/CD28 and mRNA levels of IL-2, IL-8, INFγ and IκBα were determined by qRT-PCR relative to unstimulated cells. **(B)** Relative PP1α mRNA levels in the indicated cell lines were assessed by qRT-PCR. Data are representative of five independent experiments.

PP1α silencing was induced in two cell lines, expressing independent PP1α shRNAs (shPP1a #47 and shPP1α #34). In addition, expression of non-targeting shRNA was induced in control cells (shContr.). 72 hours later, cells were stimulated *via* the TCR over various periods of time and mRNA levels of several *bona fide* NF-κB responsive genes, such as IL-2, IL-8, INFγ or IκBα, were determined by qRT-PCR.

As seen in Fig. 4.10 A, PP1α knock down, resulted in two to three fold lower levels of IL-2 and IL-8 mRNA after 60 or 90 minutes of stimulation compared to control cells. In contrast, INFγ mRNA was equally induced until 60 minutes of stimulation, but reproducibly declined in PP1α silenced cells thereafter, while in control cells, mRNA levels further increased. Thus PP1α silencing altered the kinetics of INFγ mRNA synthesis, while the overall induction of IL-2 and IL-8 mRNA was clearly lower. Interestingly, IκBα expression was only mildly affected among independent experiments (Fig. 4.10 A), together with the observation that IκBα protein is normally resynthesized after initial degradation in the absence of PP1α (Fig. 4.7).

In summary, expression profiling of the investigated genes demonstrates an impact of PP1α on transcriptional activity. Expression of several, but not all *bona fide* NF-κB target genes was shown to be influenced by PP1α. The decreased IL-2 and IL-8 mRNA levels are in line with the previous findings. Although transcription initiation is normal for all investigated mRNAs, the magnitude of synthesis appears to be controlled by PP1α, indicating that the phosphatase might regulate the occupancy or duration of NF-κB at promoter sites.

4.10 PP1α regulates DNA binding activity of NF-κB

The preceding experiment demonstrated a role for PP1α in regulation of NF-κB-mediated gene expression, presumably on the level of transcription. Two possible mechanisms may account for this phenotype: PP1α either regulates nuclear import of NF-κB dimers or modulates the DNA binding activity of the transcription factor. First, the DNA binding activity of NF-κB in PP1α-silenced *versus* non-silenced cells was determined using EMSA. In Jurkat, T cells, NF-κB was observed to exhibit high background binding activity in unstimulated cells and, thus, experiments were not always conclusive. Hence, primary T cells were used to assess the influence of PP1α on DNA binding of NF-κB.

For this purpose, primary $CD4^+$ T cells were either transfected with control or PP1α-specific siRNA. 72 hours after transfection, cells were stimulated *via* the TCR for the indicated time

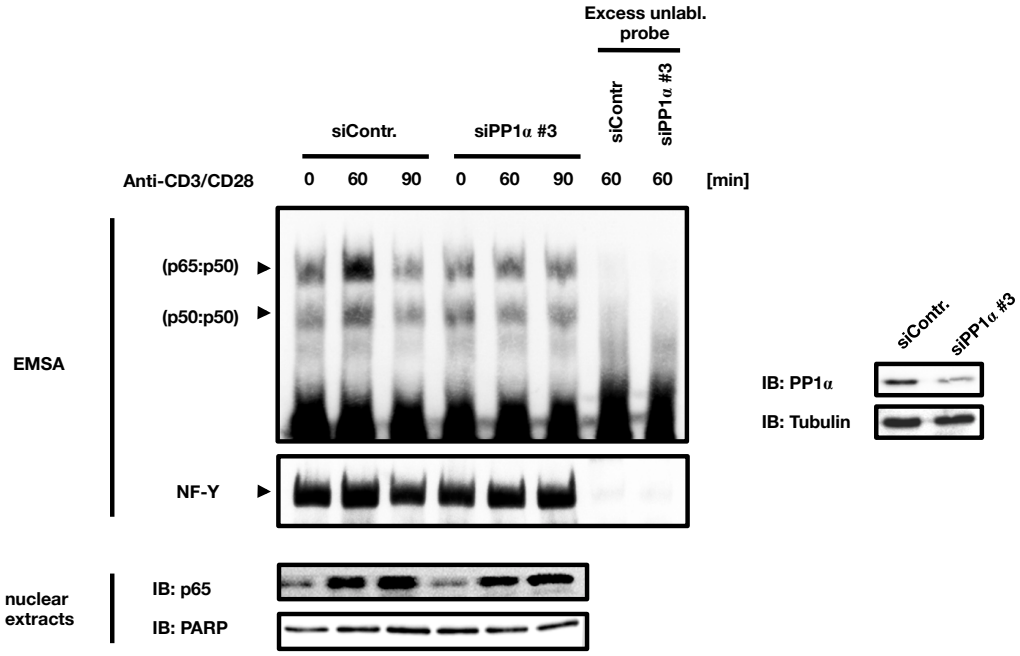

Figure 4.11 PP1α regulates DNA binding activity of NF-κB. Primary human T cells were transiently transfected with non-targeting (siContr.) or PP1α-targeting (siPP1α #3) siRNA. 72 hours later, cells were stimulated with 0.5 µg/ml anti-CD3/CD28 for the indicated periods of time. Subsequently, nuclear extracts were prepared and either subjected to EMSA using dsDNA oligonucleotides encompassing the NF-κB binding site in the IL-8 promoter or an EMSA using dsDNA oligonucleotides containing the consensus binding site of NF-Y to control for equal protein input. Specificity of protein:DNA complexes was controlled by supplying an excess of respective unlabelled dsDNA oligonucleotides. In parallel, nuclear extracts were subjected to SDS-PAGE, followed by immunoblot analysis. Immunoblots were probed with anti-p65 antibodies to monitor stimulus-dependent nuclear translocation of p65 and anti-PARP to control for equal loading. Cytosolic fractions of unstimulated cells were subjected to SDS-PAGE, followed by immunoblot analysis using indicated primary antibodies to control PP1α knock down (right panel). Results are representative of three independent experiments.

periods (Fig. 4.11). Subsequently, nuclear extracts of cells were prepared and subjected to EMSA, either using NF-κB-specific dsDNA- or NF-Y-specific dsDNA oligonucleotides, to control for equal protein input. Specificity of protein:DNA complexes was controlled, by adding anti-65 and anti-p50 antibodies to the binding reaction to induce supershifts (data not shown) or by applying unlabelled dsDNA probes in excess to compete binding of NF-κB- or NF-Y-bound labelled probes. Due to low cell viability after transfection, the analysis was limited to three time points after stimulation, which were previously tested to cover the peak of NF-κB DNA binding activity after TCR stimulation (data not shown). In addition, knock down of PP1α was controlled by immunoblot analysis.

As seen in Fig. 4.11 (top panel), binding activity of p65:p50 and p50:p50 complexes occurred in a stimulus-dependent manner and peaked at 60 minutes of TCR stimulation in control-transfected cells. In sharp contrast, knock down of PP1α (siPP1α #3), markedly reduced DNA-binding activity of p65:p50 and p50:p50 dimers (Fig. 4.11). In addition, nuclear translocation of p65 was analysed, using a portion of nuclear extracts for immunoblot analysis. Importantly, nuclear translocation of p65 was unchanged in PP1α-silenced cells (Fig. 4.11, lower panel).

Collectively, these data provide evidence that PP1α directly interferes with NF-κB function, by regulating its DNA binding activity. Nuclear translocation of p65 was unaffected in PP1α-silenced cells, indicating that albeit present in the nucleus, p65 is not competent in DNA binding in the absence of PP1α. This suggests that a so far unknown modification of p65 or a co-factor is regulated by PP1α.

4.11 Inhibition of PP1 by Tautomycetin attenuates IL-2 secretion

The presented data show that PP1α regulates NF-κB-mediated gene expression. However, this conclusion is primarily based on loss-of-function approaches. To complement these data, it was tested, whether the phospholytic activity of PP1α is required. For this purpose, Tautomycetin, a phosphatase inhibitor was used, which was shown to selectively inhibit PP1 activity (Han et al., 2003).

Hence, Jurkat or primary human $CD4^+$ T cells were treated with vehicle or increasing concentrations of Tautomycetin, ranging from 50 to 250 nM. Cyclosporine A (CsA), a known immunosuppressive drug, that counteracts NFAT nuclear translocation by inhibiting calcineurin, was used as a positive control. After five hours of pre-incubation with vehicle or inhibitors, cells were stimulated *via* the TCR and IL-2 secretion was measured by ELISA. As seen in Fig. 4.12, treatment of Jurkat (A) or primary human T cells (B) with Tautomycetin

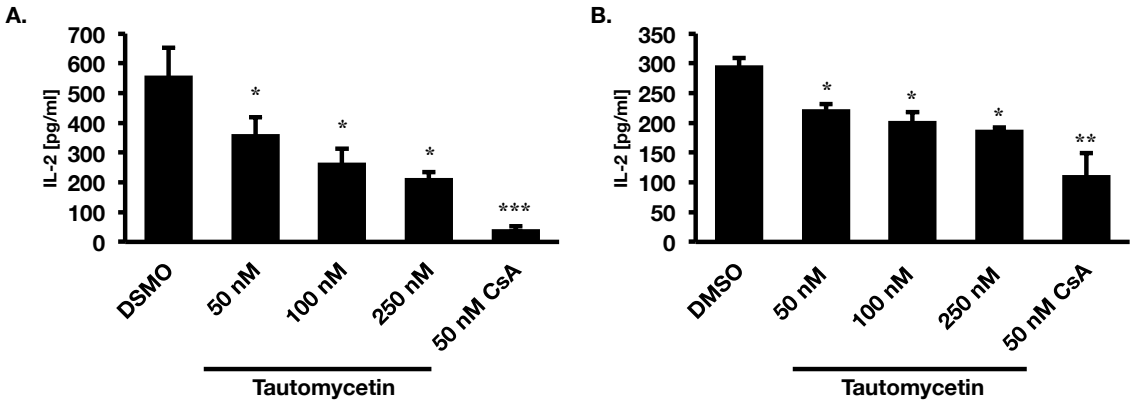

Figure 4.12 Inhibition of PP1α enzymatic activity attenuates IL-2 production. Jurkat T cells **(A)** or primary human T cells **(B)** were pre-treated with indicated concentrations of Tautomycetin, CyclosporinA (CsA) or vehicle (DMSO) as control for 5 hours. Subsequently, cells were stimulated with 0.5 µg/ml anti-CD3/CD28 overnight and levels of secreted IL-2 were measured by ELISA. Shown results are representative of five (A) or three (B) independent experiments. (mean +/- SD of three independent stimulations and replicate technical measurements); *, $p \leq 0.05$; **, $p \leq 0.005$

suppressed IL-2 secretion in a concentration-dependent manner. Although less effective than CsA, already 50 nM of Tautomycetin suppressed IL-2 by 30 to 40%, a degree comparable to the suppression of IL-2 seen in PP1α-silenced cells. Consistent with knock down of PP1α, Tautomycetin did neither affect cell viability nor cytoplasmic signalling to NF-κB (data not shown).

Taken together, inhibition of enzymatic activity largely phenocopies the previously described effect of PP1α knock down, indicating that catalytic activity is involved in regulation of NF-κB signalling by PP1α.

4.12 Inhibition or knock down of PP1α suppresses proliferation of primary human T cells

Knock down or inhibition of PP1α suppressed NF-κB-dependent cytokine secretion, like the growth factor IL-2, which is required to drive T cell proliferation. Thus, one may speculate about a role of PP1α in T cell proliferation. Hence it was tested, whether PP1α-silencing or inhibition interferes with TCR-induced proliferation.

Primary human $CD4^+$ T cells were isolated from peripheral blood of healthy donors and transfected with control or PP1α-specific siRNAs. In a second approach, primary T cells were treated with various concentrations of Tautomycetin or Cyclosporine A that were shown to suppress IL-2 secretion (Fig. 4.12). Proliferation of cells was determined using

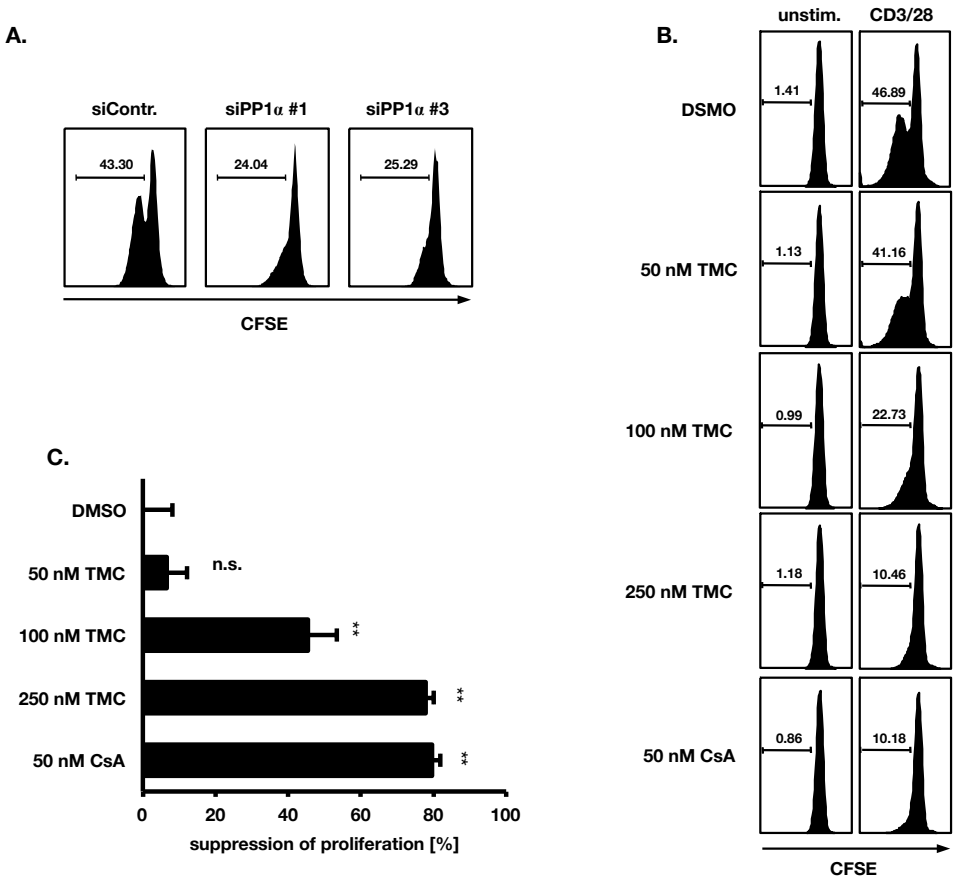

Figure 4.13 PP1α knock down or inhibition by Tautomycetin suppresses T cell proliferation. **(A)** Primary human T cells were transiently transfected with control (siContr.) or two independent PP1α-specific (siPP1α #1, siPP1α #3) siRNAs. 48 hours after transfection, cells were labelled with CFSE. On day three after transfection, labelled cells were stimulated with 0.2 µg/ml anti-CD3, 0.5 µg/ml anti-CD28 and 2 µg/ml GAM. Subsequently, CFSE dilution was measured by flow cytometry on day four after stimulation. Gated on living cells. **(B)** CFSE-labelled primary T cells were stimulated with anti-CD3/CD28 and GAM in the presence of indicated concentrations of Tautomycetin (TMC) or CsA or vehicle (DMSO) as control for five days. Inhibitors were freshly added to the culture medium on day two and four after stimulation. Subsequently, CFSE dilution was measured by flow cytometry on day five after stimulation. Gated on living cells. Results are representative of four independent donors. Numbers in histograms depict the percent of proliferating cells in the CFSE dilution gate. **(C)** Quantification of **(B)** depicted as percent suppression of proliferation compared to DMSO treated cells mean +/- SD of 4 independent donors **, $p \leq 0.005$

CFSE staining. Therefore, cells were labelled with CFSE 48 hours after transfection. 24 hours later, cells were stimulated *via* the TCR and proliferation was assessed on day four after stimulation following dilution of CFSE using flow cytometry. As shown in Fig. 4.13 A, knock down of PP1α using two independent siRNAs significantly reduced TCR-induced proliferation by 40 to 50% compared to control transfected cells. Knock down was

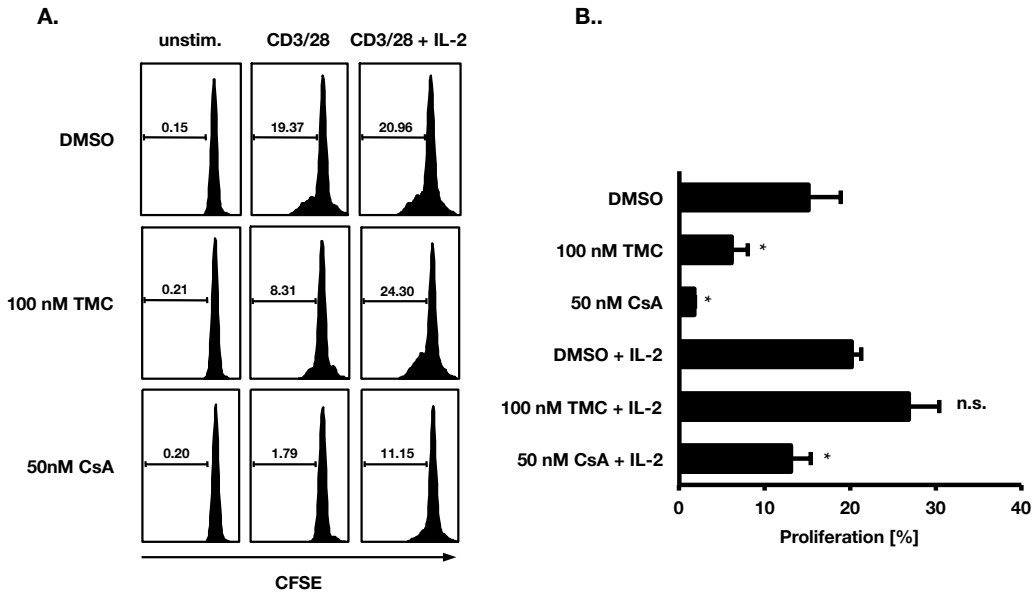

Figure 4.14 Tautomycetin-mediated suppression of proliferation is rescued by exogenous IL-2. (A) CFSE-labelled primary T cells were stimulated with 0.2 µg/ml anti-CD3, 0.5 µg/ml anti-CD28 and 2 µg/ml GAM. in the presence of indicated concentrations of Tautomycetin or CsA or vehicle (DMSO) as control for five days. In addition, cells were cultured in the presence or absence of exogenous IL-2 (100 U/ml) as indicated. Inhibitors were freshly added to the culture medium on day two and four after stimulation. Subsequently, CFSE dilution was measured by flow cytometry on day five after stimulation. Results are representative of three independent donors. **(B)** Quantification of (A) depicted as percent proliferation (mean +/- SD of three independent donors) Significance was calculated to DMSO or DMSO+IL-2 treated cells. *, $p \leq 0.05$

controlled by qRT-PCR and did result in reduced IL-2 secretion (data not shown). Congruently, inhibition of PP1α by Tautomycetin suppressed proliferation in a dose-dependent manner compared to control treated cells. Consistent with the degree of IL-2 suppression (Fig. 4.12 B), 100 nM of Tautomycetin suppressed proliferation by ~50% (Fig. 4.13 B and C). In contrast, 50 nM CsA was sufficient to suppress proliferation by 80%. Of note, neither knock down of PP1α nor Tautomycetin exhibited any effect towards cell viability, indicating that the reduced rate of proliferation was not caused by cell death. (data not shown).

To test whether the reduced production of IL-2 is causative for the lack of proliferation under these conditions, the experiment was repeated in the absence or presence of exogenous IL-2 (Fig. 4.14). Tautomycetin reproducibly suppressed proliferation by 50%, which was completely rescued by exogenous IL-2. Again, CsA abolished proliferation almost completely, but could not be fully rescued by exogenous IL-2.

In summary, these results indicate that reduced IL-2 production upon inhibition of PP1α is causative for the inhibition of proliferation in primary human T cells.

4.13 Knock down or inhibition of PP1α sensitizes NF-κB-dependent CTCL cells towards cell death

The Sézary Syndrome is an aggressive subtype of cutaneous T cell lymphoma (CTCL) and is characterised by constitutive proliferation of cells in the blood of patients. Several publications have established a direct link between persistent NF-κB activation in Sézary cells that is causal for their survival by constantly forcing expression of anti-apoptotic genes (Izban et al., 2000; Sors et al., 2006). However, to date, the molecular aetiology and abnormalities leading to persistent NF-κB activation are not well understood. However, the characterisation of CTCL cell lines reveals a differential dependence on different pathways (Brechmann, 2010). Whereas, for example Hut78 cells were shown to exhibit constitutively active Ras (Kiessling et al., 2011), HH cells rely on persistent IKK activity (Brechmann, 2010). While Ras inhibitors are already therapeutically used, systemic application of IKK inhibitors, although in clinical trials, might not be feasible. Since it was shown that IKK inhibition has unwanted side effects, causing inflammation and breakdown of barrier function in the intestinal epithelium (Pasparakis, 2009; Guma et al., 2011), it is of high interest to find novel cancer-specific molecular targets that can be therapeutically exploited.
The present study identified PP1α as a novel positive regulator of NF-κB in T cells. Intriguingly, PP1α seems to control the DNA-binding activity of NF-κB in a target gene specific manner. It is tempting to speculate that inhibition of PP1α might be a suitable therapeutic target in CTCL cells. To test this hypothesis, the influence of PP1α expression on CTCL cell survival was investigated. Therefore, two CTCL cell lines, Hut78 and HH, were transduced with inducible PP1α-specific shRNA expression constructs as described previously. Cells were selected for stable incorporation of the expression cassette into their genome and subsequently characterised for RFP positivity after Dox treatment using flow cytometry (data not shown). To test for knock down-dependent alterations in cell viability, shRNA expression was induced in Hut78, HH and Jurkat T cells. Non-Dox treated cells served as controls. Following Dox treatment, samples of cells were acquired on a daily basis. A portion of gathered samples was used to control for PP1α protein expression by immunoblot analysis. In parallel, cell viability was assessed by propidium iodide staining using flow cytometry.
Viability of Hut78 and Jurkat T cells was unaffected by Dox-mediated PP1α–silencing, but HH cells exhibited a strong increase in specific cell death in a time-dependent fashion (Fig. 4.15 A upper panel). Of note, the induction of the PP1α-specific shRNA expression led to a comparable decline of PP1α protein in both cell lines (Fig. 4.15 A lower panel), which paralleled increased cell death in HH, but not in Hut78 cells.

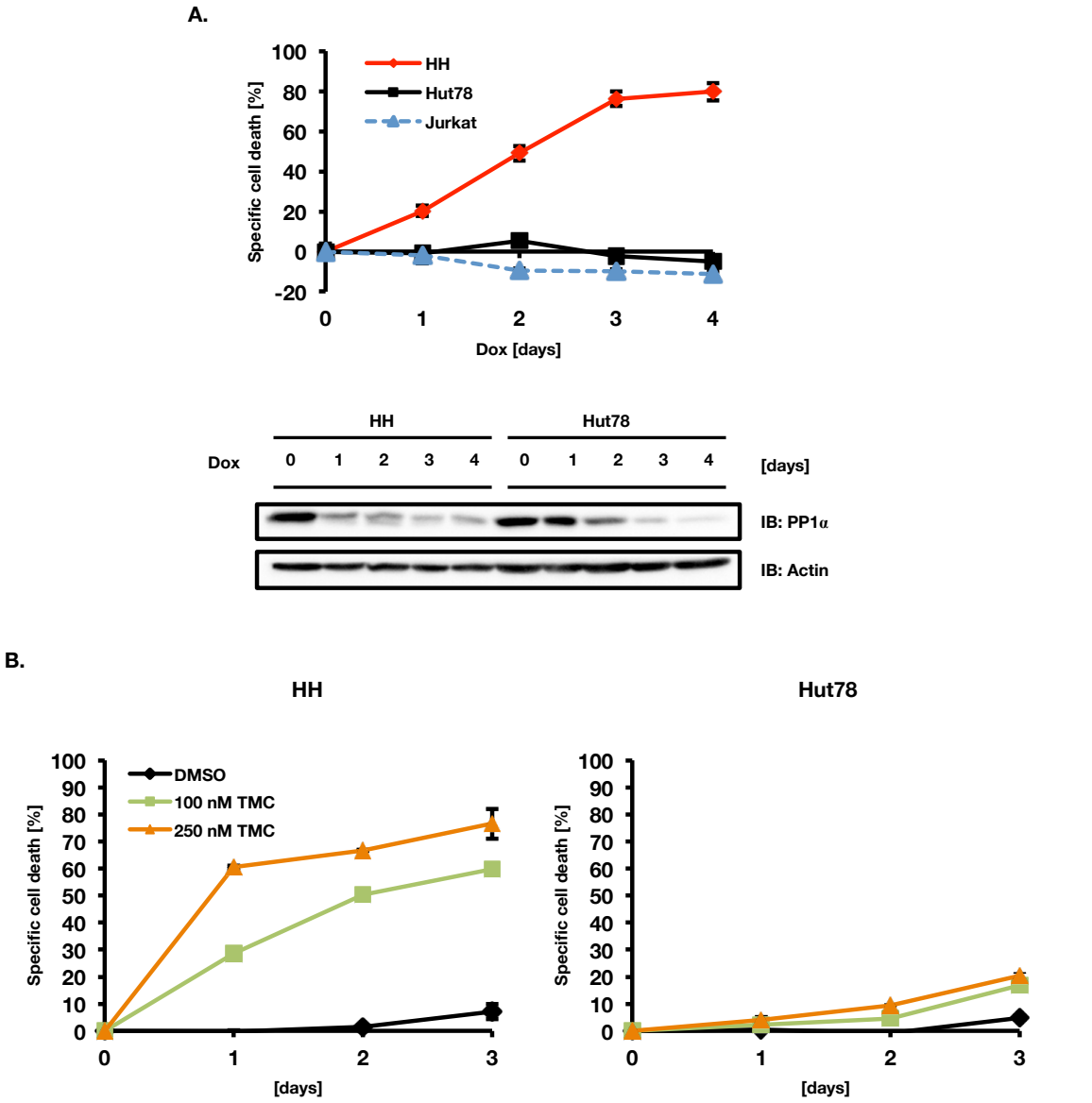

Figure 4.15 Knock down or inhibition of PP1α sensitizes the NF-κB-addicted CTCL cell line HH towards cell death. (A) Indicated cell lines were transduced with lentiviral vectors, containing a PP1α-specific Dox-inducible shRNA expression cassette. PP1α-silencing was induced by application of 2 µg/ml Dox. Subsequently, specific cell death, compared to untreated cells, was determined by propidiume iodide staining daily. WCLs were subjected to SDS-PAGE, followed by immunoblot analysis using the indicated primary antibodies, to control for PP1α-silencing (lower panel). Reprobing with anti-Actin antibodies verified equal loading. **(B)** HH (left panel) or Hut78 (right panel) cells were cultured in the presence of vehicle or indicated concentration of Tautomycetin (TMC) for three days. Viability of cells was determined daily by propidium iodide. Specific cell death, compared to untreated cells, was calculated as previously described.

Next, it was investigated whether inhibition of PP1 activity, rather than silencing, sensitises cells towards apoptosis (Fig. 4.15 B). Hence, HH and Hut78 cells were cultured in the presence of vehicle or different concentrations of Tautomycetin for up to three days. Cell

viability was assessed on a daily basis by propidium iodide staining using flow cytometry. Comparable to PP1α-silencing, HH cells were highly sensitive towards inhibition of PP1α activity, resulting in 60 to 70% specific cell death after three days of Tautomycetin treatment (Fig. 4.15 B, left panel). In contrast, PP1 inhibition exhibited significantly lower toxicity in Hut78 cells, resulting in ~15% to ~20% specific cell death after 3 days of treatment (Fig. 4.15 b right panel).

Taken together, these results demonstrate a differential role of PP1α in CTCL cell lines. HH cells seem to specifically depend on PP1α activity, indicating the phosphatase as a suitable therapeutic target.

5. Discussion

The transcription factor NF-κB is an indispensible regulator of the immune response. It mediates lymphocyte activation, proliferation and survival by controlling expression of cytokines, growth factors and anti-apoptotic genes (Schulze-Luehrmann and Ghosh, 2006). However, several lymphoid malignancies, such as CTCL or ABC-DLBCL, exploit NF-κB signalling, resulting in uncontrolled proliferation and expression of anti-apoptotic genes that render malignant cells resistant towards apoptosis and insensitive to classical chemotherapeutic treatment (Staudt, 2010). Thus, investigation of NF-κB activation as well as signal termination is of great interest.

Engagement of the TCR results in rapid signal transduction to NF-κB, mediated by posttranslational modifications of signalling mediators, such as phosphorylation. Many studies have concentrated on the identification and characterisation of kinases and their substrates, including signalling platforms, like the CBM complex or the IKKs and NF-κB subunits. Thus, phosphorylation events cover every step of TCR-induced NF-κB activation (see paragraph 1.3.5). However, phosphorylation is reversible and little is known about the role of phosphatases in modulating NF-κB activation, although phosphatases have been ascribed regulatory functions in several other signalling pathways (Virshup and Shenolikar, 2010). To date, only few genetic studies demonstrated a selective involvement of phosphatases in the NF-κB pathway (see paragraph 1.3.7). However, these studies were solely focussing on the TNFR system, using different non-lymphoid epithelial murine and human cell lines. Therefore, generalised conclusions, especially with regard to different receptor systems and cellular contexts, can not be drawn (Li et al., 2006b; Sun et al., 2009). To gain a more comprehensive picture of phosphatases in NF-κB signalling, we employed a semi-large scale RNAi screen using Jurkat T cells, allowing to simultaneously study signalling downstream of the TCR and the TNFR (Frey 2009, Brechmann, 2010). The genetic loss-of-function approach identified several known and unknown candidate phosphatases involved in NF-κB signalling (Brechmann, 2010). A subset of candidates selectively scored downstream of one of the receptor systems. Accordingly, PP1α was identified as a positive regulator of NF-κB specifically downstream of the TCR (see Fig. 4.1, Fig. 4.9) (Frey, 2009; Brechmann, 2010). The present study was conducted to validate this finding and characterise PP1α and its molecular mechanism with regard to NF-κB activation, T cell biology as well as its role as a possible therapeutic target in NF-κB-dependent T cell tumors.

5.1 RNAi screen identifies PP1α as a positive regulator of NF-κB in T cells

RNAi-screening has emerged as a powerful tool to identify components of specific cellular processes or signalling pathways. Only few RNAi screens were successfully performed in lymphocytes. Lymphocytes are largely refractory to liposome-based transfection methods and conventional electroporation requires high concentrations of siRNA and is further complicated by fluctuating cell viability (Sharma and Rao, 2009). Until now, RNAi screens in lymphocytes were primarily based on retroviral transduction of shRNA libraries. Using this method, several factors required for proliferation and survival of NF-κB-dependent B cell lymphoma cells were identified and characterised (Lenz et al., 2008; Bidère et al., 2009; Davis et al., 2010; Ngo et al., 2011). Although in the past proven to be successful, retroviral approaches entail several pitfalls especially in immune cells: viral infection of target cells may directly activate signalling pathways, thereby possibly masking a specific loss-of-function phenotype. In addition, successfully transduced cells have to be selected *via* antibiotic resistance, potentially leading to selection of unspecifically altered phenotypes induced by the technical procedure itself. Due to these obstacles, we favoured transient transfection of synthetic siRNA oligos. Although technically challenging, especially in suspension cells, we established a Jurkat T cell line, harbouring a stably integrated NF-κB-dependent reporter gene that allowed specific investigation of genes involved in NF-κB signalling. By using a siRNA library, we specifically analysed phosphatases or phosphatase-associated proteins involved in NF-κB signalling on a large scale (Brechmann, 2010). To our knowledge, only one technical report described a siRNA screen in Jurkat T cells utilising transient transfection to identify factors involved in CD95-mediated apoptosis (Zumbansen et al., 2006). In the present study, we used a commercially available nucleofection method for transfection of single siRNA oligos in an arrayed 96 well format. Nucleofection was found to be superior over other transfection methods, especially with regard to siRNA delivery, knock down efficacy and cell viability (Brechmann, 2010). The validity of the siRNA screen was confirmed by the reproducible scoring of positive controls, such as CYLD, CARMA1 or p65 (Fig. 4.1 A), which scored with high reproducibility under screening conditions. In addition, a number of phosphatases previously associated with NF-κB signalling or T cell function scored in our screen (Brechmann, 2010). Moreover, we identified and mechanistically characterised the PP4c:PP4R1 phosphatase holoenzyme as a negative regulator of IKK activity in T cells (Brechmann, 2010; Brechmann and Mock et al., manuscript in preparation), further strengthening the validity of the primary screening and analysis strategy. Taken together, these findings prompted us to investigate additional

candidate phosphatases. Accordingly, PP1α was identified as a putative positive regulator of NF-κB and, thus, was further investigated (Fig. 4.1 A).

PP1α belongs to the PP1 family of phosphoprotein phosphatases (PPP), which accounts for the majority of all phosphatase activity in eukaryotes (Bollen et al., 2010). The human genome contains three PP1-encoding genes that encode four PP1 isozymes: PP1α, PP1β and the splice variants PP1γ1 and PP1γ2. According to the BioGPS gene expression atlas (http://www.biogps.org, GeneAtlas), the four members exhibit a distinct expression pattern over different tissues. Interestingly, PP1α is predominantly expressed in cells of the hematopoietic system, suggesting a prominent role in immune cells. However, all PP1 members exhibit rather broad phospholytic activity *in vitro* and are implicated in almost all cellular processes, including mitosis, cytoskeleton organisation, transcription and signal transduction. Due to their pleiotropic activity and function, PP1 proteins are assisted by a myriad of regulatory proteins that confer substrate specificity, influence cellular localisation and control the phospholytic activity of the catalytic subunits (Ceulemans et al., 2002). At present, approximately 180 mammalian genes are known to encode direct PP1 interactors, but the actual number may be even higher (Bollen et al., 2010; Virshup and Shenolikar, 2010). PP1 proteins therefore exist in multimeric complexes, containing one catalytic subunit and one to two regulatory subunits. The RNAi library used in this study encompassed siRNA oligos targeting 20 known PP1 regulatory subunits. However, our data analysis and selection criteria did only qualify one PP1 regulatory subunit, called PP1R11, for hit selection. In contrast to PP1α though, PP1R11 was found to increase NF-κB activity, as well as cytokine secretion upon knock down (Blank, 2011). Therefore, validation and characterisation of the positive regulatory role of PP1α in TCR-induced NF-κB signalling focussed on the catalytic subunit itself.

Transient PP1α-silencing suppressed NF-κB reporter activity by 30% to 40%, a phenotype congruent with the z scores observed during the initial screen (Fig. 4.1 A). Since expression of several cytokines, including IL-2, IL-8 and IFNγ, critically depends on NF-κB function, we considered cytokine secretion as a more physiological readout than reporter gene assays. Accordingly, we observed a reduction in NF-κB-dependent cytokines, like IL-2 and IL-8, ranging from 40% to 60% in transiently PP1α silenced Jurkat T cells (Fig. 4.3). These findings were further extended to primary human T cells, suggesting that PP1α indeed plays an important role upon TCR engagement. Transient silencing by nucleofection, which harbours disadvantages, such as fluctuating cell viability and low cell numbers, limited biochemical analysis of signalling events. Hence, Jurkat T cell lines were established in which PP1α expression could be inducibly silenced (Fig. 4.5). Induced PP1α silencing reproduced the phenotypes observed by transient siRNA transfection. In addition, we could

exclude that the observed phenotypes were due to reduced cell viability, since we could not observe adverse effects of long term induced PP1α-silencing on cell survival in Jurkat T cells (data not shown). Hence, our initial findings could be validated by this independent approach (Fig. 4.6). Ectopic expression of PP1α induced NF-κB activity in HEK293T cells in the absence of any stimulus (Fig. 4.2 A). In contrast, overexpression of PP1α in Jurkat T cells augmented NF-κB activity only upon TCR-triggering, suggesting that the phosphatase is actively engaged downstream of the TCR (Fig. 4.2 B). Further underlining a role of PP1α in TCR-induced signal transduction, we found that PP1 phospholytic activity may be increased upon TCR engagement using immunoprecipitated PP1α for an *in vitro* phosphatase assay (data not shown). However, these results have to be evaluated with caution, since non-specific para-nitrophenylphosphate was used as a substrate. Thus, other unspecifically co-purified phosphatases may account for the increased phosphatase activity upon TCR stimulation.

Although one may suspect that due to its pleiotropic function, PP1α knock down may disturb several signalling pathways, we only found evidence for a function of PP1α in TCR-induced NF-κB activation. PP1α-silencing was neither found to affect TNF signalling or TNFα induced NF-κB reporter activity nor did we observe an effect on NFAT or AP-1 activation in T cells (Fig. 4.9 A and B and data not shown).

Taken together, our RNAi screening and subsequent validation strategy identified and confirmed PP1α as a novel positive regulator of NF-κB in T cells. In contrast to the here presented data, PP1α has previously been described to negatively regulate IKK activity (Li et al., 2008). However, the authors solely focused on the TNFR-induced IKK activation in HeLa cells. Moreover, critical experiments concerning interaction and activity were based on stably overexpressed proteins in antibiotically-selected HeLa cell lines and were not confirmed by more physiological approaches such as knock down or primary cell analysis.

5.2 The influence of PP1α on NF-κB signalling

Since PP1α was found to positively regulate NF-κB, we were interested whether PP1α directly interferes with signalling to NF-κB upon TCR engagement. Activation of the IKK complex is the crucial event within the canonical NF-κB pathway, mediating phosphorylation-induced degradation of IκB proteins. In the current study, different methods were employed to characterise signal transduction events, crucial for signalling to NF-κB activation in non-silenced *versus* PP1α-silenced cells. Accordingly, IKK kinase activity was assessed using *in vitro* kinase assays and signal propagation was monitored by

phospho-immunoblot analysis of critical pathway components, including IKKα, IKKβ, p65 and IκBα. PP1α-silencing correlated with a decrease in IKK activity towards recombinant substrate (Fig. 4.7). Accordingly, phosphorylation of IκBα was mildly decreased (Fig. 4.7). In contrast, phosphorylation of p65 at S536 in the transcription activation domain, which was also shown to be mediated by IKKβ, displayed no overt abnormalities (Fig. 4.7). Several questions arise from these observations: How does PP1α influence IKK activity? And, is the observed decrease in IKK activity of functional relevance for NF-κB activation?

In T cells, IKK activation is dependent on CBM complex-mediated recruitment of the IKK complex to the IS, followed by a series of posttranslational modifications of IKKα, IKKβ and NEMO that are essential to regulate kinase activity (Vallabhapurapu and Karin, 2009). In line with genetic studies, Delhase et al. have defined IKKβ as the dominant kinase component within the complex (Delhase et al., 1999), though IKKα may contribute to total IKK activity. The authors showed that phosphorylation of two conserved serine residues within the activation loop of the kinase domain of IKKα and IKKβ (S176/S180 and S177/S181, respectively) is crucial to induce kinase activity. These phosphorylation events were suggested to be mediated by transautophosphorylation. Additionally, TAK1 and MEKK3 were described to act as IKK kinases (Yang et al., 2001b; Shim et al., 2005). However, the studies could not provide evidence for a direct involvement in IKK activation loop phosphorylation *in vivo*. Hence, it was recently suggested that initial IKK activation occurs through proximity-induced transautophosphorylation, whereas TAK1 and MEKK3 assist to prolong IKK activity through a yet to be defined mechanism (Vallabhapurapu and Karin, 2009). We observed no differences in the peak of IKKα/β autophosphorylation (Fig. 4.7 A and B). However, IKKα/β autophosphorylation activity declined more rapidly in PP1α-silenced cells compared to control cells, which might be connected to reduced activity of the IKK-Ks. Interestingly, one study described a direct interaction between PP1α and MEKK3 (Bouwmeester et al., 2004). MEKK3 contains a conserved threonine residue at position 294 that when phosphorylated promotes 14-3-3 protein association resulting in decreased NF-κB activation upon TNFR and TCR triggering (Matitau and Scheid, 2008). Thus, one may speculate that PP1α, through its previously reported interaction with MEKK3, controls the IKK function, which may explain the changed kinetics of IKK activity. In contrast to the findings based on *in vitro* kinase assays, phospho-immunoblot analyses revealed no differences in IKKα/β activation loop phosphorylation on all investigated phospho-sites in PP1α-silenced cells (Fig. 4.4 and Fig. 4.7). Hence, PP1α may act on IKK phosphorylation by itself or through upstream mediators like MEKK3 *via* another mechanism. Accordingly, activation of IKK activity was described to be dependent on two separate events (Shambharkar et al., 2007). Although activation loop phosphorylation is

required, it is not sufficient to confer kinase activity. In addition, K63-linked ubiquitination of NEMO, in a CBM complex-dependent manner, was shown to be mandatory for IKK activity upon TCR stimulation. Since the present study focused on changes in phosphorylation of pathway components, it cannot be excluded that PP1α influences upstream signalling mediators required for ubiquitination of NEMO. Therefore ubiquitination of NEMO in PP1α-silenced cells should be investigated in the future. Alternatively, other means of regulation that have been shown to control IKK activity independent of activation loop phosphorylation (Delhase et al., 1999; Huxford and Ghosh, 2009) may account for the observed phenotype in PP1α-silenced cells. In this respect, two other regions within the IKKs, the HLH-motif and the NBD, are of special importance. The HLH motif directly interacts with the kinase domain and mutations within this motif have been shown to decrease IKK activity (Delhase et al., 1999). It contains several serine residues, which might be subject to regulation by PP1α. The NBD, which mediates binding of IKKα/β to NEMO harbors three phosphorylation sites (S733, S740 and S750) that control assembly and stability of the IKK complex (Higashimoto et al., 2008). However, PP1α-mediated alterations in IKK complex composition or an overall decrease of IKK complex per se were not supported by our data (Fig. 4.7 A), excluding an influence of PP1α. A prerequisite for a direct regulation of IKKs by PP1α would be a direct interaction between these proteins. Indeed, one study has previously shown a direct interaction between the IKK complex and PP1α (Li et al., 2008). In contrast to our data, this study suggested that PP1α negatively regulates IKK activity, by dephosphorylation of IKKα/β. Non-redundant roles of PP1α downstream of different receptor systems and/or different cell types might explain these contradicting results. Indeed, we have previously identified the PP4R1:PP4c phosphatase holoenzyme to negatively control IKK activation loop phosphorylation in T cells (Brechmann, 2010; Brechmann and Mock et al., manuscript in preparation), suggesting that different cell types use distinct phosphatases to counteract IKK activity. In line with this concept, one study described a positive regulatory role for the PP1-related protein PP2A by controlling NEMO function (Kray et al., 2005), although evidence exists that PP2A negatively regulates NF-κB signalling upstream of the IKK complex (see paragraph 1.3.7). Yet, the study has to be evaluated with caution, since the authors used broad range phosphatase inhibitors and methods that could potentially indicate a role for any PPP member, including PP1α. We did not observe an association between endogenous IKKs and PP1α in Jurkat or primary T cells (data not shown). However, using co-expression of IKK components and PP1α in HEK293T cells, we were able to co-purify exogenous PP1α preferentially with immunoprecipitated NEMO (data not shown). However, this preliminary finding has to be confirmed with endogenous proteins, since overexpression may lead to unspecific results.

IKK activity is regulated by a large number of posttranslational modifications, conferring conformational changes, subcellular localization and enzymatic activity. According to the phosphosite database (Hornbeck et al., 2004) IKKα, IKKβ and NEMO contain over 30 characterized phosphorylation sites, indicating a high degree of regulation. In this study though, investigation of phosphorylation sites was hampered by the availability of high-grade phospho-site-specific antibodies and, thus, the analyses were limited to a subset of phosphorylation sites. Therefore, potentially more sensitive and unbiased approaches might help to identify PP1α-regulated phosphorylation sites (discussed in paragraph 5.6). Our findings imply that PP1α acts in a TCR-dependent manner, either by regulating phosphorylation of T cell-specific signalling components or by being actively engaged after TCR engagement through an unknown mechanism. However, ectopic expression of PP1α in HEK293T cells induced NF-κB activity in the absence of any stimulus, suggesting that PP1α substrates are not T cell specific, but PP1α phospholytic activity is regulated in a TCR- or CD28-dependent manner. Based on findings of the present study, the possible mechanisms of regulation of NF-κB activation by PP1α remain elusive and it appears unlikely that the observed mild changes in IKK activity can account for the pronounced effects on cytokine secretion. IκBα phosphorylation and degradation were only mildly affected in PP1α-silenced cells, while p65 phosphorylation at serine 536 remained unchanged compared to control cells. However, PP1α as a catalytic subunit may function in different phosphatase holoenzymes at more than one level of the NF-κB activation cascade. Therefore, it is plausible that the sum of different effects, including the influence on IKK activity as well as other putative molecular alterations in the NF-κB pathway account for the observed phenotype.

5.3 Regulation of NF-κB mediated gene transcription by PP1α

Although IKK activity as well as IκBα phosphorylation were found to be mildly attenuated, subsequent signalling leading to nuclear translocation of p65, at least in scope of the used readouts, seemed to be unchanged in PP1α-silenced compared to non-silenced Jurkat T cells. In contrast, the presented data clearly demonstrates an influence of PP1α on the kinetics and strength of *bona fide* NF-κB target gene transcription, such as IL-2, IFNγ and IL-8 (Fig. 4.10). Surprisingly though, IκBα transcription and resynthesis, which is solely dependent on NF-κB activity, was mostly unaffected (see Fig. 4.8 and 4.10). To understand this dichotomy, the different regulatory elements of NF-κB target gene selectivity have to be taken into consideration. NF-κB is activated by different stimuli, such as TNFα, LPS or

antigen receptor-triggering (Sen and Smale, 2010). However, each different stimulus results in the activation of distinct sets of NF-κB target genes. In addition, the response in different cell types, like lymphocytes, macrophages or epithelial cells, to the same NF-κB activating stimulus is different as well (Smale, 2011). Therefore, several layers of regulation confer a selective NF-κB response. One mechanism of a selective NF-κB response seems to be the regulation of different target genes by distinct homo- and heterodimeric NF-κB species. In cells lacking either c-Rel or p65, most NF-κB target genes are expressed normally, suggesting highly redundant functions or compensatory mechanisms (Gerondakis et al., 2006). However, some target genes depend on one particular NF-κB subunit for expression. Both, c-Rel and p65 deficient mice (Gerondakis et al., 2006), exhibit immune defects, proving that the function of these proteins is not entirely redundant. Microarray analysis performed in c-Rel-deficient T cells revealed only few genes that show strong dependence on this particular member (Bunting et al., 2007). For example, IL-2 expression was found to be attenuated. However, the authors do not exclude that c-Rel function might not be limiting for IL-2 expression and that other NF-κB subunits are able to substitute for loss of c-Rel. Most cytoplasmic c-Rel is bound by IκBβ, which, like IκBα, is degraded in an IKK-dependent manner. However, we did not detect a defect in IκBβ degradation in PP1α-silenced Jurkat T cells (data not shown), suggesting that PP1α does not selectively interfere with c-Rel function. In line with these observations, IL-8 and IFNγ expression that have been shown to mainly depend on p65 function and being independent of c-Rel (Kunsch and Rosen, 1993; Sica et al., 1997), were suppressed in PP1α-silenced cells (Fig. 4.10), thus excluding an selective effect on c-Rel.

Another fundamental feature of canonical NF-κB activity is its transience. Indeed, relative induction of IL-2, IFNγ and IL-8 expression was not affected up to 60 minutes after stimulation (Fig. 4.10). Only after 60 (for IL-8) and 90 minutes (for IL-2 and IFNγ), relative transcript levels were significantly reduced in PP1α-silenced *versus* non-silenced cells. Most interestingly, IFNγ expression was equally induced in PP1α-deficient and sufficient cells until 60 minutes of stimulation, but abruptly declined thereafter in the former, while PP1α-sufficent cells further increased IFNγ transcript levels (Fig. 4.10). In line with these data, reduced DNA binding activity of p65:p50 dimers at 60 minutes of stimulation in PP1α-silenced primary T cells was demonstrated (Fig. 4.11). Taken together, these observations suggest that PP1α might regulate the dwell time of NF-κB in the nucleus or its occupancy at certain promoter sites. The major pathway to regulate NF-κB nuclear localisation described is *via* nuclear export of IκBα and IκBε-associated NF-κB proteins (Sen and Smale, 2010). NF-κB-mediated expression of IκBα and IκBε is rapidly induced upon NF-κB activating

stimuli. *De novo* synthesised IκBs translocate to the nucleus, associate with NF-κB dimers, and export the transcription factor to the cytoplasm *via* NESs present at the N-terminus. In addition, IκBα was observed to actively disrupt DNA-bound NF-κB complexes *in vitro* in a cell free system, which may also apply to promoter-bound NF-κB in the nucleus (Zabel and Baeuerle, 1990). However, nuclear translocation of p65 was unaffected upon PP1α-silencing (Fig. 4.11). Our analyses did not include other NF-κB subunits or IκB proteins and immunoblot analysis might be not sensitive enough to detect minor differences in NF-κB translocation, when only a subset of target genes is regulated by such a mechanism. One approach to address such a question in more detail, would be through monitoring nuclear/cytoplasmic shuttling of NF-κB subunits in PP1α-silenced *versus* non-silenced cells, using time-lapse microscopy or high throughput Image-Stream© analysis. In contrast to IκBα, IκBβ does not contain a NES and was shown to translocate to the nucleus and associate with promoter-bound NF-κB proteins to stabilize DNA-protein interactions at a subset of promoters (Suyang et al., 1996; Rao et al., 2010). Accordingly, one may envision that PP1α-silencing causes disruption of such stabilised complexes, causing normal nuclear export *via* binding of NES-containing IκB proteins. However, IκBβ stabilised NF-κB-DNA complexes have only been shown to form upon prolonged TNFα stimulation and PP1α-silencing only caused decreased NF-κB acitivity downstream of the TCR, but not of the TNFR (Frey, 2009; data not shown).

Degradation of promoter-bound p65 was reported as another regulatory mechanism to control the transient nature of NF-κB-dependent gene expression (Sen and Smale, 2010). Several laboratories have shown that an E3-ligase complex in conjunction with the ubiquitously expressed negative NF-κB regulator COMMD1 facilitates the proteasome-mediated degradation of p65 (Maine et al., 2007; Sen and Smale, 2010). In addition, methylation of p65 at lysine 314 and 315 by the methyltransferase SET9 has been implicated in marking promoter-bound p65 for degradation in an inducible and promoter-specific manner. SET9 knock down resulted in increased IL-8 expression, but had no effect on A20 or IκBα (Yang et al., 2009). Therefore, pre-bound SET9 at a subset of promoters might constitute one mechanism by which promoters are marked for down-regulation by p65 degradation. Indeed, the activity of SET methyltransferases was shown to be counteracted by phosphatases, suggesting a possible point of interference with PP1α. Another group of enzymes, the protein inhibitor of STAT (PIAS) proteins were shown to control promoter occupancy of NF-κB dimers in a promoter-specific manner. PIAS1 and PIAS4 knockout mice are hypersensitive to septic shock and exhibit enhanced DNA-binding activity to p65 (Liu et al., 2004; Liu et al., 2005). Interestingly, PIAS1 and PIAS4 regulate

expression of distinct NF-κB target genes. Whereas PIAS1 has substantial effects on TNF-induced IκBα and IL-1β expression, PIAS4 affects expression of the chemokine CXCL1 (Ruland, 2011). Yet, their exact mode of action is unknown, but involves block of DNA-binding activity and recruitment of co-repressors. A fraction of IKKα is constitutively associated with PIAS1 and can directly phosphorylate PIAS1 after inflammatory activation (Liu et al., 2007). This modification induces dissociation of PIAS1 from the kinase and stimulates its movement to promoters of NF-κB target genes to mediate transcriptional termination. Whether such a mode of regulation also occurs in T cells was not investigated so far. However, the finding that PIAS1 knockout mice exhibit normal signal transduction and normal nuclear translocation of p65 is similar to our observations in PP1α-silenced cells (Fig. 4.7; Fig. 4.11). Therefore, regulation of PIAS activity by PP1α is an appealing idea and should be analysed further.

The above discussed mechanisms give only a snapshot of the regulatory elements that contribute to the transient nature of an NF-κB response in the nucleus. The presented data strongly suggest a nuclear role of PP1α in regulating NF-κB activity, since cytoplasmic signalling events seem not overtly altered. To further analyse the influence of PP1α on promoter-specific NF-κB binding activity *via* PIAS1, SET proteins or other putative mechanisms, chromatin immunoprecipitation (ChIP) should be employed to gain an extended picture of the dynamics of NF-κB presence at selected promoters.

5.4 PP1α function is required for normal T cell proliferation

The presented data shows that knock down of PP1α in primary human $CD4^+$ T cells results in a significant reduction of IL-2 secretion. IL-2 is an essential growth factor for T cells required for their proliferation. Thus, we were interested whether the suppressed IL-2 secretion would have any impact on the proliferative capacity of T cells. Indeed, we found that knock down of PP1α resulted in a substantial decrease in proliferation of up to ~50%, correlating with the degree of IL-2 suppression (Fig. 4.3 C and Fig. 4.13 A). Since transient transfection of primary human T cells by nucleofection generally decreased cell viability and we also wanted to address whether inhibition of enzymatic activity would suffice for the observed phenotype, we explored the use of the PP1 inhibitor tautomycetin. Tautomycetin is a natural anti-fungal antibiotic extracted from the bacterium *Streptomyces spiroverticillatus.* Most phosphatase inhibitors, like ocadaic acid, calyculin A, mycrocytins or fostriecin exhibit a rather broad spectrum inhibitory activity towards several PPPs, probably due to the structural similarity of the catalytic domain of PPPs (Shi, 2009). In contrast,

tautomycetin has been defined as a highly specific inhibitor of PP1, suppressing phospholytic activity of PP1 proteins 40 fold stronger than that of PP2A or PP2B at low concentrations (Mitsuhashi et al., 2008). Application of 50 to 100 nM tautomycetin reduced IL-2 secretion by 40 to 50% in Jurkat and in primary human $CD4^+$ T cells, comparable to knock down of PP1α (Fig. 4.12). Importantly, tautomycetin exhibited no cytotoxic effects at the used concentrations. Therefore, we also assessed whether tautomycetin application would suppress T cell proliferation. In line with the degree of suppressed IL-2 secretion, 100 nM tautomycetin suppressed T cell proliferation by ~50%, again not affecting cell viability (Fig. 4.13 B). These data strongly suggest that the suppressed proliferation is directly connected to reduced IL-2 production. Indeed, the defect in proliferation by tautomycetin treatment was completely rescued by addition of exogenous IL-2 (Fig. 4.14), implying that the PP1 inhibition- or knock down-mediated suppression of IL-2 is causal for the proliferative defect. CsA, a known immunosuppressive drug targeting calcineurin and thereby NFAT function, was used as a control. In contrast to tautomycetin, CsA-mediated suppression of proliferation could not be completely rescued by IL-2 addition (Fig. 4.13 B), indicating that the inhibitor affects more than one pathway or overlapping pathways to a different extent. Accordingly, it has been known that calcineurin inhibition by CsA influences signalling to NF-κB (Marienfeld et al., 1997), resulting in lower IKK activity in T cells. Two recent publications substantiate this observation, demonstrating that calcineurin activity is needed for CBM-complex stability by dephosphorylation of Bcl-10 (Palkowitsch et al., 2011; Frischbutter et al., 2011). Hence, while CsA inhibits both NFAT and NF-κB signalling, PP1α inhibition or knock down, on the basis of our data, selectively affects NF-κB function, explaining why the CsA-mediated suppression of proliferation may not be completely rescued by exogenous IL-2. Our suggestion that PP1α selectively interferes with NF-κB function is supported by the observation that p65-deficient T cells exhibit reduced, but not completely suppressed proliferative capacity (Doi et al., 1997). Tautomycetin has been described as a T cell-specific immunosuppressive compound before (Shim et al., 2002; Han et al., 2003; Chae et al., 2004). However, most of the studies used concentrations of tautomycetin in the micromolar range, which was shown to inhibit other PPP members as well (Han et al., 2003). In line with another study that investigated the effects of tautomycetin on T cell viability (Shim et al., 2002), we observed increased cell death at these concentrations (data not shown), indicating unspecific effects. Interestingly, inhibition of PP1α by tautomycetin has also been implicated to suppress IKK activity in HEK293T cells (Mitsuhashi et al., 2008). In contrast to our data, tautomycetin almost completely suppressed IKK activity in response to TNFα. However, the different cellular setting

combined with the use of very high concentrations of tautomycetin and the lack of genetic evidence by knock down of PP1α limits comparisons of this study to ours.
Taken together, we demonstrate a direct connection between PP1α and IL-2-dependent T cell proliferation. Moreover, due to our data, demonstrating an influence of PP1α on NF-κB mediated IL-2 gene expression, we suggest that this is directly connected to regulation of NF-κB by PP1α. However, more experimental work is required to delineate the role of PP1α in T cell physiology.

5.5 Therapeutic targeting of PP1α in Sézary syndrome

The concept of "oncogenic addiction" has initially been defined by Weinstein (Weinstein, 2002) and reflects the observation that cancer cells are dependent on (or "addicted to") the activity of oncogenic factors or pathways for sustained proliferation and survival, by counteracting pro- and enhancing expression of anti-apoptotic factors (Weinstein, 2002; Hanahan and Weinberg, 2011). However, single oncogenes are not sufficient to drive tumorigenesis. Collaboration with other oncogenes or loss of tumor suppressors are required. In contrast, single oncogene suppression has been shown to restore the balance between pro-and anti-apoptotic factors, which allows a cell to reinstate its physiological checkpoint mechanisms, resulting in spontaneous apoptosis of tumor cells (Weinstein, 2002; Weinstein and Joe, 2008; Hanahan and Weinberg, 2011). Hence, oncogenes or oncogenically activated pathways can also be considered as the *Achilles heel* of cancer cells. Several studies have established the oncogenic activation of NF-κB, through a variety of oncogenic mutations of pathway components, as a hallmark of several hematologic malignancies (reviewed in paragraph 1.4). A shared consequence of these mutations is the constitutive activation of IKKs. Accordingly, many IKK inhibitors have been developed and proven to exhibit anti-tumorigenic effects in a variety of experimental *in vivo* models, ranging from lymphoma to melanoma (Amschler et al., 2010; Lam et al., 2005). However, at present no such drug has been clinically approved. Several hurdles may hamper the systemic inhibition of IKKs: (i) long-term and full inhibition of IKKβ would be expected to impair innate and adaptive immunity, (ii) since IKKβ was described to counteract IL-1β processing and secretion, IKKβ inhibition might cause severe inflammation (Greten et al., 2007) and (iii) IKK activity has been shown to be essential to maintain epithelial barrier function in the small intestine (Pasparakis, 2009; Guma et al., 2011). Therefore, it may be more applicable to target disease-specific molecular lesions. Accordingly, frequent mutations in the signalling activators CARMA1 and MyD88 have recently been described to

drive persistent activity of downstream effectors (like IKKs and IRAK1/4, respectively) in ABC-DLBCL cell lines and patient specimens, resulting in constitutive NF-κB activity (Lenz et al., 2008; Ngo et al., 2011). Knock down of these oncogenic factors or interference with their downstream effectors sensitised cells towards cell death. The identification and characterisation of oncogenic mutations and their consequences can therefore open new windows of opportunity for therapeutic intervention.

CTCLs belong to a rather heterogeneous group of skin-associated neoplasms among which the leukemic Sézary syndrome (SS) represents the most aggressive subtype (reviewed in paragraph 1.4.1), which to date is not curable. Several publications have established a direct link between SS cell survival and a dependence on persistent NF-κB activity (Izban et al., 2000; Sors et al., 2006; Sors et al., 2008). CTCL cell lines, like HH, SeAx and MyLa as well as malignant peripheral blood lymphocytes from SS patients are susceptible to inhibition of the NF-κB pathway (Sors et al., 2006; 2008; Kiessling et al., 2009). Hence, CTCL cells are defined as oncogenically addicted to NF-κB. However, the molecular aetiology of persistent NF-κB activity in SS is largely unknown (Lenz et al. 2008; Ngo et al., 2011). Our RNAi screening approach identified the PP4c:PP4R1 phosphatase holoenzyme as a negative regulator of the IKK complex in T cells (Brechmann, 2010, Brechmann and Mock et al., manuscript in preparation). In addition, we found PP4R1 expression to be reduced or absent in a subset of CTCL cell lines as well as in SS patient samples. Ectopic expression of PP4R1 in the PP4R1-deficient CTCL cell line HH inhibited constitutive IKK activity and sensitised cells towards cell death. Therefore, deficiency of PP4R1 might be one causative factor that contributes to oncogenic NF-κB addiction in a subgroup of CTCLs. However, therapeutic targeting of IKK activity by reintroducing PP4R1 in PP4R1-deficient cells is hardly applicable. Since PP1α was found as a positive regulator of NF-κB, we reasoned that the phosphatase may constitute a suitable therapeutic target for treatment of NF-κB-addicted CTCL. Therefore, we analysed the dependence of the CTCL lines HH and Hut78 on the expression of PP1α, using our Dox-inducible knock down system. Indeed, we found a strong dependence of HH cell survival on PP1α expression (Fig. 4.15 A). These findings could be further substantiated by the application of the PP1 inhibitor tautomycetin, which selectively induced apoptosis in HH, but not Hut78 or Jurkat T cells (Fig. 4.15 B and data not shown). Hence, we conclude that PP1α-targeting might be a future possibility for treatment of CTCL. Indeed, tautomycetin in addition to its immunosuppressive capacity, has been previously shown to exert anti-tumorigenic effects (Adler et al., 2009). In addition, systemic application of tautomycetin in a rodent islet allograft model for up to 100 days was not exerting specific organ toxicity (Wee et al., 2010).

However, substantial experimental work has to be conducted to show whether PP1α inhibition is causative for suppression of NF-κB acitivity in CTCL leading to cell death.

5.6 Outlook

The present study identified and characterised PP1α as a positive regulator of NF-κB signalling after TCR engagement using different experimental readouts. Loss of function approaches demonstrated a significant impact on NF-κB-driven cytokine production, most likely regulating DNA-binding activity of NF-κB. Moreover, silencing and enzymatic inhibition of PP1α was found to inhibit IL-2 dependent proliferation of primary human T cells. Furthermore, silencing and enzymatic inhibition of PP1α in HH cells identify the phosphatase as a possible therapeutic target in NF-κB-addicted CTCL cells. Although these are several lines of evidence for a physiological function of PP1α in T cells, the exact molecular mechanism of NF-κB regulation by PP1α remains to be resolved. Analysis of the NF-κB signalling pathway yielded little information, apart from a reproducibly observed decrease in IKK activity in PP1α-silenced Jurkat T cells. PP1α as a phosphatase is expected to modulate dephosphorylation of target proteins. Yet, no overt differences in phosphorylation of selected NF-κB pathway components were observed. However, the used phospho-immunoblot analysis entails several technical limitations that might hamper the identification of changes in the phospho-proteome of PP1α-silenced cells: (i) investigation of specific phosphorylated residues in a given protein is highly biased, (ii) availability of high quality phopho-site specific antibodies limits analysis to a few known phosphorylation sites, (iii) phospho-immunoblot blot analysis might be too insensitive to quantitatively detect subtle differences of low abundance phospho-sites. A recent proteomics study, which described 696 TCR-responsive phosphorylation sites further underlines the limitations of traditional techniques (David K. Han, 2009). Due to these obstacles, a more global approach is required to identify PP1α-mediated changes in the phospho-proteome of TCR-stimulated cells. Therefore, a highly sensitive proteomic screening procedure, based on stable isotope labelling with amino acids in cell culture (SILAC) was utilised, but could not be completed during the present study (collaboration with Dominic Winter, PhD, Children's Hospital Boston). SILAC relies on the incorporation of amino acids with substituted stable isotopic nuclei (e.g. ^{2}H, ^{13}C, ^{15}N) into the proteome of a cell. Thus, cell populations can be cultured in the presence of "light-" or "middle-" or "heavy-weight" isotopic amino acid analogues. Once the differentially labelled amino acids are supplied to cells, they are incorporated in every newly synthesized protein. Hence, after

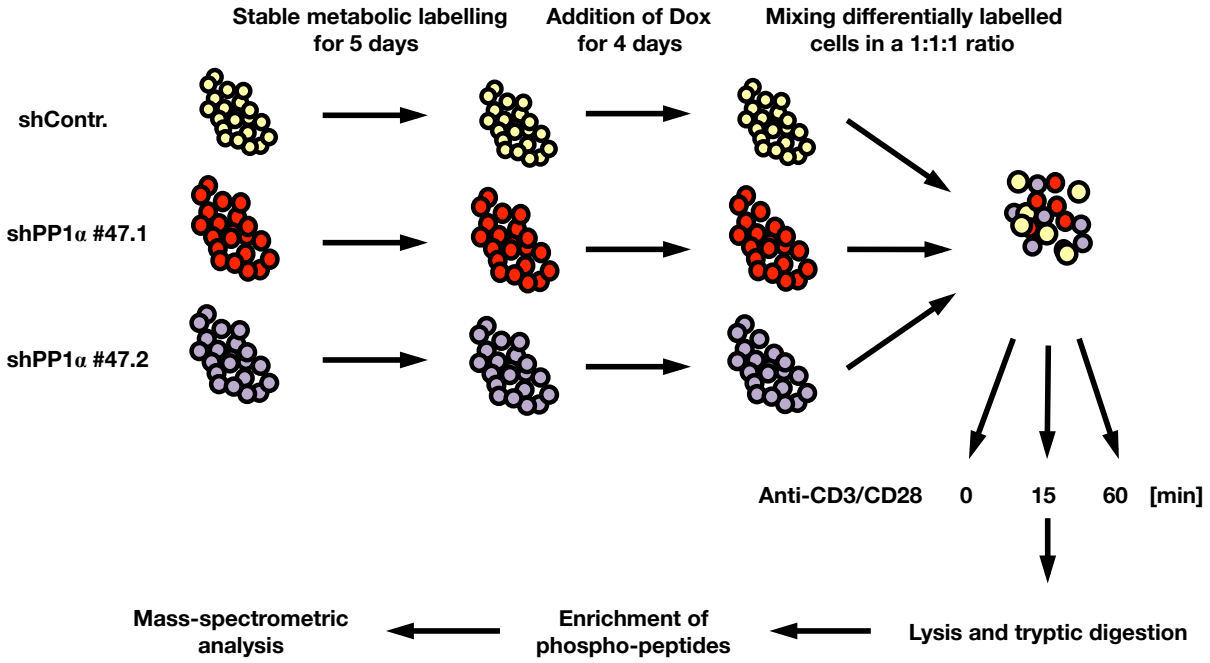

Figure 5.1: SILAC screening apporach for identification of PP1α substrates. Depicted is a schematic representation of the SILAC experiment. Indicated cell lines were cultured in the presence of light- (yellow filled circles), middle- (red filled circles) or heavy-weight (light violet filled circles) isotopic amino acids for a period of nine days. At day five of metabolic labelling, cells were supplied with 2 µg/ml doxycycline to induce control shRNA expression or PP1a-silencing in the respective cell lines. On day nine of metabolic labelling, equal numbers of cells were pooled in a 1:1:1 ratio. Subsequently, pooled cells were stimulated with 0.5 µg/ml anti-CD3/CD28 for the indicated periods of time. Samples were further processed as indicated.

a number of cell divisions, every protein incorporated the differential isotopic amino acid. To identify PP1α-dependent changes in the phospho-proteome of Jurkat T cells, we took advantage of the inducible PP1α-silencing system. Therefore, one control cell line (shContr.), inducibly expressing non-targeting shRNA, and two cell lines (shPP1α #47.1 and shPP1α #47.2) inducibly expressing the same PP1α-targeting-shRNA (as biological duplicates) were used. Fig. 5.1 depicts a schematic representation of the experimental setup. As indicated, control cells were cultured in the presence of "light-", while shPP1α #47.1 and #47.2 were cultured in the presence of "middle-" and "heavy-weight" isotopic amino acids, respectively, for a period of 9 days. After 5 days, cells were supplied with Dox to drive non- or PP1α-targeting shRNA expression for 4 days. On day 9 of metabolic labelling, all cells were counted and pooled in a 1:1:1 ratio, enabling stimulation of all cells under the same conditions and thus limiting technical variation. Pooled cells were left untreated or stimulated *via* the TCR for 15 or 60 minutes. Further handling of samples and analysis is currently carried out as indicated, concentrating on the identification of

differential occurrence of phospho-peptides. Due to the differential labelling and stimulation conditions, changes under basal conditions as well as temporal changes upon stimulation can be discriminated. The combined application of PP1α-silencing and quantitative phospho-proteomics, therefore, constitutes a powerful tool and will help to delineate the mechanism of PP1α function in T cells. Future work should concentrate on the validation and characterisation of newly identified PP1α-regulated phospho-sites and their biological impact. Based on the results of the present study, we propose that PP1α modulates NF-κB-mediated gene expression in a promoter-specific manner (Fig. 5.2). Thus, changes in phosphorylation of NF-κB pathway components as well as changes regarding nuclear proteins, which regulate gene transcription, for instance on an epigenetic level, should be of particular interest when analysing results of the SILAC screen.

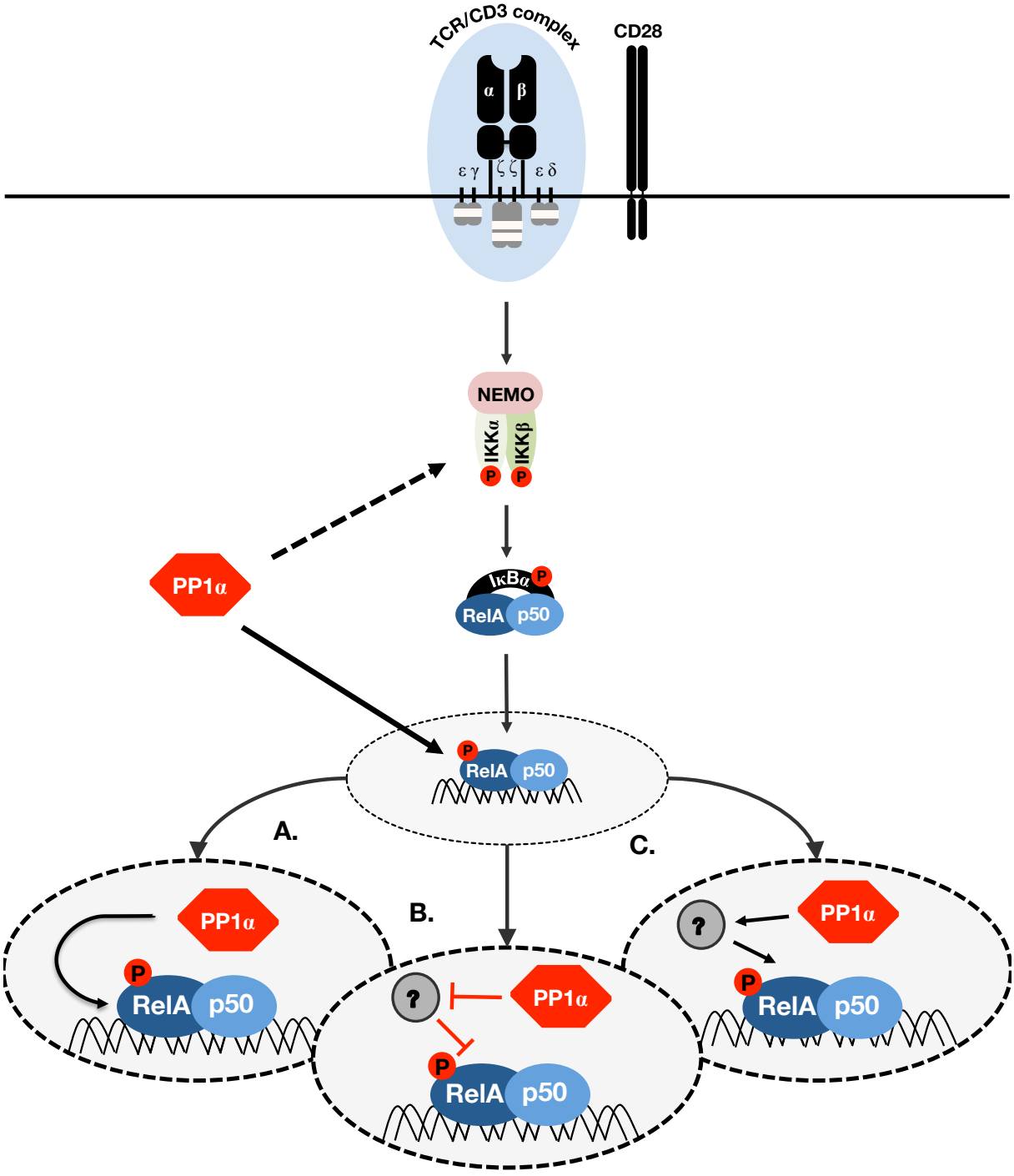

Figure 5.2: Possible mechanisms of PP1α-mediated regulation of NF-κB signalling. A possible role for PP1α in regulation of IKK activity is indicated by a dashed line. In addition, PP1α was found to control the duration of NF-κB-mediated gene transcription, presumably by regulating DNA binding activity of NF-κB in a promoter specific manner. Three possible mechanisms may explain these observations: **(A)** PP1α directly modifies NF-κB subunits on an unknown site and thereby stabilises complexes at certain promoter sites. **(B)** The duration of NF-κB-mediated gene expression is negatively controlled by an unknown factor (indicated with "?"), which is negatively regulated by PP1α. **(C)** The occupancy of NF-κB at promoter sites is stabilised by an unknown regulator that is positively controlled by PP1α. A-C may involve an influence of PP1α on recruitment or interaction of NF-κB with transcriptional co-activators, co-repressors, histone- or DNA-modifying enzymes.

6. References

Adler, J. T., Cook, M., Luo, Y., Pitt, S. C., Ju, J., Li, W., Shen, B., Kunnimalaiyaan, M., and Chen, H. (2009). Tautomycetin and tautomycin suppress the growth of medullary thyroid cancer cells via inhibition of glycogen synthase kinase-3beta. Mol. Cancer Ther. *8*, 914–920.

Akagi, T., Motegi, M., Tamura, A., and Suzuki, R. (1999). A novel gene, MALT1 at 18q21, is involved in t (11; 18)(q21; q21) found in low-grade B-cell lymphoma of mucosa-associated lymphoid tissue. Oncogene.

Akira, S., and Takeda, K. (2004). Toll-like receptor signalling. Nat Rev Immunol *4*, 499–511.

Amschler, K., Schoen, M. P., Pletz, N., Wallbrecht, K., Erpenbeck, L., and Schoen, M. (2010). NF-kappa B Inhibition through Proteasome Inhibition or IKK beta Blockade Increases the Susceptibility of Melanoma Cells to Cytostatic Treatment through Distinct Pathways. J Invest Dermatol *130*, 1073–1086.

Ashwell, J. D. (2006). The many paths to p38 mitogen-activated protein kinase activation in the immune system. Nat Rev Immunol *6*, 532–540.

Au-Yeung, B. B., Deindl, S., Hsu, L.-Y., Palacios, E. H., Levin, S. E., Kuriyan, J., and Weiss, A. (2009). The structure, regulation, and function of ZAP-70. Immunol. Rev. *228*, 41–57.

Baeuerle, P. A., and Baltimore, D. (1988). Activation of DNA-binding activity in an apparently cytoplasmic precursor of the NF-kappa B transcription factor. Cell *53*, 211–217.

Basak, S., Kim, H., Kearns, J., and Tergaonkar, V. (2007). A fourth IkB protein within the NF-kB signaling module. Cell.

Ben-Neriah, Y., and Karin, M. (2011). Inflammation meets cancer, with NF-κB as the matchmaker. Nature Publishing Group *12*, 715–723.

Bentley, G. A. (1996). The Structure of the T cell antigen receptor Annu Rev Immunol 14, 563-590.

Bidère, N., Ngo, V. N., Lee, J., Collins, C., Zheng, L., Wan, F., Davis, R. E., Lenz, G., Anderson, D. E., Arnoult, D., et al. (2009). Casein kinase 1alpha governs antigen-receptor-induced NF-kappaB activation and human lymphoma cell survival. Nature *458*, 92–96.

Birmingham, A., Selfors, L. M., Forster, T., Wrobel, D., Kennedy, C. J., Shanks, E., Santoyo-Lopez, J., Dunican, D. J., Long, A., Kelleher, D., et al. (2009). Statistical methods for analysis of high-throughput RNA interference screens. Nature Publishing Group *6*, 569–575.

Blonska, M., You, Y., and Geleziunas, R. (2004). Restoration of NF-{kappa} B activation by tumor necrosis factor alpha receptor complex-targeted MEKK3 in receptor-interacting protein-deficient cells. Molecular and cellular ….

Blonska, M., and Lin, X. (2010). NF-κB signaling pathways regulated by CARMA family of scaffold proteins. Cell Res. *21*, 55–70.

Bollen, M., Peti, W., Ragusa, M. J., and Beullens, M. (2010). The extended PP1 toolkit: designed to create specificity. Trends Biochem. Sci. *35*, 450–458.

Bond, M., Fabunmi, R., and Baker, A. (1998). Synergistic upregulation of metalloproteinase-9 by growth factors and inflammatory cytokines: an absolute requirement for transcription factor NF-[kappa] B. FEBS Lett.

Booken, N., Gratchev, A., Utikal, J., Weiss, C., Yu, X., Qadoumi, M., Schmuth,

M., Sepp, N., Nashan, D., Rass, K., et al. (2008). Sezary syndrome is a unique cutaneous T-cell lymphoma as identified by an expanded gene signature including diagnostic marker molecules CDO1 and DNM3. Leukemia *22*, 393–399.

Boomer, J. S., and Green, J. M. (2010). An Enigmatic Tail of CD28 Signaling. Cold Spring Harbor Perspectives in Biology *2*, a002436–a002436.

Boone, D. L., Turer, E. E., Lee, E. G., Ahmad, R.-C., Wheeler, M. T., Tsui, C., Hurley, P., Chien, M., Chai, S., Hitotsumatsu, O., et al. (2004). The ubiquitin-modifying enzyme A20 is required for termination of Toll-like receptor responses. Nat Immunol *5*, 1052–1060.

Bours, V., Franzoso, G., Azarenko, V., and Park, S. (1993). The oncoprotein Bcl-3 directly transactivates through [kappa] B motifs via association with DNA-binding p50B homodimers. Cell.

Bouwmeester, T., Bauch, A., Ruffner, H., Angrand, P.-O., Bergamini, G., Croughton, K., Cruciat, C., Eberhard, D., Gagneur, J., Ghidelli, S., et al. (2004). A physical and functional map of the human TNF-alpha/NF-kappa B signal transduction pathway. Nat Cell Biol *6*, 97–105.

Brancho, D., Tanaka, N., Jaeschke, A., Ventura, J., Kelkar, N., Tanaka, Y., Kyuuma, M., Takeshita, T., Flavell, R., and Davis, R. (2003). Mechanism of p38 MAP kinase activation in vivo. Genes Dev *17*, 1969–1978.

Brenner, D., Brechmann, M., Roehling, S., Tapernoux, M., Mock, T., Winter, D., Lehmann, W. D., Kiefer, F., Thome, M., Krammer, P. H., et al. (2009). Phosphorylation of CARMA1 by HPK1 is critical for NF-kappa B activation in T cells. Proc Natl Acad Sci USA *106*, 14508–14513.

Bromley, S., Burack, W., Johnson, K., Somersalo, K., Sims, T., Sumen, C., Davis, M., Shaw, A., Allen, P., and Dustin, M. (2001). The immunological synapse. Annu Rev Immunol *19*, 375–396.

Brechmann, M. (2010), Identification and Characterization of Protein Phosphatase 4, Regulatory Subunit 1 (PP4R1) as a Suppressor of NF-κB in T Lymphocytes and T cell Lymphomas. PhD thesis, Ruperto-Carola Unibersity of Heidelberg.

Bundy, D. L., and McKeithan, T. W. (1997). Diverse effects of BCL3 phosphorylation on its modulation of NF-kappaB p52 homodimer binding to DNA. J Biol Chem *272*, 33132–33139.

Bunting, K., Rao, S., Hardy, K., Woltring, D., Denyer, G. S., Wang, J., Gerondakis, S., and Shannon, M. F. (2007). Genome-wide analysis of gene expression in T cells to identify targets of the NF-kappa B transcription factor c-Rel. J Immunol *178*, 7097–7109.

Bustelo, X. R. (2000). Regulatory and signaling properties of the Vav family. Mol Cell Biol *20*, 1461–1477.

Cai, Y. C., Cefai, D., Schneider, H., Raab, M., Nabavi, N., and Rudd, C. E. (1995). Selective CD28pYMNM mutations implicate phosphatidylinositol 3-kinase in CD86-CD28-mediated costimulation. Immunity *3*, 417–426.

Carpino, N., Turner, S., Mekala, D., Takahashi, Y., Zang, H., Geiger, T. L., Doherty, P., and Ihle, J. N. (2004). Regulation of ZAP-70 activation and TCR signaling by two related proteins, Sts-1 and Sts-2. Immunity *20*, 37–46.

Ceulemans, H., Stalmans, W., and Bollen, M. (2002). Regulator-driven functional diversification of protein phosphatase-1 in eukaryotic evolution. Bioessays *24*, 371–381.

Chae, W.-J., Choi, J.-M., Yang, J.-J., and Lee, S.-K. (2004). T Cell-specific immunosuppression using tautomycetin or PTD-conjugated protein drugs. Yonsei Med. J. *45*, 978–990.

Chen, G., Cao, P., and Goeddel, D. V. (2002). TNF-induced recruitment and activation of the IKK complex require Cdc37 and Hsp90. Molecular Cell *9*, 401–410.

Chen, Z. (2005). Ubiquitin signaling in the NF-κB pathway. Nat Cell Biol.

Chew, J., Biswas, S., Shreeram, S., Humaidi, M., Wong, E. T., Dhillion, M. K., Teo, H., Hazra, A., Fang, C. C., Lopez-Collazo, E., et al. (2009). WIP1 phosphatase is a negative regulator of NF-kappa B signalling. Nat Cell Biol *11*, 659–U493.

Compagno, M., Lim, W. K., Grunn, A., Nandula, S. V., Brahmachary, M., Shen, Q., Bertoni, F., Ponzoni, M., Scandurra, M., Califano, A., et al. (2009). Mutations of multiple genes cause deregulation of NF-kappaB in diffuse large B-cell lymphoma. Nature *459*, 717–721.

Coope, H. J., Atkinson, P. G. P., Huhse, B., Belich, M., Janzen, J., Holman, M. J., Klaus, G. G. B., Johnston, L. H., and Ley, S. C. (2002). CD40 regulates the processing of NF-kappaB2 p100 to p52. EMBO J *21*, 5375–5385.

Coornaert, B., Carpentier, I., and Beyaert, R. (2009). A20: central gatekeeper in inflammation and immunity. J Biol Chem *284*, 8217–8221.

Davis, R. E., Ngo, V. N., Lenz, G., Tolar, P., Young, R. M., Romesser, P. B., Kohlhammer, H., Lamy, L., Zhao, H., Yang, Y., et al. (2010). Chronic active B-cell-receptor signalling in diffuse large B-cell lymphoma. Nature *463*, 88–92.

Davis, R., Brown, K., Siebenlist, U., and Staudt, L. (2001). Constitutive nuclear factor kappa B activity is required for survival of activated B cell-like diffuse large B cell lymphoma cells. Journal of Experimental Medicine *194*, 1861–1874.

Delhase, M., Hayakawa, M., Chen, Y., and Karin, M. (1999). Positive and negative regulation of IkappaB kinase activity through IKKbeta subunit phosphorylation. Science *284*, 309–313.

Demchenko, Y., and Glebov, O. (2010). Classical and/or alternative NF-κB pathway activation in multiple myeloma. ….

Derudder, E., Dejardin, E., Pritchard, L. L., Green, D. R., Korner, M., and Baud, V. (2003). RelB/p50 dimers are differentially regulated by tumor necrosis factor-alpha and lymphotoxin-beta receptor activation: critical roles for p100. J Biol Chem *278*, 23278–23284.

Devin, A., Lin, Y., Yamaoka, S., Li, Z., Karin, M., and Liu Zg (2001). The alpha and beta subunits of IkappaB kinase (IKK) mediate TRAF2-dependent IKK recruitment to tumor necrosis factor (TNF) receptor 1 in response to TNF. Mol Cell Biol *21*, 3986–3994.

Devin, A., Cook, A., Lin, Y., Rodriguez, Y., Kelliher, M., and Liu, Z. (2000). The distinct roles of TRAF2 and RIP in IKK activation by TNF-R1: TRAF2 recruits IKK to TNF-R1 while RIP mediates IKK activation. Immunity *12*, 419–429.

Diamandidou, E., and Cohen, P. (1996). Mycosis fungoides and Sezary syndrome. Blood.

DiDonato, J. A., Hayakawa, M., Rothwarf, D. M., Zandi, E., and Karin, M. (1997). A cytokine-responsive IkappaB kinase that activates the transcription factor NF-kappaB. Nature *388*, 548–554.

Dierlamm, J., Baens, M., Wlodarska, I., Stefanova-Ouzounova, M., Hernandez, J. M., Hossfeld, D. K., De Wolf-Peeters, C., Hagemeijer, A., Van den Berghe, H., and Marynen, P. (1999). The apoptosis inhibitor gene API2 and a novel 18q gene, MLT, are recurrently rearranged in the t(11;18)(q21;q21) associated with mucosa-associated lymphoid tissue lymphomas. Blood *93*, 3601–3609.

Dimitratos, S., Woods, D., Stathakis, D., and Bryant, P. (1999). Signaling pathways

are focused at specialized regions of the plasma membrane by scaffolding proteins of the MAGUK family. Bioessays *21*, 912–921.

Dippel, E., Klemke, C. D., and Goerdt, S. (2003). Current status of cutaneous T-cell lymphoma: molecular diagnosis, pathogenesis, therapy and future directions. Onkologie *26*, 477–483.

Dodson, L. F., Boomer, J. S., Deppong, C. M., Shah, D. D., Sim, J., Bricker, T. L., Russell, J. H., and Green, J. M. (2009). Targeted Knock-In Mice Expressing Mutations of CD28 Reveal an Essential Pathway for Costimulation. Mol Cell Biol *29*, 3710–3721.

Doi, T., Takahashi, T., Taguchi, O., Azuma, T., and Obata, Y. (1997). NF-kappa B RelA-deficient lymphocytes: Normal development of T cells and B cells, impaired production of IgA and IgG1 and reduced proliferative responses. Journal of Experimental Medicine *185*, 953–961.

Dong, C., Yang, D. D., Wysk, M., Whitmarsh, A. J., Davis, R. J., and Flavell, R. A. (1998). Defective T cell differentiation in the absence of Jnk1. Science *282*, 2092–2095.

Dong, C., Davis, R. J., and Flavell, R. A. (2002). MAP K INASES IN THEI MMUNER ESPONSE. Annu Rev Immunol *20*, 55–72.

Dower, N., Stang, S., Bottorff, D., Ebinu, J., Dickie, P., Ostergaard, H., and Stone, J. (2000). RasGRP essential for mouse thymocyte differentiation and TCR signaling. Nat Immunol *1*, 317–321.

Ducut Sigala, J. L., Bottero, V., Young, D. B., Shevchenko, A., Mercurio, F., and Verma, I. M. (2004). Activation of transcription factor NF-kappaB requires ELKS, an IkappaB kinase regulatory subunit. Science *304*, 1963–1967.

Duwel, M., Welteke, V., Oeckinghaus, A., Baens, M., Kloo, B., Ferch, U., Darnay, B. G., Ruland, J., Marynen, P., and Krappmann, D. A20 Negatively Regulates T Cell Receptor Signaling to NF-kappa B by Cleaving Malt1 Ubiquitin Chains. J Immunol *182*, 7718–7728.

Ea, C.-K., Deng, L., Xia, Z.-P., Pineda, G., and Chen, Z. J. (2006). Activation of IKK by TNFalpha requires site-specific ubiquitination of RIP1 and polyubiquitin binding by NEMO. Molecular Cell *22*, 245–257.

Ebinu, J., Stang, S., Teixeira, C., Bottorff, D., Hooton, J., Blumberg, P., Barry, M., Bleakley, R., Ostergaard, H., and Stone, J. (2000). RasGRP links T-cell receptor signaling to Ras. Blood *95*, 3199–3203.

Ebinu, J. O., Bottorff, D. A., Chan, E. Y., Stang, S. L., Dunn, R. J., and Stone, J. C. (1998). RasGRP, a Ras guanyl nucleotide-releasing protein with calcium- and diacylglycerol-binding motifs. Science *280*, 1082–1086.

Egan, S. E., Giddings, B. W., Brooks, M. W., Buday, L., Sizeland, A. M., and Weinberg, R. A. (1993). Association of Sos Ras exchange protein with Grb2 is implicated in tyrosine kinase signal transduction and transformation. Nature *363*, 45–51.

Eitelhuber, A. C., Warth, S., Schimmack, G., Duwel, M., Hadian, K., Demski, K., Beisker, W., Shinohara, H., Kurosaki, T., Heissmeyer, V., et al. (2011). Dephosphorylation of Carma1 by PP2A negatively regulates T-cell activation. EMBO J *30*, 594–605.

Ellis, J. H., Ashman, C., Burden, M. N., Kilpatrick, K. E., Morse, M. A., and Hamblin, P. A. (2000). GRID: a novel Grb-2-related adapter protein that interacts with the activated T cell costimulatory receptor CD28. J Immunol *164*, 5805–5814.

Feng, W., and Zhang, M. (2009). Organization and dynamics of PDZ-domain-related supramodules in the postsynaptic density. Nat. Rev. Neurosci. *10*, 87–99.

Frearson, J., and Alexander, D. (1998). The phosphotyrosine phosphatase SHP-2 participates in a multimeric signaling complex and regulates T cell receptor (TCR) coupling to the Ras/Mitogen-activated protein kinase (MAPK) pathway in Jurkat T cells. Journal of Experimental Medicine *187*, 1417–1426.

Freeburn, R., Wright, K., Burgess, S., Astoul, E., Cantrell, D., and Ward, S. (2002). Evidence that SHIP-1 contributes to phosphatidylinositol 3,4,5-trisphosphate metabolism in T lymphocytes and can regulate novel phosphoinositide 3-kinase effectors. J Immunol *169*, 5441–5450.

Frischbutter, S., Gabriel, C., Bendfeldt, H., Radbruch, A., and Baumgrass, R. (2011). Dephosphorylation of Bcl-10 by calcineurin is essential for canonical NF-κB activation in Th cells. Eur J Immunol *41*, 2349–2357.

Fu, D.-X., Kuo, Y.-L., Liu, B.-Y., Jeang, K.-T., and Giam, C.-Z. (2003). Human T-lymphotropic virus type I tax activates I-kappa B kinase by inhibiting I-kappa B kinase-associated serine/threonine protein phosphatase 2A. J Biol Chem *278*, 1487–1493.

Fuller, C. L., Braciale, V. L., and Samelson, L. E. (2003). All roads lead to actin: the intimate relationship between TCR signaling and the cytoskeleton. Immunol. Rev. *191*, 220–236.

Gaide, O., Favier, B., Legler, D. F., Bonnet, D., Brissoni, B., Valitutti, S., Bron, C., Tschopp, J., and Thome, M. (2002). CARMA1 is a critical lipid raft-associated regulator of TCR-induced NF-kappa B activation. Nat Immunol *3*, 836–843.

Ge, B., Gram, H., Di Padova, F., Huang, B., New, L., Ulevitch, R., Luo, Y., and Han, J. (2002). MAPKK-independent activation of p38 alpha mediated by TAB1-dependent autophosphorylation of p38 alpha. Science *295*, 1291–1294.

Gerlach, B., Cordier, S. M., Schmukle, A. C., Emmerich, C. H., Rieser, E., Haas, T. L., Webb, A. I., Rickard, J. A., Anderton, H., Wong, W. W. L., et al. (2011). Linear ubiquitination prevents inflammation and regulates immune signalling. Nature *471*, 591–596.

Germain, R. (1994). Mhc-Dependent Antigen-Processing and Peptide Presentation - Providing Ligands for T-Lymphocyte Activation. Cell *76*, 287–299.

Gerondakis, S., Grumont, R., Gugasyan, R., Wong, L., Isomura, I., Ho, W., and Banerjee, A. (2006). Unravelling the complexities of the NF-kappaB signalling pathway using mouse knockout and transgenic models. Oncogene *25*, 6781–6799.

Greten, F. R., Arkan, M. C., Bollrath, J., Hsu, L.-C., Goode, J., Miething, C., Göktuna, S. I., Neuenhahn, M., Fierer, J., Paxian, S., et al. (2007). NF-kappaB is a negative regulator of IL-1beta secretion as revealed by genetic and pharmacological inhibition of IKKbeta. Cell *130*, 918–931.

Guma, M., Stepniak, D., Shaked, H., Spehlmann, M. E., Shenouda, S., Cheroutre, H., Vicente-Suarez, I., Eckmann, L., Kagnoff, M. F., and Karin, M. (2011). Constitutive intestinal NF- B does not trigger destructive inflammation unless accompanied by MAPK activation. Journal of Experimental Medicine *208*, 1889–1900.

Haas, T. L., Emmerich, C. H., Gerlach, B., Schmukle, A. C., Cordier, S. M., Rieser, E., Feltham, R., Vince, J., Warnken, U., Wenger, T., et al. (2009). Recruitment of the Linear Ubiquitin Chain Assembly Complex Stabilizes the TNF-R1 Signaling Complex and Is Required for TNF-Mediated Gene Induction. Molecular Cell *36*, 831–844.

Hacker, H., and Karin, M. (2006). Regulation and Function of IKK and IKK-Related Kinases. Science's STKE *2006*, re13–re13.

Hale, K. K., Trollinger, D., Rihanek, M.,

and Manthey, C. L. (1999). Differential expression and activation of p38 mitogen-activated protein kinase alpha, beta, gamma, and delta in inflammatory cell lineages. J Immunol *162*, 4246–4252.

Han, D., Jeong, Y., Wee, Y., Lee, A., Lee, H., Ha, J., Lee, S., and Kim, S. (2003). Tautomycetin as a novel immunosuppressant in transplantation. In Transplantation Proceedings, pp. 547–547.

Hanahan, D., and Weinberg, R. A. (2011). Hallmarks of cancer: the next generation. Cell *144*, 646–674.

Harhaj, E. W., and Dixit, V. M. (2011). Deubiquitinases in the regulation of NF-κB signaling. Cell Res. *21*, 22–39.

Hayden, M. S., and Ghosh, S. (2008). Shared principles in NF-kappaB signaling. Cell *132*, 344–362.

Hermiston, M. L. (2002). Reciprocal regulation of lymphocyte activation by tyrosine kinases and phosphatases. Journal of Clinical Investigation *109*, 9–14.

Higashimoto, T., Chan, N., Lee, Y.-K., and Zandi, E. (2008). Regulation of I(kappa)B kinase complex by phosphorylation of (gamma)-binding domain of I(kappa)B kinase (beta) by Polo-like kinase 1. J Biol Chem *283*, 35354–35367.

Hoffmann, J. A. (1999). Phylogenetic Perspectives in Innate Immunity. Science *284*, 1313–1318.

Huang, G., Shi, L. Z., and Chi, H. (2009). Regulation of JNK and p38 MAPK in the immune system: Signal integration, propagation and termination. Cytokine *48*, 161–169.

Huxford, T., and Ghosh, G. (2009). A Structural Guide to Proteins of the NF- B Signaling Module. Cold Spring Harbor Perspectives in Biology *1*, a000075–a000075.

Hwang, S. T., Janik, J. E., Jaffe, E. S., and Wilson, W. H. Mycosis fungoides and Sézary syndrome. The Lancet *371*, 945–957.

Ikeda, F., Deribe, Y. L., Skånland, S. S., Stieglitz, B., Grabbe, C., Franz-Wachtel, M., van Wijk, S. J. L., Goswami, P., Nagy, V., Terzic, J., et al. (2011). SHARPIN forms a linear ubiquitin ligase complex regulating NF-κB activity and apoptosis. Nature *471*, 637–641.

Irving, B., and Weiss, A. (1991). The Cytoplasmic Domain of the T-Cell Receptor Zeta-Chain Is Sufficient to Couple to Receptor-Associated Signal Transduction Pathways. Cell *64*, 891–901.

Isakov, N., and Altman, A. (2002). Protein kinase C theta in T cell activation. Annu Rev Immunol *20*, 761–794.

Ishimaru, N., Kishimoto, H., Hayashi, Y., and Sprent, J. (2006). Regulation of naive T cell function by the NF-kappaB2 pathway. Nat Immunol *7*, 763–772.

Ishitani, T., Takaesu, G., Ninomiya-Tsuji, J., Shibuya, H., Gaynor, R. B., and Matsumoto, K. (2003). Role of the TAB2-related protein TAB3 in IL-1 and TNF signaling. EMBO J *22*, 6277–6288.

Iwasaki, A., and Medzhitov, R. (2010). Regulation of adaptive immunity by the innate immune system. Science *327*, 291–295.

Izban, K., Ergin, M., Qin, J., Martinez, R., Pooley, R., Saeed, S., and Alkan, S. (2000). Constitutive expression of NF-kappa B is a characteristic feature of mycosis fungoides: Implications for apoptosis resistance and pathogenesis. Hum Pathol *31*, 1482–1490.

Janeway, C. A., Jr., and Medzhitov, R. (2002). Innate Immune Recognition. Annu Rev Immunol *20*, 197–216.

Jordan, M. S., Smith, J. E., Burns, J. C., Austin, J.-E. T., Nichols, K. E., Aschenbrenner, A. C., and Koretzky, G. A. (2008). Complementation in trans of

altered thymocyte development in mice expressing mutant forms of the adaptor molecule SLP76. Immunity *28*, 359–369.

Jost, P. J., and Ruland, J. (2007). Aberrant NF-kappaB signaling in lymphoma: mechanisms, consequences, and therapeutic implications. Blood *109*, 2700–2707.

Kanayama, A., Seth, R., Sun, L., Ea, C., and Hong, M. (2004). TAB2 and TAB3 activate the NF-[kappa] B pathway through binding to polyubiquitin chains. Molecular Cell.

Kaplan, E., Rosen, S., and Norris, D. (1990). Phase II study of recombinant human interferon gamma for treatment of cutaneous T-cell lymphoma. Journal of the ….

Karin, M. (2009). NF-kappaB as a critical link between inflammation and cancer. Cold Spring Harbor Perspectives in Biology *1*, a000141.

Karin, M., and Greten, F. R. (2005). NF-kappaB: linking inflammation and immunity to cancer development and progression. Nat Rev Immunol *5*, 749–759.

Kawai, T., and Akira, S. (2010). The role of pattern-recognition receptors in innate immunity: update on Toll-like receptors. Nature Publishing Group *11*, 373–384.

Kearns, J., Basak, S., and Werner, S. (2006). IκBε provides negative feedback to control NF-κB oscillations, signaling dynamics, and inflammatory gene expression. The Journal of Cell ….

Kiessling, M. K., Oberholzer, P. A., Mondal, C., Karpova, M. B., Zipser, M. C., Lin, W. M., Girardi, M., Macconaill, L. E., Kehoe, S. M., Hatton, C., et al. (2011). High-throughput mutation profiling of CTCL samples reveals KRAS and NRAS mutations sensitizing tumors toward inhibition of the RAS/RAF/MEK signaling cascade. Blood *117*, 2433–2440.

Kiessling, M. K., Klemke, C. D., Kaminski, M. M., Galani, I. E., Krammer, P. H., and Gulow, K. (2009). Inhibition of Constitutively Activated Nuclear Factor- B Induces Reactive Oxygen Species- and Iron-Dependent Cell Death in Cutaneous T-Cell Lymphoma. Cancer Research *69*, 2365–2374.

Kishida, S., Sanjo, H., Akira, S., and Matsumoto, K. (2005). TAK1-binding protein 2 facilitates ubiquitination of TRAF6 and assembly of TRAF6 with IKK in the IL-1 signaling pathway. Genes to ….

Klemke, C. D., Mansmann, U., Poenitz, N., Dippel, E., and Goerdt, S. (2005). Prognostic factors and prediction of prognosis by the CTCL Severity Index in mycosis fungoides and Sézary syndrome. Br. J. Dermatol. *153*, 118–124.

Koretzky, G. A., Abtahian, F., and Silverman, M. A. SLP76 and SLP65: complex regulation of signalling in lymphocytes and beyond. Nat Rev Immunol *6*, 67–78.

Kray, A. E., Carter, R. S., Pennington, K. N., Gomez, R. J., Sanders, L. E., Llanes, J. M., Khan, W. N., Ballard, D. W., and Wadzinski, B. E. (2005). Positive regulation of IkappaB kinase signaling by protein serine/threonine phosphatase 2A. J Biol Chem *280*, 35974–35982.

Kunsch, C., and Rosen, C. A. (1993). NF-kappa B subunit-specific regulation of the interleukin-8 promoter. Mol Cell Biol *13*, 6137–6146.

Lam, L., Davis, R., Pierce, J., Hepperle, M., Xu, Y., Hottelet, M., Nong, Y., Wen, D., Adams, J., Dang, L., et al. (2005). Small molecule inhibitors of I kappa B kinase are selectively toxic for subgroups of diffuse large B-cell lymphoma defined by gene expression profiling. Clinical Cancer Research *11*, 28–40.

Lam, L. T., Wright, G., Davis, R. E., Lenz, G., Farinha, P., Dang, L., Chan, J. W., Rosenwald, A., Gascoyne, R. D., and Staudt, L. M. (2008). Cooperative

signaling through the signal transducer and activator of transcription 3 and nuclear factor-{kappa}B pathways in subtypes of diffuse large B-cell lymphoma. Blood *111*, 3701–3713.

Lee, E. G., Boone, D. L., Chai, S., Libby, S. L., Chien, M., Lodolce, J. P., and Ma, A. (2000). Failure to regulate TNF-induced NF-kappaB and cell death responses in A20-deficient mice. Science *289*, 2350–2354.

Lee, K.-Y., D'Acquisto, F., Hayden, M. S., Shim, J.-H., and Ghosh, S. (2005). PDK1 nucleates T cell receptor-induced signaling complex for NF-kappaB activation. Science *308*, 114–118.

Lee, T., Shank, J., Cusson, N., and Kelliher, M. (2004). The kinase activity of Rip1 is not required for tumor necrosis factor-alpha-induced I kappa B kinase or p38 MAP kinase activation or for the ubiquitination of Rip1 by Traf2. J Biol Chem *279*, 33185–33191.

Lenz, G., Davis, R. E., Ngo, V. N., Lam, L., George, T. C., Wright, G. W., Dave, S. S., Zhao, H., Xu, W., Rosenwald, A., et al. (2008). Oncogenic CARD11 mutations in human diffuse large B cell lymphoma. Science *319*, 1676–1679.

lenz, G., Davis, R. E., Ngo, V. N., Lam, L., George, T. C., Wright, G. W., Dave, S. S., Zhao, H., Xu, W. H., Rosenwald, A., et al. Oncogenic CARD11 mutations in human diffuse large B cell lymphoma. Science *319*, 1676–1679.

Lenz, G., and Staudt, L. M. (2010). Aggressive lymphomas. N. Engl. J. Med. *362*, 1417–1429.

Letourneur, F., and Klausner, R. D. (1992). Activation of T cells by a tyrosine kinase activation domain in the cytoplasmic tail of CD3 epsilon. Science *255*, 79–82.

Levine, L., Lucci, J. A., Pazdrak, B., Cheng, J.-Z., Guo, Y.-S., Townsend, C. M., and Hellmich, M. R. (2003). Bombesin stimulates nuclear factor kappa B activation and expression of proangiogenic factors in prostate cancer cells. Cancer Research *63*, 3495–3502.

Li, H., Kobayashi, M., Blonska, M., You, Y., and Lin, X. (2006a). Ubiquitination of RIP is required for tumor necrosis factor alpha-induced NF-kappaB activation. J Biol Chem *281*, 13636–13643.

Li, H.-Y., Liu, H., Wang, C.-H., Zhang, J.-Y., Man, J.-H., Gao, Y.-F., Zhang, P.-J., Li, W.-H., Zhao, J., Pan, X., et al. (2008). Deactivation of the kinase IKK by CUEDC2 through recruitment of the phosphatase PP1. Nature Publishing Group *9*, 533–541.

Li, Q. (2002). NF-kappaB regulation in the immune system. Nat Rev Immunol.

Li, S., Wang, L., Berman, M. A., Zhang, Y., and Dorf, M. E. (2006b). RNAi Screen in Mouse Astrocytes Identifies Phosphatases that Regulate NF-κB Signaling. Molecular Cell *24*, 497–509.

Lin, L., DeMartino, G. N., and Greene, W. C. (1998). Cotranslational biogenesis of NF-kappaB p50 by the 26S proteasome. Cell *92*, 819–828.

Lindquist, J. A., Simeoni, L., and Schraven, B. (2003). Transmembrane adapters: attractants for cytoplasmic effectors. Immunol. Rev. *191*, 165–182.

Liu, B., Yang, R., Wong, K., Getman, C., Stein, N., Teitell, M., Cheng, G., Wu, H., and Shuai, K. (2005). Negative regulation of NF-kappa B signaling by PIAS1. Mol Cell Biol *25*, 1113–1123.

Liu, B., Mink, S., Wong, K., Stein, N., Getman, C., Dempsey, P., Wu, H., and Shuai, K. (2004). PIAS1 selectively inhibits interferon-inducible genes and is important in innate immunity. Nat Immunol *5*, 891–898.

Liu, B., Yang, Y., Chernishof, V., Loo, R. R. O., Jang, H., Tahk, S., Yang, R., Mink, S., Shultz, D., Bellone, C. J., et al. (2007). Proinflammatory stimuli induce IKKalpha-

mediated phosphorylation of PIAS1 to restrict inflammation and immunity. Cell *129*, 903–914.

Liu, H.-H., Xie, M., Schneider, M. D., and Chen, Z. J. (2006). Essential role of TAK1 in thymocyte development and activation. Proc Natl Acad Sci USA *103*, 11677–11682.

Liu, J. O. (2009). Calmodulin-dependent phosphatase, kinases, and transcriptional corepressors involved in T-cell activation. Immunol. Rev. *228*, 184–198.

Liu, S., Fang, N., Koretzky, G., and McGlade, C. (1999). The hematopoietic-specific adaptor protein Gads functions in T-cell signaling via interactions with the SLP-76 and LAT adaptors. Curr Biol *9*, 67–75.

Liu, S., and Chen, Z. J. (2011). Expanding role of ubiquitination in NF-κB signaling. Cell Res. *21*, 6–21.

Lu, B., Yu, H., Chow, C., Li, B., Zheng, W., Davis, R. J., and Flavell, R. A. (2001). GADD45gamma mediates the activation of the p38 and JNK MAP kinase pathways and cytokine production in effector TH1 cells. Immunity *14*, 583–590.

Lucas, P., Yonezumi, M., Inohara, N., McAllister-Lucas, L., Abazeed, M., Chen, F., Yamaoka, S., Seto, M., and Nunez, G. (2001). Bcl10 and MALT1, independent targets of chromosomal translocation in MALT lymphoma, cooperate in a novel NF-kappa B signaling pathway. J Biol Chem *276*, 19012–19019.

Lühder, F., Huang, Y., Dennehy, K. M., Guntermann, C., Müller, I., Winkler, E., Kerkau, T., Ikemizu, S., Davis, S. J., Hanke, T., et al. (2003). Topological requirements and signaling properties of T cell-activating, anti-CD28 antibody superagonists. Journal of Experimental Medicine *197*, 955–966.

Macian, F. (2005). NFAT proteins: key regulators of T-cell development and function. Nat Rev Immunol *5*, 472–484.

Macián, F., López-Rodríguez, C., and Rao, A. (2001). Partners in transcription: NFAT and AP-1. Oncogene *20*, 2476–2489.

Maine, G. N., Mao, X., Komarck, C. M., and Burstein, E. (2007). COMMD1 promotes the ubiquitination of NF-kappaB subunits through a cullin-containing ubiquitin ligase. EMBO J *26*, 436–447.

Malinin, N. L., Boldin, M. P., Kovalenko, A. V., and Wallach, D. (1997). MAP3K-related kinase involved in NF-kappaB induction by TNF, CD95 and IL-1. Nature *385*, 540–544.

Manning, A. M., and Davis, R. J. (2003). Targeting JNK for therapeutic benefit: from junk to gold? Nat Rev Drug Discov *2*, 554–565.

Manning, G., Whyte, D., Martinez, R., Hunter, T., and Sudarsanam, S. (2002). The protein kinase complement of the human genome. Science *298*, 1912–.

Marengere, L., Okkenhaug, K., Clavreul, A., Couez, D., Gibson, S., Mills, G., Mak, T., and Rottapel, R. (1997). The SH3 domain of Itk/Emt binds to proline-rich sequences in the cytoplasmic domain of the T cell costimulatory receptor CD28. J Immunol *159*, 3220–3229.

Marienfeld, R., Neumann, M., Chuvpilo, S., Escher, C., Kneitz, B., Avots, A., Schimpl, A., and Serfling, E. (1997). Cyclosporin A interferes with the inducible degradation of NF-kappa B inhibitors, but not with the processing of p105/NF-kappa B1 in T cells. Eur J Immunol *27*, 1601–1609.

Massoumi, R., Chmielarska, K., Hennecke, K., and Pfeifer, A. (2006a). Cyld inhibits tumor cell proliferation by blocking bcl-3-dependent NF-[kappa] B signaling. Cell.

Massoumi, R., Chmielarska, K., Hennecke, K., Pfeifer, A., and Fässler, R. (2006b). Cyld inhibits tumor cell proliferation by blocking Bcl-3-dependent

NF-kappaB signaling. Cell *125*, 665–677.

Matitau, A. E., and Scheid, M. P. (2008). Phosphorylation of MEKK3 at threonine 294 promotes 14-3-3 association to inhibit nuclear factor kappaB activation. J Biol Chem *283*, 13261–13268.

Matsumoto, R., Wang, D., Blonska, M., Li, H., Kobayashi, M., Pappu, B., Chen, Y., Wang, D., and Lin, X. (2005). Phosphorylation of CARMA1 plays a critical role in T cell receptor-mediated NF-kappa B activation. Immunity *23*, 575–585.

Mercurio, F., Murray, B., and Shevchenko, A. (1999). Ikappa B kinase (IKK)-associated protein 1, a common component of the heterogeneous IKK complex. … and cellular biology.

Meuer, S., Fitzgerald, K., Hussey, R., Hodgdon, J., Schlossman, S., and Reinherz, E. (1983a). Clonotypic Structures Involved in Antigen-Specific Human T-Cell Function - Relationship to the T3-Molecular Complex. Journal of Experimental Medicine *157*, 705–719.

Meuer, S., Acuto, O., Hussey, R., Hodgdon, J., Fitzgerald, K., Schlossman, S., and Reinherz, E. (1983b). Evidence for the T3-Associated 90k Heterodimer as the T-Cell Antigen Receptor. Nature *303*, 808–810.

Meylan, E., Burns, K., Hofmann, K., Blancheteau, V., Martinon, F., Kelliher, M., and Tschopp, J. (2004). RIP1 is an essential mediator of Toll-like receptor 3-induced NF-kappa B activation. Nat Immunol *5*, 503–507.

Mikhailik, A., Ford, B., Keller, J., Chen, Y., Nassar, N., and Carpino, N. (2007). A phosphatase activity of Sts-1 contributes to the suppression of TCR signaling. Molecular Cell *27*, 486–497.

Miletic, A. V., Sakata-Sogawa, K., Hiroshima, M., Hamann, M. J., Gomez, T. S., Ota, N., Kloeppel, T., Kanagawa, O., Tokunaga, M., Billadeau, D. D., et al. (2006). Vav1 acidic region tyrosine 174 is required for the formation of T cell receptor-induced microclusters and is essential in T cell development and activation. J Biol Chem *281*, 38257–38265.

Misra, R. S., Russell, J. Q., Koenig, A., Hinshaw-Makepeace, J. A., Wen, R., Wang, D., Huo, H., Littman, D. R., Ferch, U., Ruland, J., et al. (2007). Caspase-8 and c-FLIPL associate in lipid rafts with NF-kappa B adaptors during T cell activation. J Biol Chem *282*, 19365–19374.

Mitsuhashi, S., Shima, H., Li, Y., Tanuma, N., Okamoto, T., Kikuchi, K., and Ubukata, M. (2008). Tautomycetin suppresses the TNFalpha/NF-kappaB pathway via inhibition of IKK activation. Int. J. Oncol. *33*, 1027–1035.

Monks, C., Freiberg, B., Kupfer, H., Sciaky, N., and Kupfer, A. (1998). Three-dimensional segregation of supramolecular activation clusters in T cells. Nature *395*, 82–86.

Moorhead, G. B. G., Trinkle-Mulcahy, L., and Ulke-Lemée, A. (2007). Emerging roles of nuclear protein phosphatases. Nat Rev Mol Cell Biol *8*, 234–244.

Moorthy, A. K., Savinova, O. V., Ho, J. Q., Wang, V. Y.-F., Vu, D., and Ghosh, G. (2006). The 20S proteasome processes NF-kappaB1 p105 into p50 in a translation-independent manner. EMBO J *25*, 1945–1956.

Morgan, J., Yin, Y., Borowsky, A., Kuo, F., Nourmand, N., Koontz, J., Reynolds, C., Soreng, L., Griffin, C., Graeme-Cook, F., et al. (1999). Breakpoints of the t(11;18)(q21;q21) in mucosa-associated lymphoid tissue (MALT) lymphoma lie within or near the previously undescribed gene MALT1 in chromosome 18. Cancer Research *59*, 6205–6213.

Motoyama, M., Yamazaki, S., Eto-Kimura, A., Takeshige, K., and Muta, T. (2005). Positive and negative regulation of nuclear

factor-kappa B-mediated transcription by I kappa B-xi, an inducible nuclear protein. J Biol Chem *280*, 7444–7451.

Nakano, H., Sakon, S., and Koseki, H. (1999). Targeted disruption of Traf5 gene causes defects in CD40-and CD27-mediated lymphocyte activation. In Proceedings of the ….

Natoli, G., and Chiocca, S. (2008). Nuclear ubiquitin ligases, NF-kappaB degradation, and the control of inflammation. Sci.STKE *1*, pe1.

Ngo, V. N., Young, R. M., Schmitz, R., Jhavar, S., Xiao, W., Lim, K.-H., Kohlhammer, H., Xu, W., Yang, Y., Zhao, H., et al. (2011). Oncogenically active MYD88 mutations in human lymphoma. Nature *470*, 115–119.

Ni, H., Ergin, M., Huang, Q., Qin, J. Z., Amin, H. M., Martinez, R. L., Saeed, S., Barton, K., and Alkan, S. (2001). Analysis of expression of nuclear factor kappa B (NF-kappa B) in multiple myeloma: downregulation of NF-kappa B induces apoptosis. Br. J. Haematol. *115*, 279–286.

Nolan, G., Fujita, T., Bhatia, K., and Huppi, C. (1993). The bcl-3 proto-oncogene encodes a nuclear I kappa B-like molecule that preferentially interacts with NF-kappa B p50 and p52 in a phosphorylation-dependent …. … and cellular biology.

O'Mahony, A., Lin, X., Geleziunas, R., and Greene, W. C. (2000). Activation of the heterodimeric IkappaB kinase alpha (IKKalpha)-IKKbeta complex is directional: IKKalpha regulates IKKbeta under both basal and stimulated conditions. Mol Cell Biol *20*, 1170–1178.

Oeckinghaus, A., Hayden, M. S., and Ghosh, S. (2011). Crosstalk in NF-κB signaling pathways. Nature Publishing Group *12*, 695–708.

Oeckinghaus, A., and Ghosh, S. (2009). The NF- B Family of Transcription Factors and Its Regulation. Cold Spring Harbor Perspectives in Biology *1*, a000034–a000034.

Oh-hora, M., and Rao, A. (2008). Calcium signaling in lymphocytes. Curr. Opin. Immunol. *20*, 250–258.

Palkowitsch, L., Marienfeld, U., Brunner, C., Eitelhuber, A., Krappmann, D., and Marienfeld, R. B. (2011). The Ca2+-dependent Phosphatase Calcineurin Controls the Formation of the Carma1-Bcl10-Malt1 Complex during T Cell Receptor-induced NF- B Activation. Journal of Biological Chemistry *286*, 7522–7534.

Park, S.-G., Schulze-Luehrman, J., Hayden, M. S., Hashimoto, N., Ogawa, W., Kasuga, M., and Ghosh, S. (2009). The kinase PDK1 integrates T cell antigen receptor and CD28 coreceptor signaling to induce NF-kappaB and activate T cells. Nature Publishing Group *10*, 158–166.

Pasparakis, M. (2009). Regulation of tissue homeostasis by NF-kappaB signalling: implications for inflammatory diseases. Nat Rev Immunol *9*, 778–788.

Perkins, N. D. (2006). Post-translational modifications regulating the activity and function of the nuclear factor kappa B pathway. Oncogene *25*, 6717–6730.

Qi, Q., and August, A. (2007). Keeping the (kinase) party going: SLP-76 and ITK dance to the beat. Science's STKE *2007*, pe39.

Quill, H., and Schwartz, R. H. (1987). Stimulation of normal inducer T cell clones with antigen presented by purified Ia molecules in planar lipid membranes: specific induction of a long-lived state of proliferative nonresponsiveness. J Immunol *138*, 3704–3712.

Radvanyi, L., Shi, Y., Vaziri, H., Sharma, A., Dhala, R., Mills, G., and Miller, R. (1996). CD28 costimulation inhibits TCR-induced apoptosis during a primary T cell response. J Immunol *156*, 1788–1798.

Rahighi, S., Ikeda, F., Kawasaki, M.,

Akutsu, M., Suzuki, N., Kato, R., Kensche, T., Uejima, T., Bloor, S., Komander, D., et al. (2009). Specific recognition of linear ubiquitin chains by NEMO is important for NF-kappaB activation. Cell *136*, 1098–1109.

Rao, P., Hayden, M. S., Long, M., Scott, M. L., West, A. P., Zhang, D., Oeckinghaus, A., Lynch, C., Hoffmann, A., Baltimore, D., et al. (2010). IκBβ acts to inhibit and activate gene expression during the inflammatory response. Nature *466*, 1115–1119.

Razani, B., Zarnegar, B., Ytterberg, A. J., Shiba, T., Dempsey, P. W., Ware, C. F., Loo, J. A., and Cheng, G. (2010). Negative Feedback in Noncanonical NF-kappa B Signaling Modulates NIK Stability Through IKK alpha-Mediated Phosphorylation. Sci.STKE *3*, –.

Reiley, W., Zhang, M., Wu, X., Granger, E., and Sun, S.-C. (2005). Regulation of the deubiquitinating enzyme CYLD by IkappaB kinase gamma-dependent phosphorylation. Mol Cell Biol *25*, 3886–3895.

Reth, M. (1989). Antigen Receptor Tail Clue. Nature *338*, 383–384.

Ricklin, D., Hajishengallis, G., Yang, K., and Lambris, J. D. (2010). Complement: a key system for immune surveillance and homeostasis. Nature Publishing Group *11*, 785–797.

Rincon, M., and Davis, R. J. (2009). Regulation of the immune response by stress-activated protein kinases. Immunol. Rev. *228*, 212–224.

Romeo, C., Amiot, M., and Seed, B. (1992). Sequence Requirements for Induction of Cytolysis by the T-Cell Antigen/Fc Receptor Zeta-Chain. Cell *68*, 889–897.

Rook, A. H., Wood, G. S., Yoo, E. K., Elenitsas, R., Kao, D. M., Sherman, M. L., Witmer, W. K., Rockwell, K. A., Shane, R. B., Lessin, S. R., et al. (1999). Interleukin-12 therapy of cutaneous T-cell lymphoma induces lesion regression and cytotoxic T-cell responses. Blood *94*, 902–908.

Roose, J. P., Mollenauer, M., Gupta, V. A., Stone, J., and Weiss, A. (2005). A diacylglycerol-protein kinase C-RasGRP1 pathway directs Ras activation upon antigen receptor stimulation of T cells. Mol Cell Biol *25*, 4426–4441.

Rosenwald, A. (2003). Gene expression profiling of diffuse large B-cell lymphoma. Leukemia & Lymphoma.

Rudd, C. E., Taylor, A., and Schneider, H. (2009). CD28 and CTLA-4 coreceptor expression and signal transduction. Immunol. Rev. *229*, 12–26.

Rudd, C., and Schneider, H. (2003). Unifying concepts in CD28, ICOS and CTLA4 co-receptor signalling. Nat Rev Immunol *3*, 544–556.

Rudolph, M. G., Stanfield, R. L., and Wilson, I. A. (2006). How TCRs bind MHCs, peptides, and coreceptors. Annu Rev Immunol *24*, 419–466.

Ruland, J. (2011). Return to homeostasis: downregulation of NF-κB responses. Nature Publishing Group *12*, 709–714.

Salvador, J., Mittelstadt, P., Guszczynski, T., Copeland, T., Yamaguchi, H., Appella, E., Fornace, A., and Ashwell, J. (2005a). Alternative p38 activation pathway mediated by T cell receptor-proximal tyrosine kinases. Nat Immunol *6*, 390–395.

Salvador, J., Mittelstadt, P., Belova, G., Fornace, A., and Ashwell, J. (2005b). The autoimmune suppressor Gadd45 alpha inhibits the T cell alternative p38 activation pathway. Nat Immunol *6*, 396–402.

Sato, S., Sanjo, H., Takeda, K., Ninomiya-Tsuji, J., Yamamoto, M., Kawai, T., Matsumoto, K., Takeuchi, O., and Akira, S. (2005). Essential function for the kinase TAK1 in innate and adaptive immune responses. Nat Immunol *6*, 1087–1095.

Savignac, M., Mellstrom, B., and Naranjo, J. R. (2007). Calcium-dependent transcription of cytokine genes in T lymphocytes. Pflug Arch Eur J Phy *454*, 523–533.

Scharschmidt, E., Wegener, E., Heissmeyer, V., Rao, A., and Krappmann, D. (2004). Degradation of Bcl10 induced by T-cell activation negatively regulates NF-kappa B signaling. Mol Cell Biol *24*, 3860–3873.

Schneider, H., Cai, Y. C., Prasad, K. V., Shoelson, S. E., and Rudd, C. E. (1995). T cell antigen CD28 binds to the GRB-2/SOS complex, regulators of p21ras. Eur J Immunol *25*, 1044–1050.

Schulze-Luehrmann, J., and Ghosh, S. (2006). Antigen-receptor signaling to nuclear factor kappa B. Immunity *25*, 701–715.

Sen, R., and Baltimore, D. (1986). Multiple nuclear factors interact with the immunoglobulin enhancer sequences. Cell *46*, 705–716.

Sen, R., and Smale, S. T. (2010). Selectivity of the NF-{kappa}B response. Cold Spring Harbor Perspectives in Biology *2*, a000257.

Senftleben, U., Cao, Y., Xiao, G., Greten, F. R., Krahn, G., Bonizzi, G., Chen, Y., Hu, Y., Fong, A., Sun, S. C., et al. (2001). Activation by IKKalpha of a second, evolutionary conserved, NF-kappa B signaling pathway. Science *293*, 1495–1499.

Serfling, E., Berberich-Siebelt, F., and Avots, A. (2007). NFAT in Lymphocytes: A Factor for All Events? Science's STKE *2007*, pe42–pe42.

Shaffer, A. L., Emre, N. C. T., Romesser, P. B., and Staudt, L. M. (2009). IRF4: Immunity. Malignancy! Therapy? Clinical Cancer Research *15*, 2954–2961.

Shambharkar, P. B., Blonska, M., Pappu, B. P., Li, H., You, Y., Sakurai, H., Darnay, B. G., Hara, H., Penninger, J., and Lin, X. (2007). Phosphorylation and ubiquitination of the IkappaB kinase complex by two distinct signaling pathways. EMBO J *26*, 1794–1805.

Shan, X., Czar, M., Bunnell, S., Liu, P., Liu, Y., Schwartzberg, P., and Wange, R. (2000). Deficiency of PTEN in Jurkat T cells causes constitutive localization of Itk to the plasma membrane and hyperresponsiveness to CD3 stimulation. Mol Cell Biol *20*, 6945–6957.

Sharma, S., and Rao, A. (2009). RNAi screening: tips and techniques. Nat Immunol *10*, 799–804.

Shembade, N., Harhaj, N. S., Parvatiyar, K., Copeland, N. G., Jenkins, N. A., Matesic, L. E., and Harhaj, E. W. (2008). The E3 ligase Itch negatively regulates inflammatory signaling pathways by controlling the function of the ubiquitin-editing enzyme A20. Nature Publishing Group *9*, 254–262.

Shi, Y. (2009). Serine/threonine phosphatases: mechanism through structure. Cell *139*, 468–484.

Shim, J., Lee, H., Chang, E., Chae, W., Han, J., Han, D., Morio, T., Yang, J., Bothwell, A., and Lee, S. (2002). Immunosuppressive effects of tautomycetin in vivo and in vitro via T cell-specific apoptosis induction. Proc Natl Acad Sci USA *99*, 10617–10622.

Shim, J., Xiao, C., Paschal, A., Bailey, S., Rao, P., Hayden, M., Lee, K., Bussey, C., Steckel, M., Tanaka, N., et al. (2005). TAK1, but not TAB1 or TAB2, plays an essential role in multiple signaling pathways in vivo. Genes Dev *19*, 2668–2681.

Sica, A., Dorman, L., Viggiano, V., Cippitelli, M., Ghosh, P., Rice, N., and Young, H. A. (1997). Interaction of NF-kappaB and NFAT with the interferon-gamma promoter. J Biol Chem *272*, 30412–30420.

Smale, S. T. (2011). Hierarchies of NF-κB target-gene regulation. Nature Publishing Group *12*, 689–694.

Smith-Garvin, J. E., Koretzky, G. A., and Jordan, M. S. (2009). T cell activation. Annu Rev Immunol *27*, 591–619.

Soderling, T. R. (1999). The Ca-calmodulin-dependent protein kinase cascade. Trends Biochem. Sci. *24*, 232–236.

Solan, N. J., Miyoshi, H., Carmona, E. M., Bren, G. D., and Paya, C. V. (2002). RelB cellular regulation and transcriptional activity are regulated by p100. J Biol Chem *277*, 1405–1418.

Sommer, K., Guo, B., Pomerantz, J., Bandaranayake, A., Moreno-Garcia, M., Ovechkina, Y., and Rawlings, D. (2005). Phosphorylation of the CARMA1 linker controls NF-kappa B activation. Immunity *23*, 561–574.

Sommers, C., Samelson, L., and Love, P. (2004). LAT: a T lymphocyte adapter protein that couples the antigen receptor to downstream signaling pathways. Bioessays *26*, 61–67.

Sommers, C. L., Lee, J., Steiner, K. L., Gurson, J. M., Depersis, C. L., El-Khoury, D., Fuller, C. L., Shores, E. W., Love, P. E., and Samelson, L. E. (2005). Mutation of the phospholipase C-gamma1-binding site of LAT affects both positive and negative thymocyte selection. Journal of Experimental Medicine *201*, 1125–1134.

Sors, A., Jean-Louis, F., Pellet, C., Laroche, L., Dubertret, L., Courtois, G., Bachelez, H., and Michel, L. (2006). Down-regulating constitutive activation of the NF-kappa B canonical pathway overcomes the resistance of cutaneous T-cell lymphoma to apoptosis. Blood *107*, 2354–2363.

Sors, A., Jean-Louis, F., Pellet, C., Laroche, L., Dubertret, L., Courtois, G., Bachelez, H., and Michel, L. Down-regulating constitutive activation of the NF-{kappa}B canonical pathway overcomes the resistance of cutaneous T-cell lymphoma to apoptosis. Blood *107*, 2354–2363.

Sors, A., Jean-Louis, F., Begue, E., Parmentier, L., Dubertret, L., Dreano, M., Courtois, G., Bachelez, H., and Michel, L. (2008). Inhibition of I B Kinase Subunit 2 in Cutaneous T-Cell Lymphoma Down-Regulates Nuclear Factor- B Constitutive Activation, Induces Cell Death, and Potentiates the Apoptotic Response to Antineoplastic Chemotherapeutic Agents. Clinical Cancer Research *14*, 901–911.

Starr, T. K., Jameson, S. C., and Hogquist, K. A. (2003). Positive and negative selection of T cells. Annu Rev Immunol *21*, 139–176.

Staudt, L. M. (2010). Oncogenic activation of NF-kappaB. Cold Spring Harbor Perspectives in Biology *2*, a000109–.

Staudt, L., and Dave, S. (2005). The biology of human lymphoid malignancies revealed by gene expression profiling. Adv Immunol *87*, 163–.

Stefansson, B., and Brautigan, D. L. (2006). Protein phosphatase 6 subunit with conserved Sit4-associated protein domain targets IkappaBepsilon. J Biol Chem *281*, 22624–22634.

Su, B., Jacinto, E., Hibi, M., Kallunki, T., Karin, M., and Ben-Neriah, Y. (1994). JNK is involved in signal integration during costimulation of T lymphocytes. Cell *77*, 727–736.

Sun, L., Deng, L., Ea, C., Xia, Z., and Chen, Z. (2004). The TRAF6 ubiquitin ligase and TAK1 kinase mediate IKK activation by BCL10 and MALT1 in T lymphocytes. Molecular Cell *14*, 289–301.

Sun, S. (2010a). Controlling the fate of NIK: a central stage in noncanonical NF-kappaB signaling. Sci.STKE.

Sun, S. C. (2010b). CYLD: a tumor suppressor deubiquitinase regulating NF-

kappaB activation and diverse biological processes. Cell Death Differ *17*, 25–34.

Sun, S.-C. (2011). Non-canonical NF-κB signaling pathway. Cell Res. *21*, 71–85.

Sun, W., Yu, Y., Dotti, G., Shen, T., Tan, X., Savoldo, B., Pass, A. K., Chu, M., Zhang, D., Lu, X., et al. (2009). PPM1A and PPM1B act as IKKbeta phosphatases to terminate TNFalpha-induced IKKbeta-NF-kappaB activation. Cell Signal *21*, 95–102.

Sun, W., Wang, H., Zhao, X., Yu, Y., Fan, Y., Wang, H., Wang, X., Lu, X., Zhang, G., Fu, S., et al. (2010). Protein phosphatase 2A acts as a mitogen-activated protein kinase kinase kinase 3 (MEKK3) phosphatase to inhibit lysophosphatidic acid-induced IkappaB kinase beta/nuclear factor-kappaB activation. Journal of Biological Chemistry *285*, 21341–21348.

Suyang, H., Phillips, R., Douglas, I., and Ghosh, S. (1996). Role of unphosphorylated, newly synthesized I kappa B beta in persistent activation of NF-kappa B. Mol Cell Biol *16*, 5444–5449.

Tacke, M., Hanke, G., Hanke, T., and Hunig, T. (1997). CD28-mediated induction of proliferation in resting T cells in vitro and in vivo without engagement of the T cell receptor: Evidence for functionally distinct forms of CD28. Eur J Immunol *27*, 239–247.

Tada, K., Okazaki, T., Sakon, S., Kobarai, T., Kurosawa, K., Yamaoka, S., Hashimoto, H., Mak, T., Yagita, H., Okumura, K., et al. (2001). Critical roles of TRAF2 and TRAF5 in tumor necrosis factor-induced NF-kappa B activation and protection from cell death. J Biol Chem *276*, 36530–36534.

Tanaka, T., Grusby, M. J., and Kaisho, T. (2007). PDLIM2-mediated termination of transcription factor NF-kappaB activation by intranuclear sequestration and degradation of the p65 subunit. Nat Immunol *8*, 584–591.

Tavano, R., Contento, R. L., Jimenez Baranda, S., Soligo, M., Tuosto, L., Manes, S., and Viola, A. (2006). CD28 interaction with filamin-A controls lipid raft accumulation at the T-cell immunological synapse. Nat Cell Biol *8*, 1270–U46.

Tergaonkar, V., Correa, R. G., Ikawa, M., and Verma, I. M. (2005). Distinct roles of IkappaB proteins in regulating constitutive NF-kappaB activity. Nat Cell Biol *7*, 921–923.

Thome, M. CARMA1, BCL-10 and MALT1 in lymphocyte development and activation 2. Nat Rev Immunol *4*, 348–359.

Thome, M., Charton, J. E., Pelzer, C., and Hailfinger, S. (2010). Antigen Receptor Signaling to NF- B via CARMA1, BCL10, and MALT1. Cold Spring Harbor Perspectives in Biology *2*, a003004–a003004.

Thompson, C. B., Lindsten, T., Ledbetter, J. A., Kunkel, S. L., Young, H. A., Emerson, S. G., Leiden, J. M., and June, C. H. (1989). CD28 activation pathway regulates the production of multiple T-cell-derived lymphokines/cytokines. Proc Natl Acad Sci USA *86*, 1333–1337.

Ting, A., and Pimentel-Muinos, F. (1996). RIP mediates tumor necrosis factor receptor 1 activation of NF-kappaB but not Fas/APO-1-initiated apoptosis. EMBO J.

Tokunaga, F., Nakagawa, T., Nakahara, M., Saeki, Y., Taniguchi, M., Sakata, S.-I., Tanaka, K., Nakano, H., and Iwai, K. (2011). SHARPIN is a component of the NF-κB-activating linear ubiquitin chain assembly complex. Nature *471*, 633–636.

Tonegawa, S. (1993). The Nobel Lectures in Immunology - the Nobel-Prize for Physiology or Medicine, 1987 - Awarded to Tonegawa,Susumu - Biography. Scand J Immunol *38*, 318–319.

Trombetta, E. S., and Mellman, I. (2005). CELL BIOLOGY OF ANTIGEN PROCESSING IN VITRO AND IN VIVO.

Annu Rev Immunol *23*, 975–1028.

Trompouki, E., Hatzivassiliou, E., Tsichritzis, T., Farmer, H., Ashworth, A., and Mosialos, G. (2003). CYLD is a deubiquitinating enzyme that negatively regulates NF-kappa B activation by TNFR family members. Nature *424*, 793–796.

Uren, A., O'Rourke, K., Aravind, L., Pisabarro, M., Seshagiri, S., Koonin, E., and Dixit, V. (2000). Identification of paracaspases and metacaspases: Two ancient families of caspase-like proteins, one of which plays a key role in MALT lymphoma. Molecular Cell *6*, 961–967.

Vallabhapurapu, S., Matsuzawa, A., and Zhang, W. (2008). Nonredundant and complementary functions of TRAF2 and TRAF3 in a ubiquitination cascade that activates NIK-dependent alternative NF-κB signaling. Nature.

Vallabhapurapu, S., and Karin, M. (2009). Regulation and Function of NF-kappa B Transcription Factors in the Immune System. Annu Rev Immunol *27*, 693–733.

Vanhaesebroeck, B., and Alessi, D. (2000). The PI3K-PDK1 connection: more than just a road to PKB. Biochem J *346*, 561–576.

Villalba, M., Bi, K., Hu, J., and Altman, Y. (2002). Translocation of PKCθ in T cells is mediated by a nonconventional, PI3-K– and Vav-dependent pathway, but does not absolutely require phospholipase C. The Journal of Cell ….

Virshup, D. M., and Shenolikar, S. (2010). From Promiscuity to Precision: Protein Phosphatases Get a Makeover. Molecular Cell *33*, 537–545.

Wagner, S., Carpentier, I., Rogov, V., Kreike, M., Ikeda, F., Löhr, F., Wu, C.-J., Ashwell, J. D., Dötsch, V., Dikic, I., et al. (2008). Ubiquitin binding mediates the NF-kappaB inhibitory potential of ABIN proteins. Oncogene *27*, 3739–3745.

Wan, Y., Chi, H., Xie, M., and Schneider, M. (2006). The kinase TAK1 integrates antigen and cytokine receptor signaling for T cell development, survival and function. Nat Immunol.

Wang, C., Deng, L., Hong, M., Akkaraju, G. R., Inoue, J., and Chen, Z. J. (2001). TAK1 is a ubiquitin-dependent kinase of MKK and IKK. Nature *412*, 346–351.

Wang, D., You, Y., Case, S., and McAllister-Lucas, L. (2002). A requirement for CARMA1 in TCR-induced NF-κB activation. Nature.

Wardenburg, J., Fu, C., Jackman, J., Flotow, H., Wilkinson, S., Williams, D., Johnson, R., Kong, G., Chan, A., and Findell, P. (1996). Phosphorylation of SLP-76 by the ZAP-70 protein-tyrosine kinase is required for T-cell receptor function. J Biol Chem *271*, 19641–19644.

Wee, Y.-M., Choi, M. Y., Kang, C.-H., Kim, Y.-H., Kim, J.-H., Lee, S.-K., Yu, S.-Y., Kim, S.-C., and Han, D.-J. (2010). The Synergistic Effect of Tautomycetin on Cyclosporine A-Mediated Immunosuppression in a Rodent Islet Allograft Model. Mol Med *16*, 298–306.

Wegener, A., Letourneur, F., Hoeveler, A., Brocker, T., Luton, F., and Malissen, B. (1992). The T-Cell Receptor/Cd3 Complex Is Composed of at Least 2 Autonomous Transduction Modules. Cell *68*, 83–95.

Wegener, E., Oeckinghaus, A., Papadopoulou, N., Lavitas, L., Schmidt-Supprian, M., Ferch, U., Mak, T. W., Ruland, J., Heissmeyer, V., and Krappmann, D. (2006). Essential role for IkappaB kinase beta in remodeling Carma1-Bcl10-Malt1 complexes upon T cell activation. Molecular Cell *23*, 13–23.

Weinstein, I. (2002). Cancer: Addiction to oncogenes - The Achilles heal of cancer. Science *297*, 63–64.

Weinstein, I. B., and Joe, A. (2008). Oncogene addiction. Cancer Research *68*, 3077–80; discussion 3080.

Wertz, I. E., O'Rourke, K. M., Zhou, H., Eby, M., Aravind, L., Seshagiri, S., Wu, P., Wiesmann, C., Baker, R., Boone, D. L., et al. (2004). De-ubiquitination and ubiquitin ligase domains of A20 downregulate NF-kappaB signalling. Nature *430*, 694–699.

Woronicz, J., Gao, X., Cao, Z., Rothe, M., and Goeddel, D. (1997). I kappa B kinase-beta: NF-kappa B activation and complex formation with I kappa B kinase-alpha and NIK. Science *278*, 866–869.

Wu, C.-J., Conze, D. B., Li, T., Srinivasula, S. M., and Ashwell, J. D. (2006). Sensing of Lys 63-linked polyubiquitination by NEMO is a key event in NF-kappaB activation [corrected]. Nat Cell Biol *8*, 398–406.

Wulczyn, F. G., Naumann, M., and Scheidereit, C. (1992). Candidate proto-oncogene bcl-3 encodes a subunit-specific inhibitor of transcription factor NF-kappa B. Nature *358*, 597–599.

Xiao, G., Harhaj, E. W., and Sun, S. C. (2001). NF-kappaB-inducing kinase regulates the processing of NF-kappaB2 p100. Molecular Cell *7*, 401–409.

Xu, C., Gagnon, E., Call, M. E., Schnell, J. R., Schwieters, C. D., Carman, C. V., Chou, J. J., and Wucherpfennig, K. W. (2008). Regulation of T cell receptor activation by dynamic membrane binding of the CD3epsilon cytoplasmic tyrosine-based motif. Cell *135*, 702–713.

Xu, G., Lo, Y.-C., Li, Q., Napolitano, G., Wu, X., Jiang, X., Dreano, M., Karin, M., and Wu, H. (2011). Crystal structure of inhibitor of κB kinase β. Nature *472*, 325–330.

Yaffe, M. B. (2002). MAGUK SH3 domains--swapped and stranded by their kinases? Structure *10*, 3–5.

Yamamoto, M., Yamazaki, S., Uematsu, S., Sato, S., Hemmi, H., Hoshino, K., Kaisho, T., Kuwata, H., Takeuchi, O., Takeshige, K., et al. (2004). Regulation of Toll/IL-1-receptor-mediated gene expression by the inducible nuclear protein IkappaBzeta. Nature *430*, 218–222.

Yamamoto, Y., Verma, U. N., Prajapati, S., Kwak, Y.-T., and Gaynor, R. B. (2003). Histone H3 phosphorylation by IKK-alpha is critical for cytokine-induced gene expression. Nature *423*, 655–659.

Yang, D. D., Conze, D., Whitmarsh, A. J., Barrett, T., Davis, R. J., Rincón, M., and Flavell, R. A. (1998). Differentiation of CD4+ T cells to Th1 cells requires MAP kinase JNK2. Immunity *9*, 575–585.

Yang, J., Fan, G. H., Wadzinski, B. E., Sakurai, H., and Richmond, A. (2001a). Protein phosphatase 2A interacts with and directly dephosphorylates RelA. J Biol Chem *276*, 47828–47833.

Yang, J., Lin, Y., Guo, Z., Cheng, J., Huang, J., Deng, L., Liao, W., Chen, Z., Liu, Z., and Su, B. (2001b). The essential role of MEKK3 in TNF-induced NF-kappaB activation. Nat Immunol *2*, 620–624.

Yang, J., Liao, X., Agarwal, M. K., Barnes, L., Auron, P. E., and Stark, G. R. (2007). Unphosphorylated STAT3 accumulates in response to IL-6 and activates transcription by binding to NF kappa B. Genes Dev *21*, 1396–1408.

Yang, X.-D., Huang, B., Li, M., Lamb, A., Kelleher, N. L., and Chen, L.-F. (2009). Negative regulation of NF-kappaB action by Set9-mediated lysine methylation of the RelA subunit. EMBO J *28*, 1055–1066.

Yawalkar, N., Ferenczi, K., Jones, D. A., Yamanaka, K., Suh, K.-Y., Sadat, S., and Kupper, T. S. (2003). Profound loss of T-cell receptor repertoire complexity in cutaneous T-cell lymphoma. Blood *102*, 4059–4066.

Yeh, W., Shahinian, A., Speiser, D., and Kraunus, J. (1997). Early lethality, functional NF-[kappa] B activation, and increased sensitivity to TNF-induced cell death in TRAF2-deficient mice. Immunity.

Zabel, U., and Baeuerle, P. (1990). Purified Human I-Kappa-B Can Rapidly Dissociate the Complex of the Nf-Kappa-B Transcription Factor with Its Cognate Dna. Cell *61*, 255–265.

Zandi, E. (1997). The IkB kinase complex (IKK) contains two kinase subunits, IKKa and IKKb, necessary for IkB phosphorylation and NF-kB activation. Cell.

Zhang, J., Salojin, K. V., Gao, J. X., Cameron, M. J., Bergerot, I., and Delovitch, T. L. (1999). p38 mitogen-activated protein kinase mediates signal integration of TCR/CD28 costimulation in primary murine T cells. J Immunol *162*, 3819–3829.

Zhang, J., Chang, C., Lombardi, L., and Dallafavera, R. (1994). Rearranged Nfkb2 Gene in the Hut78 T-Lymphoma Cell-Line Codes for a Constitutively Nuclear Factor Lacking Transcriptional Repressor Functions. Oncogene *9*, 1931–1937.

Zhang, W., Sloan-Lancaster, J., Kitchen, J., Trible, R., and Samelson, L. (1998). LAT: The ZAP-70 tyrosine kinase substrate that links T cell receptor to cellular activation. Cell *92*, 83–92.

Zhou, L., Chong, M. M. W., and Littman, D. R. (2009). Plasticity of CD4+ T Cell Lineage Differentiation. Immunity *30*, 646–655.

Zikherman, J., Jenne, C., Watson, S., Doan, K., Raschke, W., Goodnow, C. C., and Weiss, A. (2010). CD45-Csk phosphatase-kinase titration uncouples basal and inducible T cell receptor signaling during thymic development. Immunity *32*, 342–354.

7. Appendix

7.1 List of abbreviations

°C	Degree Celsius
AA	Amino acid
ABC-DLBCL	Activated B cell-like DLBCL
ADAP	Adhesion- and degranulation-promoting adapter protein
Ag	Antigen(s)
ANK	Ankyrin repeat motif
AP-1	Activating protein 1
APC	Antigen presenting cell
APS	Ammonium persulfate
ATL	Adult T cell lymphoma/leukemia
ATP	Adenosine triphosphate
Bcl	B cell lymphoma
BCR	B cell antigen receptor
bp (kb)	Base pair (kilo base pair)
CARD	Caspase recruitment domain
Caspase	Cysteine-aspartate specific protease
CBM complex	Carma1-Bcl10-MALT1 complex
Cbp	Csk-binding protein
CD	Cluster of differentiation
CD95L	CD95 ligand
cDNA	Complementary DNA
CED	Caspase-8 deficiency
c-FLIP	Cellular FLICE inhibitory protein
c-IAP	Cellular inhibitor of apoptosis
CRAC	Calcium release activated calcium channel
Csk	Cellular src kinase
CTCL	Cutaneous T cell lymphoma
CYLD	Cylindromatosis tumor suppressor
d	Day
DAG	Diacylglycerol
DC	Dendritic cell
DD	Death domain
DLBCL	Diffuse large B cell lymphoma
Dlgh1	Discs large homolog 1
DMEM	Dulbecco’s Modified Eagle Medium
DMSO	Dimethyl sulfoxide
DNA	Desoxyribonucleic acid
DTT	Dithiothreitol

DUB	Deubiquitinating enzyme
ECL	Enhanced chemiluminescence
EDTA	Ethylenediaminetetraacetic acid
EGFP	Enhanced GFP
ELISA	Enzyme-linked immunosorbent assay
ER	Endoplasmic reticulum
ERK	Extracellularsignal-regulatedkinase
EtOH	Ethanol
FACS	Fluorescence activated cell sorter
FCS	Fetal calf serum
FHC	Ferritin heavy chain Fig.
GAPDH	Glyceraldehyde-3-phosphate dehydrogenase
GCB-DLBCL	Germinal center B cell-like DLBCL
Grb2	Growth factor receptor-bound protein 2 GRP
GUK	Guanylate kinase h
HTLV-1	Human T-lymphotropic virus type I HTS
FHC	Ferritin heavy chain
Fig.	Figure
g	Gramm
Gads	Grb2-related adaptor downstream of Shc
GAP	GTPase-activating protein
GAPDH	Glyceraldehyde-3-phosphate dehydrogenase
GCB-DLBCL	Germinal center B cell-like DLBCL
GEF	Guanine-nucleotide-exchange factor
GFP	Green fluorescent protein
Grb2	Growth factor receptor-bound protein 2
GRP	GDP release protein
GRR	Glycine rich region
GUK	Guanylate kinase
h	Hour
HLH	Helix-loop-helix
HPK1	Haematopoietic progenitor kinase 1
HPRT1	Hypoxanthine phosphoribosyl-transferase 1
HRP	Horseradish peroxidase
HTLV-1	Human T-lymphotropic virus type I
HTS	High throughput screening
IB	Immunoblot(ting)
IFNγ	Interferon gamma
IgG	Immunoglobulin
IgGH	Immunoglobulin heavy chain
IgGL	Immunoglobulin light chain
IKK	IκB kinase
IL	Interleukin
IMDM	Iscove's modified Eagles medium
Iono	Ionomycin
IP	Immunoprecipitation

IP3	Inositol 3,4,5-trisphosphate
IRES	Internal ribosomal entry site
ITAM	Immunoreceptor tyrosine-based activation motif
Itk	IL-2 inducible Tec kinase
IkB	Inhibitor of kB proteins
JNK/SAPK	c-Jun N-terminal kinase/stress-activated protein kinase
KBD	Kinase binding domain
KD	Kinase domain
kDa	Kilo Dalton
l	Liter
LAT	Linker of activated T cells
LZ	Leucine zipper
mAb	Monoclonal antibody
MACS	Magnetic activated cell sorter
MAGUK	Membrane-associated guanylate kinase
MALT1	Mucosa-associated lymphoid tissue lymphoma translocation protein 1
MAPK	Mitogen-activated protein kinase
MEF	Murine embryonic fibroblast
MEKK	MAPK/ERK Kinase Kinase
MeOH	Methanol
MF	Mycosis fungoides
MFI	Mean fluorescence intensity
MHC	Major histocompatibility complex
min	Minute(s)
MLK	Mixed-lineage protein kinase
MM	Multiple myeloma
mRNA	Messenger ribonucleic acid
NBD	Nemo-binding-domain
NBP	NBDpeptide
Nck	Non-catalytic region of tyrosine kinase
NEMO	NF-kB essential modulator
NES	Nuclear export sequence
NFAT	Nuclear factor of activated T cells
NF-κB	Nuclear factor-kappaB
NIK	NF-kB-inducing kinase
NK cells	Natural killer cells
NLS	Nuclear translocation sequence
p	Peptide
PAGE	Polyacrylamide gel electrophoresis
PAMP	Pathogen-associated molecular pattern
PBL	Peripheral blood leukocyte
PBS	Phosphate buffered saline
PCR	Polymerase chain reaction
PDK1	3-Phosphoinositide-dependent kinase 1
PHA	Phytohemagglutinin
PI3K	Phosphoinositide-3 kinase

PKC	Protein kinase C
PLCγ1	Phospholipase C gamma 1
PMA	Phorbol 12-myristate-13-acetate
PP1CA	Protein phosphatase 1, catalytic subunit alpha
PP2A	Protein phosphatase 2A
PP2Ac	Protein phosphatase 2A catalytic subunit
PP4c	Protein phosphatase 4 catalytic subunit
PP4R	Protein phosphatase 4 regulatory subunit
PPP	Phosphoprotein phosphatase
PRD	PKC-regulated domain
PRR	Pattern recognition receptor
PSK	Protein serine/threonine kinase
PSP	Protein serine/threonine phosphatase
PSP	Protein serine/threonine phosphatases
PTEN	Phosphatase and tensin homolog
PTK	Protein tyrosine kinase
PTP	Protein tyrosine phosphatase
PTPN	Protein tyrosine phosphatase, non-receptor type
PTPR	Protein tyrosine phosphatase, receptor type
pUb	Poly-ubiquitin
RHD	Rel homology domain
RIP1	Receptor-interacting protein 1
RLU	Relative light unit
RNA	Ribonucleic acid
RNAi	RNA interference
ROS	Reactive oxygen species
rpm	Rotations per minute
RT	Room temperature
RT-PCR	Reverse transcription PCR
SDS	Sodium dodecyl sulfate
S	Second
SFK	Src family protein tyrosine kinase
SH	Src homology
SHIP1	SH2 domain-containing inositol phosphatase 1
SHP1	SH2 domain-containing phosphatase 1
shRNA	Short hairpin RNA
siRNA	Small interfering RNA
SLP76	SH2-domain-containing leukocyte protein of 76 kd
SOCE	Store-operated calcium entry
SOS	Son of sevenless
Sts	Suppressor of TCR signaling
Syk	Spleen tyrosine kinase
TAD	Transactivationdomain
TAK1	TGF-b-activated kinase 1
T-ALL	T cell acute lymphocytic leukaemia
TCR	T cell antigen receptor

TEMED	N,N,N',N'-Tetramethyl-ethylenediamine T
NFR	TNF receptor
TNF-RSC	TNFR signaling complex
TNFα	Tumor necrosis factor alpha
TRADD	TNFR1-associated death domain protein
TRAF	TNFR-associated factor
Tris	Tris-[hydroxymethyl]amino-methane
Ub	Ubiquitin
vs.	versus
wt	Wild type
ZAP-70	Zeta chain-associated kinase of 70 kDa
ZF	Zinc finger

7.2 List of publications

CD95 stimulation results in the formation of a novel death effector domain protein-containing complex.
Lavrik IN, **Mock T**, Golks A, Hoffmann JC, Baumann S, Krammer PH
J Biol Chem. 2008 Sep 26;283(39):26401-8. Epub 2008 Jul 17.

Phosphorylation of CARMA1 by HPK1 is critical for NF-κB activation in T cells.
Brenner D, Brechmann M, Röhling S, Tapernoux M, **Mock T**, Winter D, Lehmann WD, Kiefer F, Thome M, Krammer PH, Arnold R.
Proc Natl Acad Sci U S A. 2009 Aug 25;106(34):14508-13

A PP4 holoenzyme inhibits NF-κB activation in T lymphocytes and suppresses human lymphoma cell survival
Brechmann M*, **Mock T***, Nickles D, Kiessling M, Weit N, Breuer R, Müller W, Wabnitz G, Frey F, Booken N, Samstag Y, Klemke CD, Herling M, Boutros M, Krammer PH and Arnold R
(Revised version in preparation for resubmission to Immunity)

***The authors contributed equally to the publication**

8. Declaration

Herewith, I declare that I wrote this thesis independently under supervision, and no other sources and aids than those indicated were used. Furthermore, my submission as a whole is not substantially the same as any that I have previously made or I am currently making, whether in published or unpublished form, for a degree, diploma, or similar qualification at any university or similar institution.

Heidelberg,

(Ort, Datum)

Thomas Mock (Dipl. Biol.)